



저작자표시-비영리-변경금지 2.0 대한민국

이용자는 아래의 조건을 따르는 경우에 한하여 자유롭게

- 이 저작물을 복제, 배포, 전송, 전시, 공연 및 방송할 수 있습니다.

다음과 같은 조건을 따라야 합니다:



저작자표시. 귀하는 원저작자를 표시하여야 합니다.



비영리. 귀하는 이 저작물을 영리 목적으로 이용할 수 없습니다.



변경금지. 귀하는 이 저작물을 개작, 변형 또는 가공할 수 없습니다.

- 귀하는, 이 저작물의 재이용이나 배포의 경우, 이 저작물에 적용된 이용허락조건을 명확하게 나타내어야 합니다.
- 저작권자로부터 별도의 허가를 받으면 이러한 조건들은 적용되지 않습니다.

저작권법에 따른 이용자의 권리는 위의 내용에 의하여 영향을 받지 않습니다.

이것은 [이용허락규약\(Legal Code\)](#)을 이해하기 쉽게 요약한 것입니다.

[Disclaimer](#)

이학박사 학위논문

혈관신생 과정에서 칼슘/칼모듈린에
의한 Tie2 신호 조절 기작 및
천연물 유도체의 혈소판 인테그린
활성 기작에 관한 연구

(Studies on the Mechanism of Tie2 Signaling
by Ca^{2+} /Calmodulin in Angiogenesis and of
Integrin $\alpha\text{IIb}\beta 3$ Activation by Natural
Products)

2019 년 2월

서울대학교 대학원

생명과학부

양 찬 식

Abstract

Angiogenesis, the process of building complex vascular structures, begins with sprout formation on preexisting blood vessels, followed by extension of the vessels through proliferation and migration of endothelial cells. Based on the potential therapeutic benefits of preventing angiogenesis in pathological conditions, many studies have focused on the mechanism of its initiation as well as control. However, how the extension of vessels is terminated remains obscure. Thus, I investigated the negative regulation mechanism.

I report that increased intracellular calcium can induce dephosphorylation of the endothelial receptor tyrosine kinase Tie2. The calcium-mediated dephosphorylation was found to be dependent on Tie2-calmodulin interaction. The Tyr1113 residue in the C-terminal end loop of the Tie2 kinase domain was mapped and found to be required for this interaction. Moreover, mutation of this residue into Phe impaired both the Tie2-calmodulin interaction and calcium-mediated Tie2 dephosphorylation. Furthermore, expressing a mutant Tie2 incapable of binding to calmodulin or inhibiting calmodulin function *in vivo* causes unchecked growth of the vasculature in *Xenopus*. Specifically, knockdown of Tie2 in *Xenopus* embryo retarded the sprouting and extension of intersomitic veins. Although human Tie2 expression in the Tie2-deficient animals almost completely rescued the retardation, the Tie2(Y1113F) mutant caused overgrowth of intersomitic veins with strikingly complex and excessive branching patterns.

I propose that the calcium/calmodulin-dependent negative

regulation of Tie2 can be used as an inhibitory signal for vessel growth and branching to build proper vessel architecture during embryonic development.¹⁾

Key Words : angiogenesis, calcium, calmodulin, embryogenesis, Tie2

1) All of contents in here published in *Arterioscler. Thromb. Vasc. Biol.* 2016 Jul;36(7):1406-1416 and I participated as a main author.

Epigallocatechin gallate (EGCG) is the principal bioactive ingredient in green tea and has been reported to have many health benefits. EGCG influences multiple signal transduction pathways related to human diseases, including redox, inflammation, cell cycle, and cell adhesion pathways. However, the molecular mechanisms of these varying effects are unclear, limiting further development and utilization of EGCG as a pharmaceutical compound. Here, I examined the effect of EGCG on two representative transmembrane signaling receptors, integrin $\alpha\text{IIb}\beta\text{3}$ and epidermal growth factor receptor (EGFR). I report that EGCG inhibits talin-induced integrin $\alpha\text{IIb}\beta\text{3}$ activation, but it activates $\alpha\text{IIb}\beta\text{3}$ in the absence of talin both in a purified system and in cells. This apparent paradox was explained by the fact that the activation state of $\alpha\text{IIb}\beta\text{3}$ is tightly regulated by the topology of β3 transmembrane domain (TMD); increases or decreases in TMD embedding can activate integrins. Talin increases the embedding of integrin β3 TMD, resulting in integrin activation, whereas I observed here that EGCG decreases the embedding, thus opposing talin-induced integrin activation. In the absence of talin, EGCG decreases the TMD embedding, which can also disrupt the integrin α - β TMD interaction, leading to integrin activation. EGCG exhibited similar paradoxical behavior in EGFR signaling. EGCG alters the topology of EGFR TMD and activates the receptor in the absence of EGF, but inhibits EGF-induced EGFR activation. Thus, this widely ingested polyphenol exhibits pleiotropic effects on transmembrane signaling by modifying the topology of TMDs.²⁾

2) All of contents in here published in *J. Biol. Chem.* 2017 Jun 16;292(24):9858–9864, and I participated as a main author.

Key Words : EGCG, Integrin $\alpha\text{IIb}\beta\text{3}$, transmembrane domain, Epidermal growth factor receptor

Cardiovascular disease, which is caused by unregulated platelet aggregation, is one of the main causes of deaths worldwide. Many studies have focused on natural products with antiplatelet effects as a safe alternative therapy to prevent the disease. In this context, an in-house chemical library was screened to find natural products capable of inhibiting the interaction between platelet integrin $\alpha\text{IIb}\beta\text{3}$ and fibrinogen, which is an essential step in platelet aggregation. On the basis of the screening results, indothiazinone, an alkaloid found in microbial culture, was identified as a potential antiplatelet agent. Specifically, indothiazinone treatment significantly inhibited the binding of fibrinogen to Chinese hamster ovary cells expressing integrin $\alpha\text{IIb}\beta\text{3}$. It also restricted thrombin- and adenosine diphosphate-dependent spreading of human platelets on a fibrinogen matrix. More importantly, surface plasmon resonance and molecular dynamics studies suggested that indothiazinone suppressed talin-induced activation of integrin $\alpha\text{IIb}\beta\text{3}$ presumably by inhibiting talin-integrin interaction. In conclusion, these results suggest that indothiazinone can be used as a lead compound for the development of antiplatelet drugs with a novel mode of action.³⁾

Key Words : antiplatelet drug, indothiazinone, integrin $\alpha\text{IIb}\beta\text{3}$, platelet, talin

3) All of contents in here published in *Chem. Biol. Drug Design* 2017 Nov;90(5): 873-882, and I participated as a main author.

Table of Contents

Abstract	i
List of figures	ii
Part I	1
Abstract	3
Introduction	5
Materials and methods	7
Results	13
Conclusion	48
References	53
Part II	60
Abstract	62
Introduction	64
Materials and methods	66
Results	69
Conclusion	99
References	100
Part III.	106
Abstract	108
Introduction	110
Materials and methods	113
Results	117
Conclusion	145
References	148
국문초록	153

List of figures

Figure 1. Treatment of calcium ionophore dephosphorylate endogenously expressed Tie2 in HUVEC.	14
Figure 2. Effects of calcium ionophore and Ang1 treatment on HUVEC.	17
Figure 3. Characterization of FLAG-Tie2 Δ ECD.	19
Figure 4. Calcium-and calmodulin-dependent dephosphorylation of Tie2.	21
Figure 5. Effects of calcium ionophore on phosphorylation of FLAG-Tie2 Δ ECD expression level.	23
Figure 6. Interaction between Tie2 and calmodulin.	27
Figure 7. Endogenous Tie2-calmodulin interaction in HUVECs	29
Figure 8. Effect of calcium ionophore on Tie2 mutant which defective in calmodulin bound.	33
Figure 9. Effects of Y1113 mutation on Tie2 signaling.	36
Figure 10. Role of Tyr1113 residue in calcium-induced dephosphorylation.	38
Figure 11. Evolutionarily conserved amino acid sequences in vertebrates.	41
Figure 12. Regulation of embryonic angiogenesis by Tie2 in <i>Xenopus tropicalis</i>	43
Figure 13. Uncontrolled angiogenesis caused by disruption of Tie2-calmodulin interaction.	46
Figure 14. Summary and hypothetical model.	51
Figure 15. Scheme of talin head domain induced integrin	

α IIb β 3 activation.	70
Figure 16. EGCG both activates and inhibits activation of integrin α IIb β 3 in cells.	73
Figure 17. EGCG reversibly induces integrin activation in CHO/ α IIb β 3 cells.	75
Figure 18. EGCG both activates and inhibits activation of integrin α IIb β 3 in a reconstituted system.	77
Figure 19. EGCG has distinct effects on talin-dependent and talin-independent α IIb β 3 activation.	80
Figure 20. Diagram of environment sensitive fluorescence spectroscopy.	83
Figure 21. EGCG decreases embedding angle of β 3 TMD.	85
Figure 22. EGCG induces β 3 TMD topological changes in the opposite direction to talin.	88
Figure 23. Proposed model of EGCG's action.	90
Figure 24. EGCG decreases EGF induced phosphorylation of EGFR.	93
Figure 25. EGCG alone increases phosphorylation of EGFR	95
Figure 26. Effects of EGCG on lipid embedding of EGFR TMD.	97
Figure 27. Antiplatelet activity of indothiazinone.	118
Figure 28. Representative images of platelet spreading on fibrinogen matrix.	120
Figure 29. Quantification of Indothiazinone effects on platelet spreading.	122
Figure 30. Effect of indothiazinone on talin-induced integrin activation.	125
Figure 31. Effect of indothiazinone on cell surface	

expression of integrin $\alpha\text{IIb}\beta\text{3}$	127
Figure 32. Interaction between indothiazinone and talin.	132
Figure 33. Purification of mutant talin head domain.	134
Figure 34. Effects of mutation in talin on talin- indothiazinone interaction.	136
Figure 35. Effect of indothiazinone and its derivatives.	139
Figure 36. Enhanced antiplatelet effect of KCH-1569.	141
Figure 37. Effects of indothiazinone or KCH-1569 on integrin $\alpha\text{IIb}\beta\text{3}$ surface expression levels in GFP-THD -transfected cells.	143
Figure 38. Graphical abstract	146

Part I.

Calmodulin Mediates Ca²⁺-Dependent Inhibition of Tie2 Signaling and Acts as a Developmental Brake During Embryonic Angiogenesis

Chansik Yang,* Jiyeon Ohk,* Ji Yeun Lee,* Eun Jin Kim, Jiyeon Kim, Sangyeul Han, Dongeun Park, Hosung Jung, Chungho Kim

Objective—Angiogenesis, the process of building complex vascular structures, begins with sprout formation on preexisting blood vessels, followed by extension of the vessels through proliferation and migration of endothelial cells. Based on the potential therapeutic benefits of preventing angiogenesis in pathological conditions, many studies have focused on the mechanisms of its initiation as well as control. However, how the extension of vessels is terminated remains obscure. Thus, we investigated the negative regulation mechanism.

Approach and Results—We report that increased intracellular calcium can induce dephosphorylation of the endothelial receptor tyrosine kinase Tie2. The calcium-mediated dephosphorylation was found to be dependent on Tie2-calmodulin interaction. The Tyr1113 residue in the C-terminal end loop of the Tie2 kinase domain was mapped and found to be required for this interaction. Moreover, mutation of this residue into Phe impaired both the Tie2-calmodulin interaction and calcium-mediated Tie2 dephosphorylation. Furthermore, expressing a mutant Tie2 incapable of binding to calmodulin or inhibiting calmodulin function in vivo causes unchecked growth of the vasculature in *Xenopus*. Specifically, knockdown of Tie2 in *Xenopus* embryo retarded the sprouting and extension of intersomitic veins. Although human Tie2 expression in the Tie2-deficient animals almost completely rescued the retardation, the Tie2(Y1113F) mutant caused overgrowth of intersomitic veins with strikingly complex and excessive branching patterns.

Conclusions—We propose that the calcium/calmodulin-dependent negative regulation of Tie2 can be used as an inhibitory signal for vessel growth and branching to build proper vessel architecture during embryonic development. (*Arterioscler Thromb Vasc Biol.* 2016;36:1406-1416. DOI: 10.1161/ATVBAHA.116.307619.)

Key Words: angiogenesis ■ calcium ■ calmodulin ■ embryogenesis ■ Tie2

During embryogenesis, vascular network formation depends on 2 distinct and sequential processes. The first is vasculogenesis, wherein endothelial progenitor cells differentiate, migrate, and coalesce to form the primordial vessels and heart.¹ This is followed by angiogenesis, in which endothelial cells in the primordial vessels sprout and branch, forming the complex vascular system.¹ A key regulator of these events is the receptor tyrosine kinase Tie2, which is expressed exclusively in endothelial cells.^{2,3} Genetically inhibiting Tie2 in mice impairs vasculogenesis by decreasing proliferation and survival of the endothelial cells.⁴ In addition, Tie2 knock-out mice exhibit significant defects in angiogenesis, such as reduced capillary sprouting in the head region and indistinct large and smaller blood vessels.⁵ In contrast, increasing the Tie2 activity by overexpressing its agonistic ligand, angiopoietin-1 (Ang1),⁶ in the skin increases the number, size, and

branching of blood vessels in mice.⁷ Meanwhile, overexpressing the antagonistic ligand, Ang2, phenocopies the loss of Tie2 function.⁸ Therefore, Ang/Tie2 signaling plays a pivotal role in formation of the vascular network during development.

In adult vasculature, modulation of Tie2 signaling is essential for vessel remodeling, especially in pathological conditions.⁹ Notably, rapidly growing tumors release angiogenic factors and promote vessel growth toward themselves to maintain a constant supply of oxygen and nutrients. Improper blood vessel remodeling is also key to eye diseases, such as age-related macular degeneration and diabetic retinopathy.¹⁰ In addition, during sepsis, impaired vessel integrity increases the permeability of immune cells, leading to systematic inflammation.¹¹⁻¹³ Because enhancing the vessel-stabilizing effect of Tie2 signaling might be beneficial to the treatment of these diseases, many research laboratories and pharmaceutical

Received on: November 17, 2015; final version accepted on: May 5, 2016.

From the Department of Life Sciences, Korea University, Seoul, Republic of Korea (C.Y., J.Y.L., E.J.K., J.K., C.K.); School of Biological Sciences, Seoul National University, Seoul, Republic of Korea (C.Y., D.P.); Department of Anatomy, Brain Research Institute, and Brain Korea 21 PLUS Project for Medical Science, Yonsei University College of Medicine, Seoul, Republic of Korea (J.O., H.J.); and Center for Vascular Research, Institute for Basic Science, Daejeon, Korea (S.H.).

*These authors contributed equally to this article.

The online-only Data Supplement is available with this article at <http://atvb.ahajournals.org/lookup/suppl/doi:10.1161/ATVBAHA.116.307619/-DC1>. Correspondence to Hosung Jung, Department of Anatomy, Yonsei University College of Medicine, Seoul 120-752, Republic of Korea. E-mail hosungjung@yonsei.ac.kr; or Chungho Kim, Department of Life Sciences, Korea University, Seoul 136-701, Republic of Korea. E-mail chungho@korea.ac.kr

© 2016 American Heart Association, Inc.

Arterioscler Thromb Vasc Biol is available at <http://atvb.ahajournals.org>

DOI: 10.1161/ATVBAHA.116.307619

This work was published in *Arterioscler. Thromb. Vasc. Biol.* 2016 Jul;36(7):1406-1416.

Study on the Mechanism of Tie2 Signaling by Ca²⁺/Calmodulin in Angiogenesis

Chansik Yang

School of biological sciences

The graduate school

Seoul National University

Angiogenesis, the process of building complex vascular structures, begins with sprout formation on preexisting blood vessels, followed by extension of the vessels through proliferation and migration of endothelial cells. Based on the potential therapeutic benefits of preventing angiogenesis in pathological conditions, many studies have focused on the mechanism of its initiation as well as control. However, how the extension of vessels is terminated remains obscure. Thus, I investigated the negative regulation mechanism.

I report that increased intracellular calcium can induce dephosphorylation of the endothelial receptor tyrosine kinase Tie2. The calcium-mediated dephosphorylation was found to be dependent on Tie2-calmodulin interaction. The Tyr1113 residue in the C-terminal end loop of the Tie2 kinase domain was mapped and found to be required for this interaction. Moreover, mutation of this residue into Phe impaired both the Tie2-calmodulin interaction and calcium-mediated Tie2 dephosphorylation. Furthermore, expressing a mutant Tie2 incapable of binding to calmodulin or inhibiting calmodulin function in vivo causes unchecked growth of the

vasculature in *Xenopus*. Specifically, knockdown of Tie2 in *Xenopus* embryo retarded the sprouting and extension of intersomitic veins. Although human Tie2 expression in the Tie2-deficient animals almost completely rescued the retardation, the Tie2(Y1113F) mutant caused overgrowth of intersomitic veins with strikingly complex and excessive branching patterns.

I propose that the calcium/calmodulin-dependent negative regulation of Tie2 can be used as an inhibitory signal for vessel growth and branching to build proper vessel architecture during embryonic development.⁴⁾

Key Words : angiogenesis, calcium, calmodulin, embryogenesis, Tie2
Student Number : 2013-20302

4) All of contents in here published in *Arterioscler. Thromb. Vasc. Biol.* 2016 Jul;36(7):1406-1416 and I participated as a main author.

INTRODUCTION

During embryogenesis, vascular network formation depends on 2 distinct and sequential processes. The first is vasculogenesis, wherein endothelial progenitor cells differentiate, migrate, and coalesce to form the primordial vessels and heart (Herbert SP *et al.*, 2011). It is followed by angiogenesis, in which endothelial cells in the primordial vessels sprout and branch, forming the complex vascular system (Herbert SP *et al.*, 2011). A key regulator of these events is the receptor tyrosine kinase Tie2, which is expressed exclusively in endothelial cells (Jeltsch M *et al.*, 2013; Augustin HG *et al.*, 2009). Genetically inhibiting Tie2 in mice impairs vasculogenesis by decreasing proliferation and survival of the endothelial cells (Dumont DJ *et al.*, 1994). In addition, Tie2 knockout mice exhibit significant defects in angiogenesis, such as reduced capillary sprouting in the head region and indistinct large and smaller blood vessels (Sato TN *et al.*, 1995). In contrast, increasing the Tie2 activity by overexpressing its agonistic ligand, angiopoietin-1 (Ang1) (Davis S *et al.*, 1996), in the skin increases the number, size, and branching of blood vessels in mice (Suri C *et al.*, 1998). Meanwhile, overexpressing the antagonistic ligand, Ang2, phenocopies the loss of Tie2 function (Maisonpierre PC *et al.*, 1997). Therefore, Ang/Tie2 signaling plays a pivotal role in formation of the vascular network during development.

In adult vasculature, modulation of Tie2 signaling is essential for vessel remodeling, especially in pathological conditions (Jeltsh M *et al.*, 2013; Koh GY *et al.*, 2013). Notably, rapidly growing tumors release angiogenic factors and promote vessel growth toward themselves to maintain a constant supply of oxygen and nutrients. Improper blood vessel remodeling is also key to eye diseases, such as age-related macular degeneration and

diabetic retinopathy (Ferrara N *et al.*, 2004). In addition, during sepsis, impaired vessel integrity increases the permeability of immune cells, leading to systematic inflammation (Thomas M *et al.*, 2009; Ziegler T *et al.*, 2013; Fiedler U *et al.*, 2006). Because enhancing the vessel-stabilizing effect of Tie2 signaling might be beneficial to the treatment of these diseases, many research laboratories and pharmaceutical companies are working toward developing drugs, which can modulate Tie2 activity (Wu FT *et al.*, 2015; Lee J *et al.*, 2013; Holopainen T *et al.*, 2012; Koh YJ *et al.*, 2010).

Despite the importance of Tie2 regulation in both embryonic vascular development and pathological angiogenesis, negative regulatory mechanisms of the receptor have not been elucidated. Dephosphorylation of Tie2 by tyrosine phosphatases, such as Src homology region 2-containing protein tyrosine phosphatase-2 (SH-PTP2) and vascular endothelial protein tyrosine phosphatase (VE-PTP), has been suggested previously (Fachinger G *et al.*, 1999; Huang L *et al.*, 1995). However, what controls such dephosphorylation remains largely unknown.

Here I show that increased intracellular calcium in endothelial cells induces dephosphorylation of Tie2. I also demonstrate that the calcium-mediated Tie2 dephosphorylation depends on Tie2-calmodulin interaction. Disrupting this interaction during embryogenesis leads to uncontrolled vessel growth and branching. Thus I propose that the calcium/calmodulin-dependent negative regulation of Tie2 acts as a developmental brake for vessel outgrowth to build a proper vascular network.

MATERIALS AND METHODS

Plasmids and reagents

FLAG-human Tie2 (hTie2) cDNA and human Tie2-GFP construct in lentivirusvector (FuGW/Tie2-GFP) were kindly provided by Dr. Gou-Young Koh (Korea Advanced Institute of Science and Technology). Calmodulin cDNA was purchased from Korea Human Gene Bank (Clone ID : hMU000001) and used to generate HA-tagged calmodulin. The Tac-Tie2 construct, a fusion of the extracellular domain of Tac (Interleukin-2 receptor α) and transmembrane-cytoplasmic domain of hTie2, was generated by overlapping polymerase chain reaction (PCR) using the primers IL-2Ra_ *Hind*III (F)(5'-gggtcaagcttatggattcatacctgctg-3'), Tac-Tie2 (R)(5'-gaggtccgctggtgcttgctctgttgtaaataatgga-3'), Tac-Tie2 (F)(5'-tccatatttacaacagagcaagcaccagcggacctc-3'), and Tie2-*Xba*I (R)(5'-tgttctagactaggccgcttcttcagc-3'). The Tac-Tie2 fused PCR product was digested with *Hind*III and *Xba*I and cloned into pcDNA3.1. Tac-Tie2 construct was used as template for site-specific mutagenesis to generate stop mutants, Tac-Tie2 Δ 840, Tac-Tie2 Δ 879, and Tac-Tie2 Δ 909. The FLAG-Tie2 Δ ECD construct was previously described (Kim C *et al.*, 2011). It was used to generate the Y992F, 1102F, 1108F, 1113F, 1113E, and Δ 1102 mutant constructs by site-specific mutagenesis. The α IIBTM-TAP construct was previously described (Kim C *et al.*, 2012). The calcium ionophore A23187 (Cat. C7522), W-7 (Cat. A3281), and proximity ligation assay kit (Cat. DUO92101) were purchased from Sigma-Aldrich. Anti-FLAG (M2; Sigma-Aldrich), anti-Tie2 (against intracellular domain; Santa Cruz Biotechnology, Inc., Cat. SC-324), anti-Tie2 (against extracellular domain; clone Ab33; Merck Millipore Corporation, Cat.05-584), anti-Tie2 (phospho-Y992; Abcam, Cat. ab151704), anti-RPTP ξ (BD bioscience, Cat. 610180), anti-Akt (Cell Signaling Technology, Cat. 9272),

anti-phospho-Akt(Ser473) (Cell Signaling Technology, Cat. 4051), anti-calmodulin antibody (Merck Millipore Corporation, Cat. 05-173), anti-ERK (Cell Signaling Technology, Cat. 4695), anti-phospho-ERK (Cell Signaling Technology, Cat. 9101), and anti-phosphotyrosine (4G10; Merck Millipore Corporation, 05-321) antibodies were purchased from commercial sources. Tie2 antisense morpholino (Tie2 MO), 5'-atggtttccacaatctctccatcca-3'; and Control MO, 5'-atggtttccacaatctctccatcca-3' conjugated to fluorescein were purchased from Gene-Tools (Philomath, OR, USA).

Cell culture, transfection, and pull-down experiments

Human embryonic kidney 293T cells (HEK293T) and Chinese hamster ovary (CHO) cells were maintained in Dulbecco's modified Eagle's medium supplemented with 10% fetal bovine serum (FBS), 1% penicillin, and 1% non-essential amino acids in a 5% CO₂ incubator at 37°C. For transfection, 10 µg cDNA was introduced into HEK293T cells using Lipofectamine LTX and Plus reagent (Life technologies) according to the manufacturer's guidelines. After 24 h, the cells were washed twice with ice-cold phosphate-buffered saline (PBS) and lysed by lysis buffer A (20 mM HEPES pH 7.4, 150 mM NaCl, 1% Triton-X 100, 2 mM CaCl₂, protease inhibitor cocktail (Roche), phosphatase inhibitor cocktail (Roche)). The lysates were clarified by centrifugation and the supernatants mixed with 20 µL of 50% calmodulin Sepharose (GE Healthcare). The clarified lysates with beads were incubated overnight at 4°C with agitation. The bound proteins were then analyzed by sodium dodecyl sulfate polyacrylamide gel electrophoresis (SDS PAGE) and western blotting. Lentivirus were generated and infected to make stable cell lines as previously described (Kim C *et al.*, 2012).

Immunoprecipitation

HEK293T cells were transfected with either Tie2 Δ ECD or its mutants using either Lipofectamine LTX and Plus reagent or polyethylenimine. After 24 h, the cells were starved for serum for 12 h and then treated with 10 μ M calcium ionophore for 10 min and/or 200 μ M W-7. For investigating effects of divalent cation-dependent dephosphorylation, cells transfected with Tie Δ ECD and HA-tagged calmodulin were serum-starved as above, washed twice with Tyrode's buffer (140 mM NaCl, 2.7 mM KCl, 0.4 mM sodium phosphate monobasic, 10 mM NaHCO₃, 5 mM Dextrose and 10 mM HEPES, pH 7.4) without divalent cations, and treated ionophore in the presence of 2 mM CaCl₂, MnCl₂, or MgCl₂ in Tyrodes buffer. Next, the cells were washed twice with ice-cold PBS before being lysed by lysis buffer B (20 mM HEPES pH 7.4, 150 mM NaCl, 1% Triton-X 100, 1 mM EDTA, protease inhibitor cocktail, phosphatase inhibitor cocktail). The lysates were clarified by centrifugation, mixed with anti-FLAG antibody and protein G agarose (Pierce), and incubated overnight at 4°C. The bead-bound proteins were analyzed by SDS-PAGE and western blotting with anti-Tie2 and anti-phosphotyrosine antibodies.

For immunoprecipitation of endogenous Tie2 in HUVECs, cells were starved for serum for 6 h and then treated with 10 μ M calcium ionophore and/or 200 ng/ml Ang1 as indicated. Clarified cell lysates in lysis buffer B were incubated overnight with anti-Tie2 extracellular domain antibody (clone Ab33) and further incubated with protein G agarose for 4 h at 4°C. The bead-bound proteins were analyzed by western blotting with anti-Tie2 (phospho-Y992) antibody and subsequently with anti-Tie2 intracellular domain antibody (conjugated with horse radish peroxidase).

Immunocytochemistry

Human umbilical vein endothelial cells (HUVECs) were maintained in

EGMTM-2 endothelial cell growth medium-2 (Lonza). HUVECs grown on 0.1% gelatin-coated cover glasses were starved for serum by incubating in EBMTM-2 endothelial basal medium containing 0.5% FBS for 1 day. Next, the cells were stimulated with 500 ng/mL Ang1 (R&D Systems, Cat. 923-AN-025) and/or 10 μ M calcium ionophore for 15 min, and fixed with 3.7% formaldehyde in Dulbecco's phosphate-buffered saline (DPBS, Hyclone, SH30243.01). Cells were then blocked with blocking solution (0.1%gelatin, 10% normal goat serum, 0.1% triton X-100 in PBS), and stained with anti-Tie2 (phospho-Y992; Abcam) and anti-Tie2 (against extracellular domain; clone Ab33) followed by staining with rhodamine-conjugated anti rabbit IgG and fluorescein isothiocyanate-conjugated anti mouse IgG antibodies. For proximity ligation assay (PLA), HUVECs grown on 0.1% gelatin-coated cover glasses were washed with ice-cold DPBS and fixed with 3.7% formaldehyde in DPBS. Tie2-calmodulin interaction was monitored according to manufacturer's instruction using anti-Tie2 (against intracellular domain; Santa Cruz Biotechnology, Inc.) antibody (or normal rabbit IgG as a control) and anti-calmodulin antibody. The stained cells were mounted on slide glasses with mounting medium (Dako), and the fluorescent images were acquired by a fluorescence microscope (Ti-E, Nikon) equipped with 100X (1.4 N.A) Plan-Apochromat objective lens and charge-coupled camera device (DS-Qi2, Nikon).

Embryonic angiogenesis assay in *Xenopus*

Xenopus tropicalis embryos were prepared by in vitro fertilization, raised in 0.1X Modified Barth's Saline (MBS) at 21 - 24 °C, and staged according to the tables of Nieuwkoop and Faber (1967) (Nieuwkoop PD *et al.*, 1967). For loss-of-function studies, injections of 4 ng of either Tie2 (5'-ATGGTTTCCACAATCTCTCCATCCA-3') or control MO (5'-CCTCTTA-

CCTCAGTTACAATT-TATA-3') were injected to one blastomere at the two-cell stage. For rescue experiments, 600 pg of control (mCherry), hTie2 or hTie2(Y1113F) RNA, transcribed in vitro with the mMACHINE mMACHINE kit (Ambion), was co-injected with the MOs conjugated to fluorescein (which was used as a tracer and an injection control). Total amounts of MO and RNA were identical in all groups. Embryos exhibiting a similar level of green fluorescence were selected and analyzed for vascular phenotypes. For the calmodulin inhibitor W-7 experiments, normally developing embryos were treated with 50 μ M W-7 or vehicle (methanol) from stage 33 to stage 42. For the experiment to confirm the binding of *Xenopus* Ang1 to human Tie2, *Xenopus* Ang1 cDNA clone (IMAGE clone5513391) or control plasmid (pcDNA3.1) was transfected into HEK293T cells using FuGENE® 6 Transfection Reagent (Promega E2693) according to the manufacturer's instructions. After 6 hours, culture medium was replaced with serum-free OPTI-MEM (Gibco 31985-070). The conditioned medium was collected every 24 hours for 72 hours. 24 ml of medium collected from Ang1- or control plasmid-transfected cells was concentrated using Amicon Ultra-15 Centrifugal Filter device (Millipore UFC903024) according to the manufacturer's instructions.

Vasculature labeling with low density lipoprotein from human plasma, acetylated, DiI complex (DiI-AcLDL)

Either stage 37/8 or 42 embryos, anesthetized in tricaine mesylate (MS222) solution (0.4 mg/mL in 0.1X MBS), were placed in a mold made of Sylgard 184 (Sigma-Aldrich). DiI-AcLDL (50 - 80 nL; Life Technologies) was injected into the heart of each embryo, which were then fixed for 2 h with 4% paraformaldehyde in PBS. The fixed embryos were imaged under either a fluorescence dissection or a confocal microscope (LSM700, Zeiss)

equipped with a 20X Plan-Apochromat objective(numerical aperture 0.8). To obtain a high resolution image spanning the entire body of an embryo, we used the tile scan function of LSM700.

RESULTS

Raising concentration of intracellular calcium decrease Tie2 phosphorylation

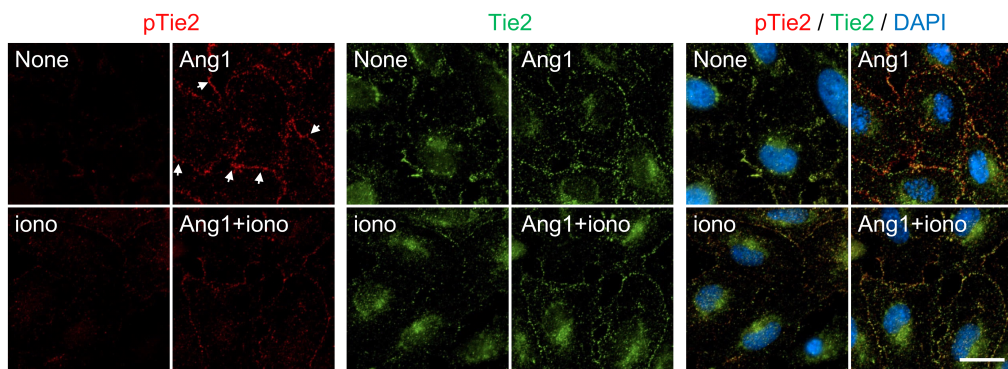
To investigate a possible connection between calcium and Tie signaling, I treated human umbilical vein endothelial cells (HUVECs) with Ang1 (an agonistic ligand of Tie2) and calcium ionophore. I then visualized Tie2-phosphorylation using an antibody that specifically detects the phosphorylated form of Tie2. Compared with untreated controls, Ang1-treated cells were clearly stained for phosphorylated Tie2, particularly at the cell-cell contact regions (Figure 1A). This observation agrees with previous reports that Ang1 and Tie2 form complexes at cell-cell contacts (Saharinen P *et al.*, 2008; Fukuhara S *et al.*, 2008). Treatment with calcium ionophore caused retraction of the cells, leading to loss of cell-cell contacts (Figure 2A and Figure 2B). This pattern of responses was more evident when Tie2 expression was increased in HUVECs by infecting them with lentivirus encoding Tie2 fused with green fluorescent protein (Tie2-GFP) (Figure 2C). This result indicates that intracellular calcium and Ang1 can antagonistically regulate Tie2 phosphorylation. Subsequent biochemical analysis also showed that calcium ionophore reduces Ang1 dependent Tie2 phosphorylation (Figure 1B, lane 2 and lane 4). Therefore, I concluded that increased intracellular calcium levels negatively regulate Tie2 phosphorylation.

Next, to investigate the molecular mechanism underlying the calcium-induced Tie2 dephosphorylation, I used a constitutively active form of Tie2 Δ ECD (Kim C *et al.*, 2011), expressed in human embryonic kidney 293T cells (HEK293T). The Tie2 mutant lacking the extracellular domain

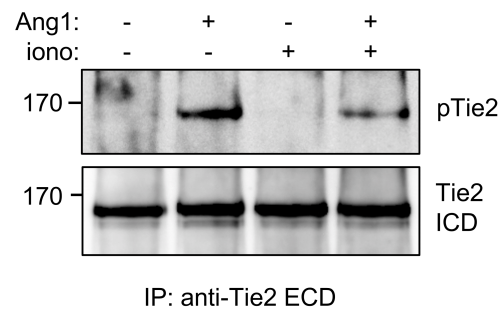
Figure 1. Treatment of calcium ionophore dephosphorylates endogenously expressed Tie2 in HUVEC.

A, Human umbilical vein endothelial cells (HUVECs) grown on coverslips were starved for serum, treated with 0.5µg/ml Ang1 and 10 µmol/L calcium ionophore for 15minutes as indicated, and subsequently stained with a phospho-specific Tie2-pY992 antibody (red) and an anti-Tie2 extracellular domain (anti-Tie2 ECD) antibody (green). Phosphotyrosine staining pattern in cell-cell contact regions is evident in Ang1-treated cells (arrows), but co-treatment with ionophore reduced the staining in the region. Scale bar, 10µm. **B**, Subconfluent HUVECs were starved for serum and stimulated with Ang1 and calcium ionophore as indicated. The degree of Tie2 phosphorylation in these cells was analyzed by immunoprecipitation using anti-Tie2 ECD antibody and Western blot using the phospho-specific Tie2-pY992 antibody (top). Equal amounts of precipitated Tie2 in each condition were also analyzed using anti-Tie2 intracellular domain (ICD) antibody (bottom)

A



B

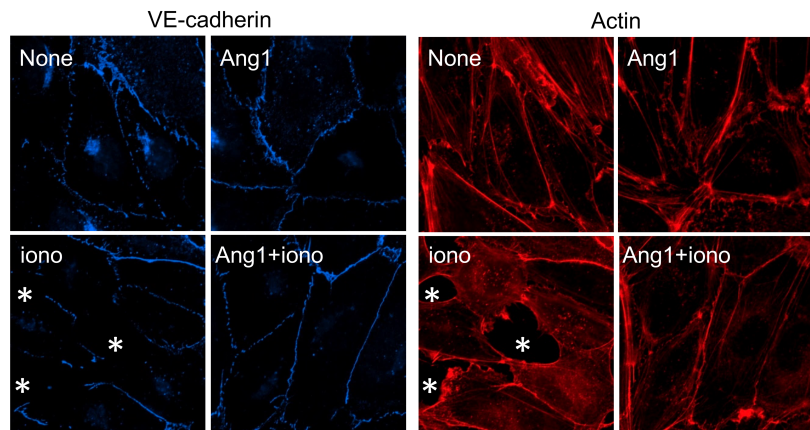


(ECD) was properly targeted to the cell surface (Figure 3) and exhibited a high level of ligand-independent phosphorylation (Figure 4A, lane 2) as previously reported (Kim C *et al.*, 2011). It may be attributed to its propensity to dimerize, even in the absence of a ligand, through its coiled-coil domain in the membrane proximal region of the Tie2 cytoplasmic tail (Kim C *et al.*, 2011). Unlike the endogenous Tie2 protein expressed in HUVECs, however, calcium ionophore treatment did not reduce the phosphorylation of Tie2 Δ ECD, ectopically expressed in HEK293T cells (Figure 1C, lane 3). I reasoned that this might result from the amount of ectopically expressed Tie2 molecules, which exceeds the relatively lower amount of, if any, an endogenously expressed calcium effector molecule. In agreement with this idea, when expression of the Tie2 Δ ECD decreased, phosphotyrosine levels were reduced by calcium ionophore in HEK293T cells (Figure 5). In addition, co-expression of a calcium effector protein, calmodulin, with Tie2 Δ ECD in HEK293T cells fully restored calcium-mediated reduction of tyrosine phosphorylation (Figure 4A, lane 5), indicating that calmodulin can work as a calcium effector mediating the calcium-induced Tie2 dephosphorylation. The reduction of Tie2 phosphorylation by calcium ionophore is calcium-specific because it did not occur when extracellular calcium ion was replaced with magnesium or manganese ion (Figure 4B). I also found that W-7, a calmodulin antagonist that inhibits calcium-dependent interaction between calmodulin and its target (Osawa M *et al.*, 1998), inhibits the ionophore-induced Tie2 dephosphorylation (Figure 4C), indicating that calmodulin mediates calcium-induced Tie2 dephosphorylation.

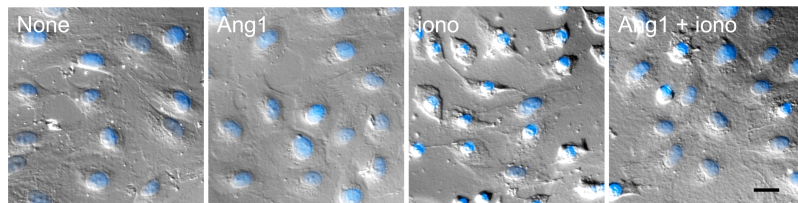
Figure 2. Effects of calcium ionophore and Ang1 treatment on HUVECs

A, HUVECs were grown on cover slips, starved for serum, and treated with angiopoietin-1(Ang1) and/or calcium ionophore. Those cells were stained with anti-VE-cadherin (blue) and phalloidin (red). Empty areas not covered by cells (indicated with asterisks) were noticeably increased in ionophore-treated HUVEC monolayer. Scale bar, 10 μ m. **B**, Differential interference contrast images of HUVECs treated as in A were shown. Scale bar, 10 μ m. **C**, HUVECs infected with lentivirus encoding GFP-fused Tie2 (Tie2-GFP) were treated as in **A**, and stained with a phospho-specific Tie2-pY992 antibody (red). Fluorescence from Tie2-GFP is shown as green. Scale bar, 10 μ m.

A.



B.



C.

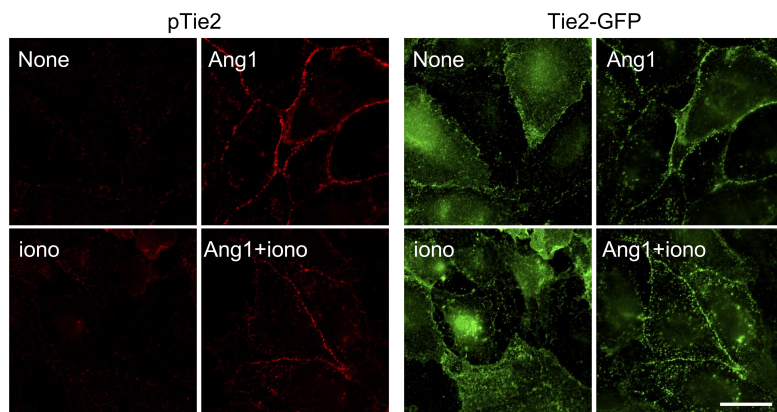


Figure 3. Characterization of FLAG-Tie2ΔECD.

FLAG-Tie2ΔECD was transfected into HEK293T cells with pEGFP-C1 as a transfection marker. 24 h after transfection, cells were detached and stained with anti-FLAG antibody and subsequently anti-mouse IgG conjugated with allophycocyanin. GFP-positive cells were gated and the degree of anti-FLAG antibody binding was shown as histogram. RLU, relative light unit.

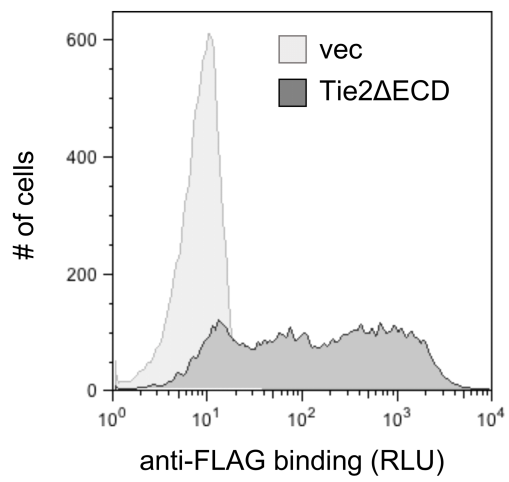
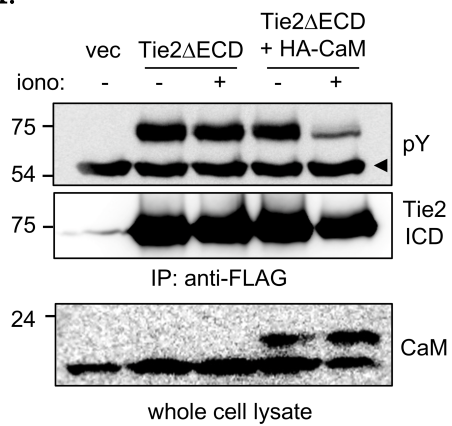


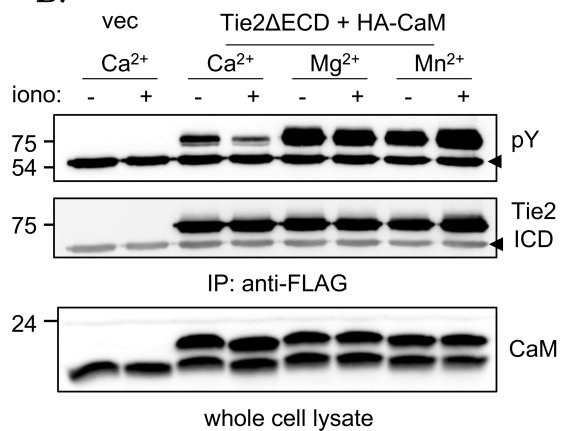
Figure 4. Calcium- and calmodulin-dependent dephosphorylation of Tie2.

A, FLAG-tagged Tie2 Δ ECD (extracellular domain-deleted Tie2 construct, FLAG-Tie2 Δ ECD) was transfected into human embryonic kidney 293T (HEK293T) cells with or without HA-tagged calmodulin (HA-CaM). Cells were treated with calcium ionophore, FLAG-Tie2 Δ ECD was immunoprecipitated (IP) by anti-FLAG antibody, and the phosphotyrosine level was measured by Western blotting (WB) using anti-phosphotyrosine antibody (anti-pY, upper panel). The membrane was reprobbed with horseradish peroxidase (HRP)-conjugated anti-Tie2 antibody to examine the degree of Tie2 precipitation in each condition (middle). Calmodulin expression in whole cell lysates was monitored by Western blotting using anti-calmodulin antibody (lower). Both endogenous (lower) and overexpressed HA-tagged (upper) calmodulin are visible. **B**, HEK293T cells transfected with FLAG-Tie2 Δ ECD and HA-CaM were starved for serum and incubated in the presence of divalent cations as described in Materials and Methods. The degree of phosphorylation of FLAG-Tie2 Δ ECD was analyzed as in **A**. **C**, HEK293T cells transfected with FLAG-Tie2 Δ ECD and HA-CaM were treated with ionophore alone or together with an calmodulin antagonist, W-7. Arrowheads in **A**, **B**, and **C** indicate immunoglobulin heavy chain.

A.



B.



C.

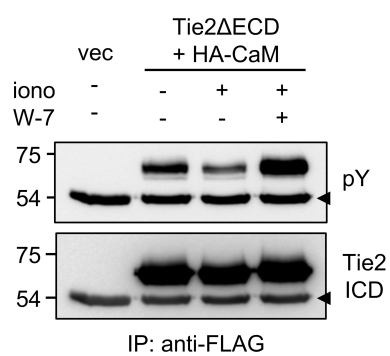
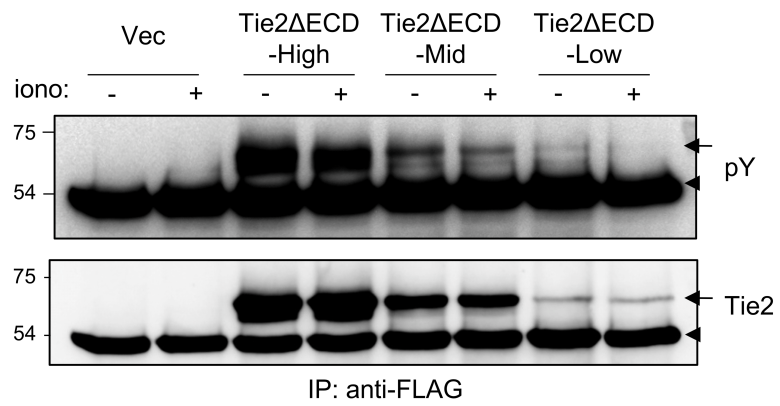


Figure 5. Effects of calcium ionophore on phosphorylation of FLAG-Tie2 Δ ECD expression level

Decreasing amounts (High, Mid Low) of FLAG-Tie2 Δ ECD were transfected into HEK293T cells, and the degrees of phosphorylation of FLAG-Tie2 Δ ECD were analyzed as in **Figure 4A**. Note that dephosphorylation of Tie2 becomes evident in cells with low amount of Tie2 expressed. Arrows and arrow heads indicate Tie2 Δ ECD and immunoglobulin heavy chains, respectively.



Calmodulin binds to C-terminal region of the Tie2 cytoplasmic Tail

Calmodulin relay calcium signaling by binding to and regulating the activity of their partners in a calcium-dependent manner (Berridge MI *et al.*, 2003). Having established that calcium-dependent dephosphorylation of Tie2 requires calmodulin (Figure 4A), I asked whether calmodulin binds to Tie2. I found that Tie2 expressed in HEK293T cells binds to calmodulin-conjugated (but not control) beads (Figure 6A), indicating that Tie2 and calmodulin may form a complex. Proximity ligation assay performed in HUVECs using antibodies against calmodulin and Tie2 also suggested that Tie2 and calmodulin form complexes in physiological conditions (Figure 7). By deletion mutants studies of Tie2 cytoplasmic lobe, I observed that calmodulin specifically binds to the cytoplasmic domain of Tie2 (not shown). To pinpoint the calmodulin-binding site in Tie2, I hypothesized that tyrosine residues in the C-terminal loop are involved in calmodulin binding. To test this, I mutated 3 tyrosine residues, Y992, Y1108, and Y1113, in the C-terminal loop (Figure 6B) into phenylalanine (F) and measured the calmodulin binding. Y1113F dramatically reduced the binding, showing that this residue is critical for the Tie2-calmodulin interaction. Introduction of the negatively charged glutamic acid (E) at the Tyr1113 site also reduced its binding to calmodulin (not shown), suggesting that any modification of the Tyr1113 residue inhibits calmodulin binding.

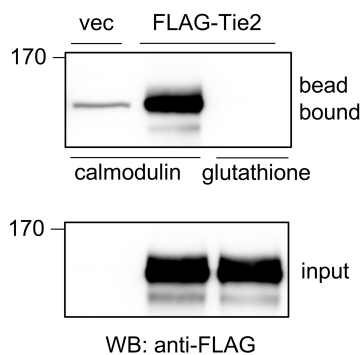
A close examination of the crystal structure of the Tie2 kinase domain revealed that the hydroxyl group in the side chain of the Tyr1113 residue forms a hydrogen bond with the backbone amino group of Leu920 (Figure 6C). This places the phenyl ring of Tyr1113 in the hydrophobic pockets formed by neighboring amino acids (Shewchuck LM *et al.*, 2000). This

interaction positions the C-terminal loop region near the C-terminal lobe of the kinase domain. The possibility that Tyr1113 is the direct binding interface between Tie2 and calmodulin cannot be rule out. However, the position of the hydroxyl group of the Tyr residue inside the hydrophobic pocket, in all crystal structures published to date, suggests that the conformation of the C-terminal loop itself is more likely to be responsible for calmodulin interaction. Therefore, either absence of the hydroxyl group on the aromatic ring (in case of Y1113F) or presence of the bulky and negatively charged residue (in case of Y1113E) might displace the C-terminal loop region away from the C-terminal lobe of the kinase domain, as suggested previously (Shewchuk LM *et al.*, 2000; Niu XL *et al.*, 2002). I reason that this structural change might prevent calmodulin binding in Y1113F mutant.

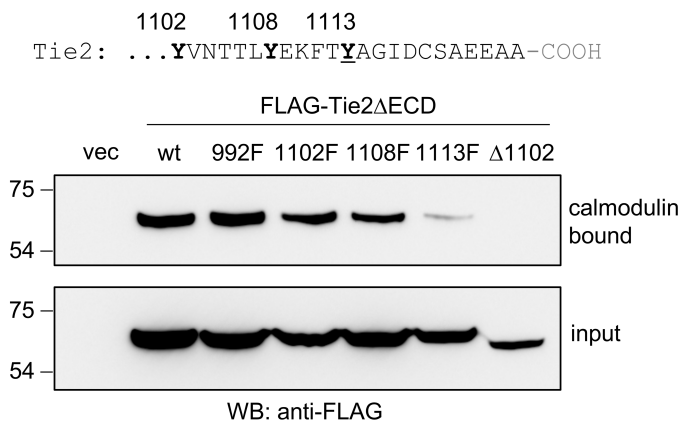
Figure 6. Interaction between Tie2 and calmodulin.

A, FLAG-tagged Tie2 was expressed in HEK293T cells (input), and its binding to calmodulin-conjugated Sepharose beads was analyzed, with glutathione Sepharose beads binding as negative control. **B**, Amino acid sequence of the C-terminal end of Tie2 is shown. FLAG-Tie2 Δ ECD constructs containing either tyrosine-to-phenylalanine mutation (Y992F, Y1102F, Y1108F, or Y1113F) or C-terminal deletion (Δ 1102) were transfected into HEK293T cells, and their binding to calmodulin was analyzed as in **A**. **C**, Structural model of the Tie2 kinase domain is shown, focusing on the C-terminal loop region (indicated in red). Note that the hydroxyl group in the side chain of Tyr1113 forms a hydrogen bond (arrow) with the backbone amino group of Leu920. The hydrogen bond is indicated with green dotted line.

A.



B.



C.

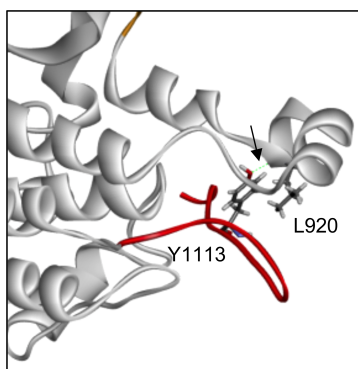
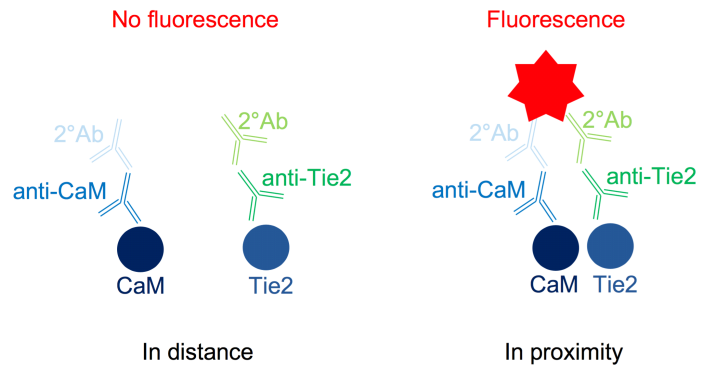


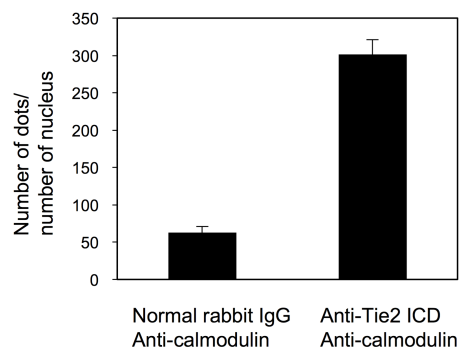
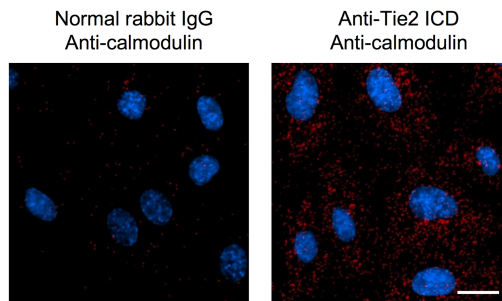
Figure 7. Endogenous Tie2-calmodulin interaction in HUVECs.

A, Schematic diagram of proximity ligation assay (PLA). When two antigens are close enough (left), two different oligonucleotides attached to species-specific secondary antibodies can be ligated, which in turn can be polymerized resulting in red fluorescence. **B**, HUVECs grown on gelatin-coated coverslips were fixed with 3.7% formaldehyde, and stained with anti-calmodulin antibody and anti-Tie2 intracellular domain (ICD) antibody (or its isotype control, normal rabbit IgG). Then, the cells were further incubated with secondary antibodies against anti-mouse and anti-rabbit antibody conjugated with Duolink™ PLA probes. The colocalization of two proteins was visualized by subsequent ligation/amplification reactions according to the manufacture's instruction. The PLA fluorescence (red) and nucleus staining (blue) were show. Scale bar, 10 μm. **C**, The numbers of red dots in three random microscopic fields in two independent experiments were counted, and the numbers of red dots divided by number of nucleus in each images were calculated and shown as bars ± standard errors (n=6).

A.



B.



Tie2-Calmodulin interaction is required for calcium-mediated Tie2 inactivation

Having identified the mutation that disrupt the Tie2-calmodulin interaction, I used a calmodulin binding-defective Tie2 mutant to test the importance of this interaction in calcium-mediated Tie2 inactivation. To this end, I transfected HEK293T cells with the constitutively active Tie2 Δ ECD construct, containing either the wild-type sequence or Y1113F mutation, treated them with calcium ionophore, and measured the phosphotyrosine levels in the immunoprecipitated Tie2 proteins. In contrast to wild-type Tie2, whose phosphorylation was significantly decreased by calcium ionophore (Figure 8A and 8B), the calmodulin binding-defective Y1113F mutant was resistant to calcium ionophore-induced dephosphorylation (Figure 8A and 8B). These results indicate that together with the requirement for calmodulin expression in calcium-dependent inactivation of Tie2 (Figure 4A), binding of calmodulin to the Tie2 C-terminal loop is essential for calcium-mediated Tie2 inactivation. Next, by using lentiviruses encoding the full length, wild-type Tie2 or the Y1113F mutant fused to GFP to its C-terminus, I generated CHO cells stably expressing either Tie2-GFP or Tie2(Y1113F)-GFP (Figure 9A and 9B) and investigated whether the Y1113F mutation affects Ang1-dependent Tie2 signaling. Ang1 increased phosphorylation of Akt and extracellular signal-regulated kinase (ERK) both in cells expressing the wild-type and mutant Tie2 (Figure 9C). However, the basal level of Akt and ERK phosphorylation were higher in cells expressing Tie2(Y1113F)-GFP than the wild-type Tie2-GFP-expressing cells (Figure 9C lane 5), suggesting that the basal activity of Tie2 may be suppressed by a calcium- and calmodulin-dependent mechanism. This is consistent with my result that depleting extracellular calcium ion and thereby decreasing intracellular calcium concentration

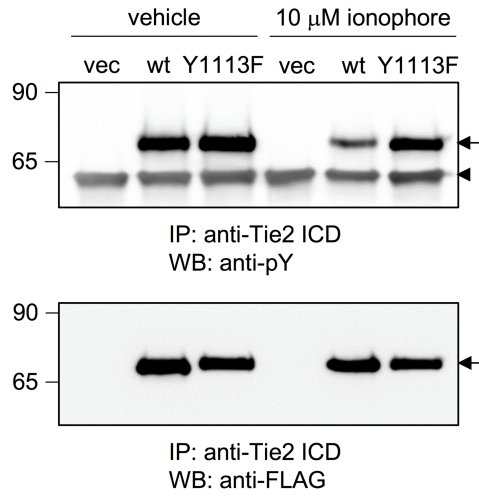
increases the basal level of phosphorylation of Tie2 Δ ECD (Figure 4B, lane 3 versus lanes 5 and 7).

Calcium binding to calmodulin causes a conformational change, which often regulates its ability to bind to its targets (Berridge MI *et al.*, 2003). Therefore, I next tested whether Tie2-calmodulin interaction is regulated by calcium. Lysate of HEK293T cells transfected with Tie2 Δ ECD was incubated with calmodulin beads in the presence of calcium as before or in the presence of calcium chelator EDTA. In the experiment, removing calcium by EDTA did not disrupt this interaction (Figure 10A, lanes 2 and 5). In sharp contrast, addition of EDTA completely abolished calmodulin binding to a nonrelevant control protein(integrin α IIb transmembrane domain-cytoplasmic tail) containing a known calcium-dependent calmodulin-binding region (Kim C *et al.*, 2009) (Figure 10A, lanes 3 and 6). These results suggest that the Tie2-calmodulin interaction is maintained independently of intracellular calcium concentrations and that calmodulin bound to Tie2 may recruit a negative regulator in a calcium-dependent manner. As VE-PTP (or receptor protein tyrosine phosphatase[RPTP] β), a member of RPTP family, is well-known as a negative regulator of Tie2 dephosphorylation (Winderlich M *et al.*, 2009), it might be a candidate responsible for the calcium-and calmodulin-dependent Tie2 dephosphorylation. However, I observed calcium-dependent Tie2 dephosphorylation not only in endothelial cells (HUVECs, Figure 1B) but also in epithelial cells (HEK293T, Figure 4A), and the expression of VE-PTP seems to be restricted to endothelial cells (Fachinger G *et al.*, 1999). Thus, I reasoned that other phosphatases capable of binding to calmodulin can also mediate calcium-induced Tie2 dephosphorylation. One possible candidate of such phosphatase I found is RPTP ζ , another member of RPTP family. The phosphatase is expressed in both endothelial and epithelial cells and interacts with calmodulin beads in a calcium-dependent

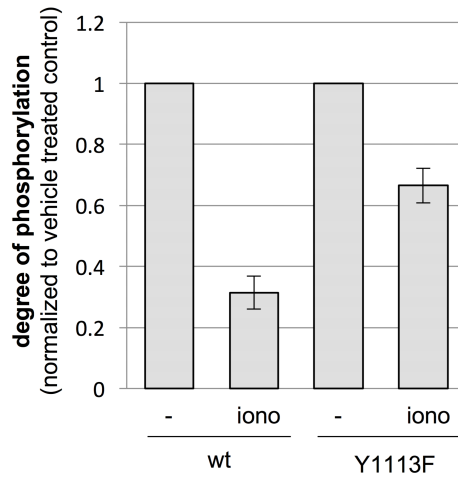
Figure 8. Effect of calcium ionophore on Tie2 mutant which defective of calmodulin bound.

A, Either wild-type or Y1113F mutant FLAG-Tie2 Δ ECD construct together with HA-calmodulin were transfected into HEK293T cells and treated with calcium ionophore as indicated. Phosphorylation of Tie2 in each condition was tested as in **Figure 4A**. **B**, The average degree of phosphorylation in calcium ionophore-treated cells compared with untreated controls is shown as a bar graph for each Tie2 construct. Error bars represent standard errors of 3 independent experiments.

A.



B.



manner (Figure 10C). However, I do not rule out the possible involvement of other tyrosine phosphatases in calcium and calmodulin-dependent Tie2 dephosphorylation. Taken, these results suggest that calcium-loaded calmodulin may recruit phosphatases, such as RPTP ζ , which mediate calcium- and calmodulin-dependent Tie2 dephosphorylation and also suggest that VE-PTP may not be the only phosphatase that can mediate Tie2 dephosphorylation.

Expressing Tie2(Y1113F) or inhibiting calmodulin function causes uncontrolled angiogenesis in vivo⁵⁾

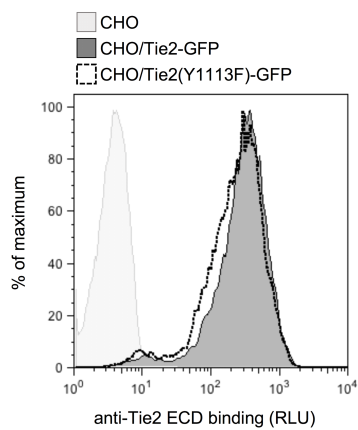
Tie2 exhibits evolutionarily conserved amino acid sequences in vertebrates (Figure 11). Particularly, the cytoplasmic domains of human and *Xenopus* Tie2 are highly conserved (94% amino acid identity and 96% similarity), and the key amino acids responsible for conformation of the C-terminal loop are identical in most vertebrates (Figure 11). To understand the importance of the calmodulin-Tie2 interaction in vivo, I used the vertebrate animal model, *Xenopus*, in which a stereotyped pattern of vascular development can be efficiently visualized using fluorescent dyes (Levine AJ *et al.*, 2003) (Figure 12A). The venous systems of zebrafish and *Xenopus* are particularly useful for studying developmental angiogenesis (Levine AJ *et al.*, 2003; Li W *et al.*, 2014). In *Xenopus*, the posterior cardinal vein (PCV) extends longitudinally at the ventral trunk region from the heart to the cloaca, and intersomitic veins (ISVs) sprout off the PCV in a rostrocaudal sequence and grow dorsally (Levine AJ *et al.*, 2003) (Figure 12B). At stage 42, the rostral-most two thirds of the ISVs can be clearly seen (Figure 12B, asterisk, and Figure 12C).

5) In this section *in vivo* experiment performed and analyzed by J. Ohk at Yeonsei Univ. Hosung Jung's lab.

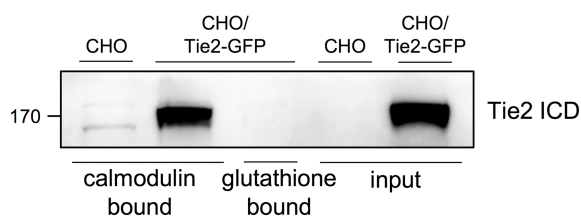
Figure 9. Effects of Y1113 mutation on Tie2 signaling.

A, Chinese hamster ovary (CHO) cells infected with lentivirus encoding Tie2-GFP or Tie2(Y1113F)-GFP, CHO/Tie2-GFP and CHO/Tie2(Y1113F)-GFP, were analyzed for the surface expression of Tie2 by flow cytometry. **B**, Lysates of CHO/Tie2-GFP cells were incubated with calmodulin (or control) beads to test whether the C-terminal fusion of GFP does not impair Tie2-calmodulin interaction. **C**, CHO/Tie2-GFP and CHO/Tie2(Y1113F)-GFP cells were starved for serum, and stimulated with 0.5 $\mu\text{g/ml}$ Ang1 for 15 minutes. Phosphorylation of Tie2, (pTie2), phosphorylation of AKT (pAKT), phosphorylation of ERK (pERK) were analyzed by western blots. The expression levels of Tie2, Akt, ERK and calmodulin (CaM) were also analyzed.

A.



B.



C.

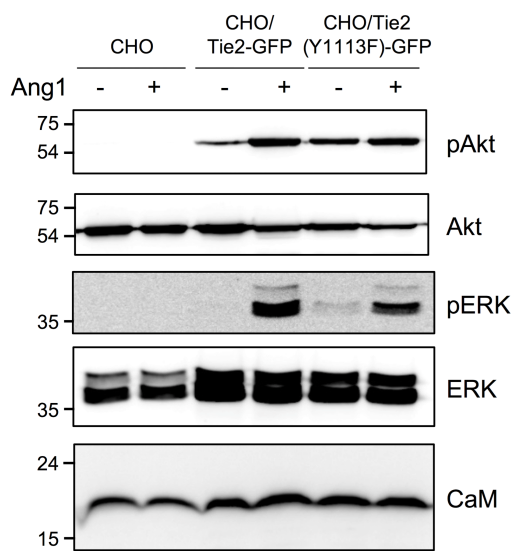
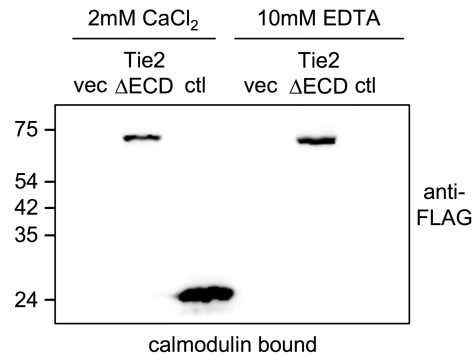


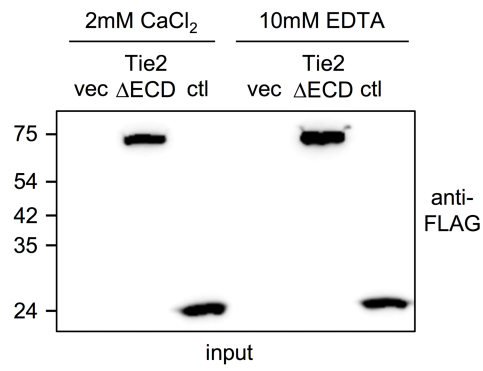
Figure 10. Role of Tyr1113 residue in calcium-induced dephosphorylation.

A, HEK293T cells transfected with FLAG-Tie2 Δ ECD or a control construct, integrin α IIb transmembrane domain-tail construct (α IIb-TAP) fused with N-terminal FLAG-tag, and C-terminal tandem affinity purification tag containing the calmodulin-binding region. Cells were lysed, and the lysates were incubated with calmodulin beads in the presence of 2mmol/L CaCl₂ or 10mmol/L EDTA in the lysis buffer, and bead-bound proteins were analyzed by Western blot using anti-FLAG antibody. **B**, Aliquots of lysate used for the calmodulin binding experiment in A analyzed to shown input levels. **C**, Lysates of HUVECs (upper) and HEK293T cells (lower) were incubated with calmodulin beads (or control beads) in the presence of 2 mmol/L CaCl₂ or 10mmol/L EDTA, and the bound proteins were analyzed with anti-receptor-type protein-tyrosine phosphatase ζ (RPTP ζ) antibody.

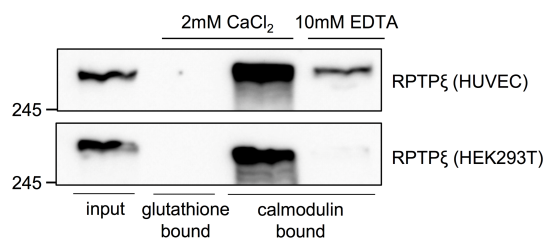
A.



B.



C.



First, I knocked down the expression of Tie2 by introducing an antisense morpholino oligonucleotide (MO), which specifically binds to the 5' untranslated region of the Tie2 mRNA and inhibits its translation by steric hindrance (Corey DR *et al.*, 2001). Knockdown of Tie2 did not perturb formation of either the heart or PCV, corroborating previous reports that vasculogenesis occurs normally in Tie2-null mice(5) and Tie2-depleted zebrafish (Li W *et al.*, 2014) (Figure 12C). However, development of ISVs from the PCV was significantly impaired, indicating that Tie2 function is required for sprouting and growth of the vasculature (Figure 12C). At stage 42, when the normal embryo presented fully defined rostral ISVs (Figure 12C, top right panel), Tie2-depleted embryos showed much shorter ISVs (Figure 12C, bottom right panel). These results confirm previous finding that Tie2 signaling is required for developmental angiogenesis in vertebrates (Sato TN *et al.*, 1995; Li W *et al.*, 2014).

To confirm that this defect is specific to the loss of Tie2 function, I investigated whether human Tie2 (hTie2) expression in these embryos can rescue the Tie2 knockdown phenotype (Figure 13A-D). First, I tested whether hTie2 is functional in *Xenopus* by asking whether *Xenopus* Ang1 can activate hTie2. I treated CHO cells stably expressing hTie2 with the culture medium harvested from cells transfected with with *Xenopus* Ang1 or control plasmid. I found that *Xenopus* Ang1 was as efficient as recombinant human Ang 1 in activating hTie2, as evidenced by increased Tie2 phosphorylation (Figure 13G). This result indicates that *Xenopus* Ang1 can bind to and activate hTie2 and that expressing hTie2 is a valid strategy to rescue the loss of endogenous Tie2 in *Xenopus*. In accordance with the evolutionarily conserved role of Tie2 in angiogenesis, hTie2 almost completely restored the growth of ISV (Figure 13C). This indicates that the angiogenic defect in Tie2 MO-injected embryo was specifically because of the loss of Tie2 function. Next I expressed the calmodulin

Figure 11. Evolutionarily conserved amino acid sequences in vertebrates.

Cytoplasmic domain of Tie2 is conserved in vertebrates. Amino acid sequence identity and similarity were calculated using Clustal Omega.

L920

human HRDFAGELEVLCKLGHHPNI INLLGACEHRGYLYLAIEYAPHGNLLDFLRKSRVLETDPA
mouse HRDFAGELEVLCKLGHHPNI INLLGACEHRGYLYLAIEYAPHGNLLDFLRKSRVLETDPA
chicken HRDFAGELEVLCKLGHHPNI INLLGACEHRGYLYLAIEYAPHGNLLDFLRKSRVLETDPA
xenopus HRDFAGELEVLCKLGHHPNI INLLGACEHRGYLYLAIEYAPHGNLLDFLRKSRVLETDPA
zebrafish HRDFAGELEVLCKLGHHPNI INLLGACEHRGYLYLAIEYAPHGNLLDFLRKSRVLETDPA
*****: * * * * . *****: *****: *****: *****

human FAIANSTASTLSSQQLLHFAADVARGMDYLSQKQFIHRDLAARNILVGENYVAKIADFG
mouse FAIANSTASTLSSQQLLHFAADVARGMDYLSQKQFIHRDLAARNILVGENYVAKIADFG
chicken FAIANSTASTLSSQQLLHFAADVARGMDYLSQKQFIHRDLAARNILVGENYVAKIADFG
xenopus FAIANSTASTLSSQQLLHFAADVARGMDYLSQKQFIHRDLAARNILVGENYVAKIADFG
zebrafish FAIAHRSTASTLSSQQLLHFAADVARGMSYLSQKQFIHRDLAARNILVGENYVAKIADFG
. **: *****: *****: *****: *****: *****

Y992

human SRGQEVYVKKTMGRLPVRWMAIESLNYSVYTTNSDVWSYGVLLWEIVSLGGTPYCGMTC
mouse SRGQEVYVKKTMGRLPVRWMAIESLNYSVYTTNSDVWSYGVLLWEIVSLGGTPYCGMTC
chicken SRGQEVYVKKTMGRLPVRWMAIESLNYSVYTTNSDVWSYGVLLWEIVSLGGTPYCGMTC
xenopus SRGQEVYVKKTMGRLPVRWMAIESLNYSVYTTNSDVWSYGVLLWEIVSLGGTPYCGMTC
zebrafish SRGQEVYVKKTMGRLPVRWMAIESLNYSVYTTNSDVWSYGVLLWEIVSLGGTPYCGMTC
*****: *****: *****: *****: *****: *****

human ELYEKLPGQYRLEKPLNCDEDEVYDLMRQCWREKPYERPSFAQIILVSLNRMLEERKTYVNT
mouse ELYEKLPGQYRLEKPLNCDEDEVYDLMRQCWREKPYERPSFAQIILVSLNRMLEERKTYVNT
chicken ELYEKLPGQYRLEKPLNCDEDEVYDLMRQCWREKPYERPSFAQIILVSLNRMLEERKTYVNT
xenopus ELYEKLPGQYRLEKPLNCDEDEVYDLMRQCWREKPYERPSFAQIILVSLNRMLEERKTYVNT
zebrafish ELYEKLPLGQRLEKPLNCDEDEVYELMQQCWREKPERPSESQIILSLGRMLEERKTYVNT
*****: *****: *****: *****: *****: *****

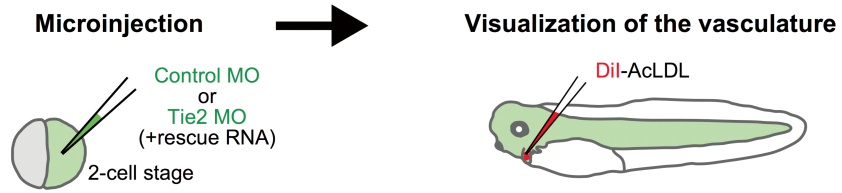
Y1108 Y1113

human TLYEKFTYAGIDCSAEAAA
mouse TLYEKFTYAGIDCSAEAAA
chicken TLYEKFTYAGIDCSAEAAA
xenopus TLYEKFTYAGIDCSAEAAA
zebrafish TLYEKFTYAGIDCSAEAAE

Figure 12. Regulation of embryonic angiogenesis by Tie2 in *Xenopus tropicalis*.

A, Experimental scheme. Embryos were injected with morpholino (MO) and RNA at the 2-cell stage, and their vasculature was visualized by low-density lipoprotein from human plasma, acetylated, Dil complex (Dil-AcLDL). **B**, Development of the intesomatic veins (ISVs). ISV growth from the posterior cardinal vein (PCV) is a well-known model of embryonic angiogenesis. The rostral-most ISVs (brackets) fully develop by stage 42. **C**, Tie2 is required for ISV formation. Scale bar, 500 μm .

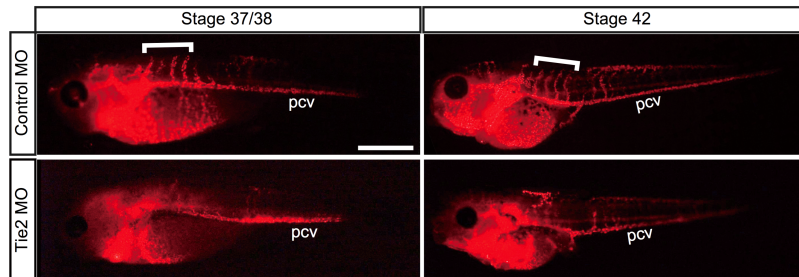
A.



B.



C.



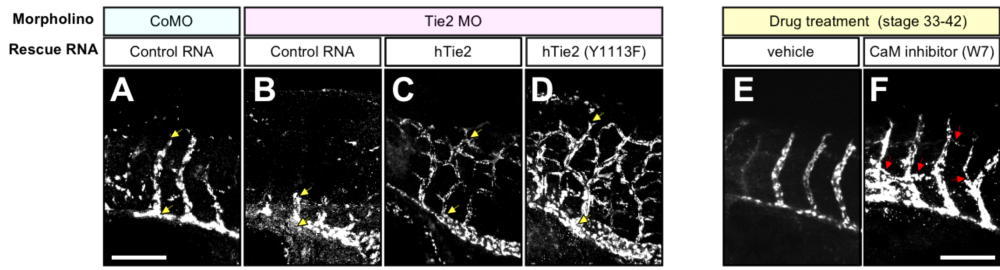
binding-defective hTie2 mutant, hTie2(Y1113F), in Tie2-depleted embryos. This led to further increase in the lengths of the ISVs and strikingly complex branching patterns (Figure 13D). The different degree of rescue by hTie2 and hTie2(Y1113F) was not because of different levels of expression because the same amount of RNAs was injected and the similar amounts of wild type and mutant Tie2 proteins were expressed in these embryos (Figure 13H). This result indicates that the activity of hTie2(Y1113F) caused ISV hyper branching (Figure 13D).

Having established that the calmodulin binding-defective mutant hTie2 causes excessive branching of the vasculature, I took an independent approach to address the involvement of calmodulin in this process. I treated W-7 to normally developing embryos at the onset of ISV formation and assessed the vessel growth (Figure 13E and F). I first optimized the W-7 regimen and found that treating embryos with 50 $\mu\text{mol/L}$ W-7 from stage 33 to stage 42 (when ISV growth occurs) did not cause toxicity (not shown) strikingly, inhibiting calmodulin function caused formation of ectopic branches that connect adjacent ISVs (Figure 13F), consistent with my model that calmodulin-mediated inhibition of Tie2 activity regulates vessel growth and branching.

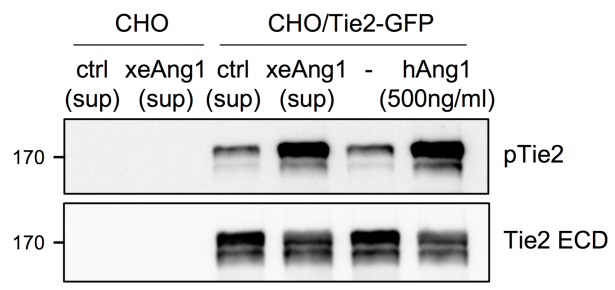
Together with my biochemical data, these *in vivo* data suggest that calmodulin might mediate calcium-mediated negative regulation of Tie2 activity and angiogenesis *in vivo*.

Figure 13. Uncontrolled angiogenesis caused by disruption of Tie2-calmodulin interaction

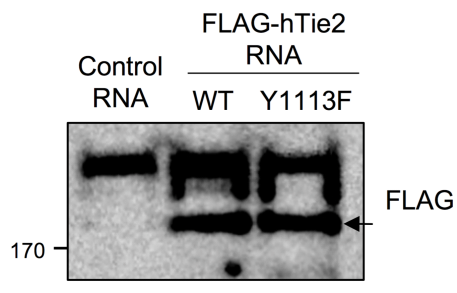
A-D, Representative images of the 4 rostral-most ISVs of embryos injected with either control morpholino (CoMO) or Tie2 MO and rescued with control (mCherry), wild-type human (h)Tie2 or hTie2(Y1113F) RNA. Yellow arrows indicate the start and end of one ISV. Note that increased branching of ISV in **D**. **E and F**, Similar images were taken from embryos treated with the calmodulin inhibitor W-7 or vehicle. Note ectopic ISV branches in F (red arrows). **G**, Xenopus cDNA encoding Ang1 or vector plasmid was transfected into HEK293T, and secreted Ang1 was collected in serum-free media which was subsequently concentrated. Ang1-conditioned or control medium was treated to CHO/Tie2-GFP for 15 minutes. Purified human Ang1 was also treated for comparison. The degree of Tie2 phosphorylation was analyzed by western blot using the phospho-specific Tie2-Y992 antibody. **H**, Xenopus embryos injected with wild type or Y1113F mutant FLAG-Tie2 constructs were lysed, and the lysates were analyzed for expression of FLAG-Tie2 (arrow). Note that the size of FLAG-Tie2 seem to be bigger than the one expressed in mammalian cells, presumable due to different glycosylation of the protein.



G.



H.



CONCLUSION

In this study, I demonstrated that calcium signaling negatively regulates Tie2 phosphorylation, and this requires Tie2-calmodulin interaction. I also found that the Tyr1113 residue in the C-terminal loop of Tie2 is essential for calmodulin binding and calcium-mediated negative regulation. Finally, I showed that expressing calmodulin binding-defective Tie2 or inhibiting calmodulin function *in vivo* causes overgrowth and excessive branching of vessels, suggesting a novel mechanism by which calmodulin mediates calcium-mediated negative regulation of Tie2 activity and angiogenesis.

A potential negative role of Tyr1113 in Tie2 phosphorylation has been proposed previously. The first line of evidence came from an expression library screening study using the autophosphorylated kinase domain of Tie2. In the study, an SH2 domain-containing tyrosine phosphatase, SH-PTP2, was identified as a Tie2-binding protein, and this binding was suggested to depend on the phosphorylation of Tyr1113 (Huang L *et al.*, 1995). This raised the possibility that this Tyr residue might be responsible for Tie2 dephosphorylation by recruiting SH-PTP2 in a phosphorylation-dependent manner. Later studies, however, revealed that Tyr1113 is not essential for the interaction with SH-PTP2 because SH-PTP2 can bind Tie2 through phosphotyrosine residues other than Tyr1113 as well (Jones N *et al.*, 1999). Moreover, Tie2 can phosphorylate SH-PTP2 even in presence of the Y1113F mutation, suggesting that SH-PTP2 is a downstream effector of Tie2, rather than it negative regulator (Sturk C *et al.*, 2010).

Another line of evidence for the negative role of the Tyr1113 comes from a structural study (Murray BW *et al.*, 2001). The study showed that the Tie2 C-terminal loop region containing Tyr1113 partially occupies the

ATP-binding site in the kinase domain, inhibiting the kinase activity of Tie2, and that Tyr1113 is required for the C-terminal loop to maintain this conformation (Shewchuk LM *et al.*, 2000). Concordantly, deletion of the C-terminal loop enhanced Tie2 activity and its downstream signaling (Niu XL *et al.*, 2002). In addition, the Y1113F mutation, predicted to displace the inhibitory C-terminal loop region from the ATP-binding site, also enhanced the kinase activity of Tie2 (Murray BW *et al.*, 2001). This model predicts that phosphorylation of Tyr1113 would, similar to Y1113F mutation, displace the C-terminal loop from the ATP-binding site and relieve its negative regulation. However, whether Tyr1113 is phosphorylated *in vivo* remains unclear because mass spectroscopy analysis failed to detect phosphorylated Tyr1113 even in a highly activated, autophosphorylated Tie2 (Murray BW *et al.*, 2001). Similarly, phosphorylation of the Y1113 residue was not detected on Ang1-induced Tie2 phosphorylation (Sturk C *et al.*, 2010). Together, these studies implicate Tyr1113-dependent conformation of the C-terminal loop in negative regulation of Tie2 activity. However, whether this is regulated by phosphorylation of Tyr1113 remains to be elucidated.

Here I proposed a novel negative regulatory mechanism for Tie2 through the Tyr1113 residue. I show that Tyr1113 is essential for the Tie2-calmodulin interaction and calcium-induced Tie2 dephosphorylation. I also propose that conformation of the C-terminal loop, which requires Tyr1113, facilitates the binding of calmodulin in a calcium-independent manner and that the Tie2-bound calmodulin may recruit a phosphatase in response to increased calcium level.

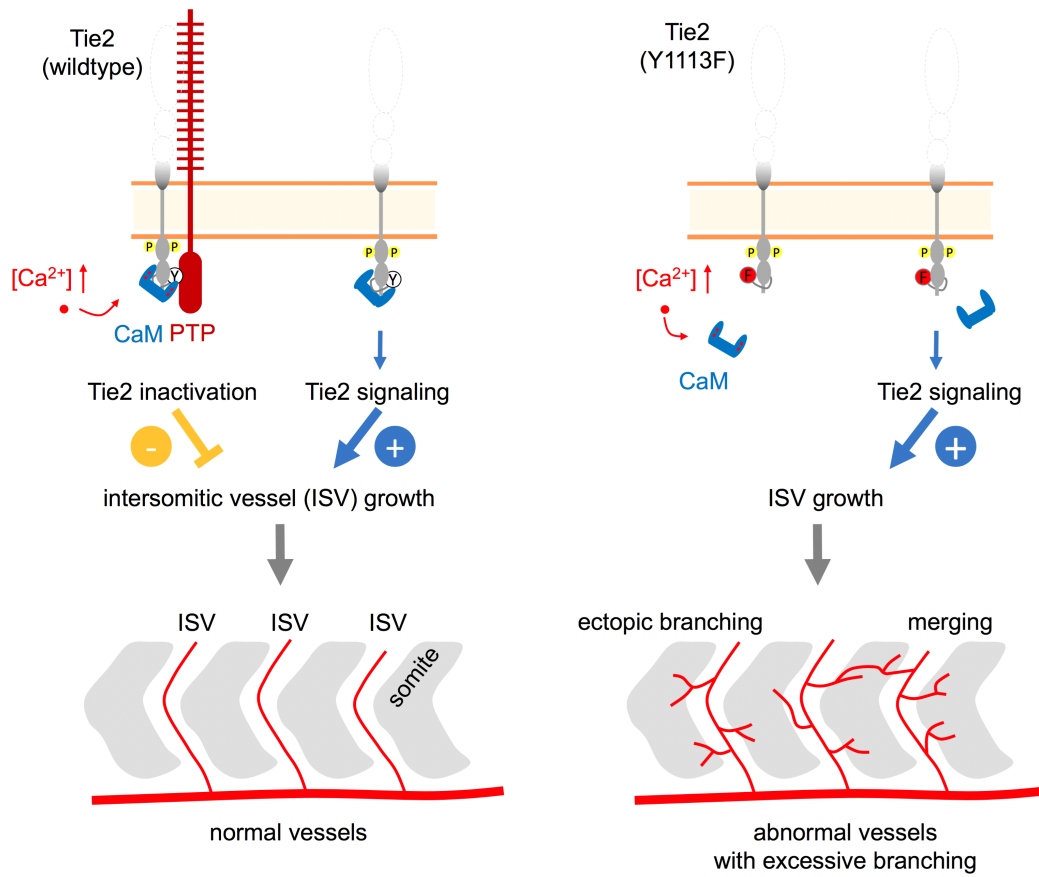
Moving forth, I extended our biochemical studies to understand the significance of the results in formation of the vascular network during development. I found that Tie2 depletion causes a specific defect in the formation of ISVs, which sprout off from the PCV that spans the entire

body. My result is consistent with an earlier Tie2 knockout mouse study, which showed that Tie2 plays a more important role in angiogenesis than in vasculogenesis during development (Sato TN *et al.*, 1995). A more recent study using zebrafish showed that depleting Tie2 expression inhibits migration and proliferation of endothelial cells that give rise to ISVs (Li W *et al.*, 2014), supporting my interpretation that Tie2 signaling is required for developmental angiogenesis (however, see also Gjini *et al.*, 2011, which reports to apparent vessel abnormality in a Tie2 deletion mutant line). It was, however, unknown how endothelial cells terminate their growth to form ISVs of appropriate size and number of branches. I showed that expressing calmodulin binding-defective (Y1113F), but not wild-type Tie2, causes overgrowth and hyperbranching of the ISVs (Figure 14), suggesting that switching off Tie2 activity during embryonic angiogenesis requires calmodulin binding, and possibly, calcium signaling. Intriguingly, neutralizing antibodies against VE-PTP, a negative regulator of Tie2 activity, also induce uncontrolled vessel growth in allantois explants and juvenile mice (Winderlich M *et al.*, 2009), consistent with our observation that a balanced Tie2 activity is key to normal vessel development.

In conclusion, my study highlights a novel connection between calcium and Tie2 signaling and a calcium/calmodulin-dependent Tie2 inactivation. I also show evidence that this mechanism of action may regulate embryonic vascularization *in vivo*. Given that negative regulation of Tie2 signaling is associated with pathological angiogenesis, I propose that relieving its negative regulation by inhibiting Tie2-calmodulin interaction is a promising therapeutic approach for angiogenesis-related diseases.

Figure 14. Summary and hypothetical model.

Extrinsic cues, possible from the somites, might induce a rise in the intracellular calcium in the endothelial cells, which would recruit protein tyrosine phosphatases (PTPs) to Tie2-bound calmodulin (CaM). PTPs dephosphorylate and inhibit Tie2, and as a result, vessel growth slows down (left, bottom). The calmodulin-binding defective Tie2 mutant, Tie2(Y1113F), is not inhibited by calcium, resulting hyperactivation of Tie2 signaling, which leads to abnormal intersomitic vessel (ISV) growth (right, bottom)



REFERENCES

Augustin HG, Koh GY, Thurston G, Alitalo K. Control of vascular morphogenesis and homeostasis through the angiotensin-Tie system. *Nat Rev Mol Cell Biol.* 2009 Mar;10(3):165-77

Berridge MJ, Bootman MD, Roderick HL. Calcium signalling: dynamics, homeostasis and remodelling. *Nat Rev Mol Cell Biol.* 2003 Jul;4(7):517-29

Corey DR, Abrams JM. Morpholino antisense oligonucleotides: tools for investigating vertebrate development. *Genome Biol.* 2001;2(5):REVIEWS1015. Epub 2001 Apr 26.

Davis S, Aldrich TH, Jones PF, Acheson A, Compton DL, Jain V, et al. Isolation of angiotensin-1, a ligand for the TIE2 receptor, by secretion-trap expression cloning. *Cell.* 1996 Dec 27;87(7):1161-9.

Dumont DJ, Gradwohl G, Fong GH, Puri MC, Gertsenstein M, Auerbach A, et al. Dominant-negative and targeted null mutations in the endothelial receptor tyrosine kinase, tek, reveal a critical role in vasculogenesis of the embryo. *Genes Dev.* 1994 Aug 15;8(16):1897-909.

Fachinger G, Deutsch U, Risau W. Functional interaction of vascular endothelial-protein-tyrosine phosphatase with the angiotensin receptor Tie-2. *Oncogene.* 1999 Oct 21;18(43):5948-53.

Ferrara N. Vascular endothelial growth factor: basic science and clinical progress. *Endocr Rev.* 2004 Aug;25(4):581-611.

Fiedler U, Augustin HG. Angiopoietins: a link between angiogenesis and inflammation. *Trends Immunol.* 2006 Dec;27(12):552-8. Epub 2006 Oct 12

Fukuhara S, Sako K, Minami T, Noda K, Kim HZ, Kodama T, et al. Differential function of Tie2 at cell-cell contacts and cell-substratum contacts regulated by angiopoietin-1. *Nat Cell Biol.* 2008 May;10(5):513-26.

Gjini E, Hekking LH, K uchler A, Saharinen P, Wienholds E, Post JA, Alitalo K, Schulte-Merker S. Zebrafish Tie-2 shares a redundant role with Tie-1 in heart development and regulates vessel integrity. *Dis Model Mech.* 2011 Jan;4(1):57-66.

Herbert SP, Stainier DY. Molecular control of endothelial cell behaviour during blood vessel morphogenesis. *Nat Rev Mol Cell Biol.* 2011 Aug 23;12(9):551-64.

Holopainen T, Saharinen P, D'Amico G, Lampinen A, Eklund L, Sormunen R, et al. Effects of angiopoietin-2-blocking antibody on endothelial cell-cell junctions and lung metastasis. *J Natl Cancer Inst.* 2012 Mar 21;104(6):461-75

Huang L, Turck CW, Rao P, Peters KG. GRB2 and SH-PTP2: potentially important endothelial signaling molecules downstream of the TEK/TIE2 receptor tyrosine kinase. *Oncogene.* 1995 Nov 16;11(10):2097-103.

Jeltsch M, Leppanen VM, Saharinen P, Alitalo K. Receptor tyrosine kinase-mediated angiogenesis. *Cold Spring Harb Perspect Biol.* 2013 Sep 1;5(9). pii: a009183.

Jones N, Dumont DJ. Tek/Tie2 signaling: new and old partners. Cancer metastasis reviews. *Cancer Metastasis Rev.* 2000;19(1-2):13-7.

Jones N, Master Z, Jones J, Bouchard D, Gunji Y, Sasaki H, et al. Identification of Tek/Tie2 binding partners. Binding to a multifunctional docking site mediates cell survival and migration. *J Biol Chem.* 1999 Oct 22;274(43):30896-905.

Jones N, Chen SH, Sturk C, Master Z, Tran J, Kerbel RS, et al. A unique autophosphorylation site on Tie2/Tek mediates Dok-R phosphotyrosine binding domain binding and function. *Mol Cell Biol.* 2003 Apr;23(8):2658-68.

Kim C, Lau TL, Ulmer TS, Ginsberg MH. Interactions of platelet integrin alphaIIb and beta3 transmembrane domains in mammalian cell membranes and their role in integrin activation. *Blood.* 2009 May 7;113(19):4747-53

Kim C, Lee HS, Lee D, Lee SD, Cho EG, Yang SJ, et al. Epithin/PRSS14 proteolytically regulates angiotensin receptor Tie2 during transendothelial migration. *Blood.* 2011 Jan 27;117(4):1415-24.

Kim C, Schmidt T, Cho EG, Ye F, Ulmer TS, Ginsberg MH. Basic amino-acid side chains regulate transmembrane integrin signalling. *Nature.* 2011 Dec 18;481(7380):209-13

Koh GY. Orchestral actions of angiotensin-1 in vascular regeneration. *Trends Mol Med.* 2013 Jan;19(1):31-9.

Koh YJ, Kim HZ, Hwang SI, Lee JE, Oh N, Jung K, et al. Double

antiangiogenic protein, DAAP, targeting VEGF-A and angiopoietins in tumor angiogenesis, metastasis, and vascular leakage. *Cancer Cell*. 2010 Aug 9;18(2):171-84.

Kontos CD, Stauffer TP, Yang WP, York JD, Huang L, Blonar MA, et al. Tyrosine 1101 of Tie2 is the major site of association of p85 and is required for activation of phosphatidylinositol 3-kinase and Akt. *Mol Cell Biol*. 1998 Jul;18(7):4131-40.

Lee J, Kim KE, Choi DK, Jang JY, Jung JJ, Kiyonari H, et al. Angiopoietin-1 guides directional angiogenesis through integrin $\alpha\beta 5$ signaling for recovery of ischemic retinopathy. *Sci Transl Med*. 2013 Sep 18;5(203):203ra127.

Levine AJ, Munoz-Sanjuan I, Bell E, North AJ, Brivanlou AH. Fluorescent labeling of endothelial cells allows in vivo, continuous characterization of the vascular development of *Xenopus laevis*. *Dev Biol*. 2003 Feb 1;254(1):50-67.

Longair MH, Baker DA, Armstrong JD. Simple Neurite Tracer: open source software for reconstruction, visualization and analysis of neuronal processes. *Bioinformatics*. 2011 Sep 1;27(17):2453-4

Li W, Chen J, Deng M, Jing Q. The zebrafish Tie2 signaling controls tip cell behaviors and acts synergistically with Vegf pathway in developmental angiogenesis. *Acta Biochim Biophys Sin (Shanghai)*. 2014 Aug;46(8):641-6

Maisonpierre PC, Suri C, Jones PF, Bartunkova S, Wiegand SJ, Radziejewski C, et al. Angiopoietin-2, a natural antagonist for Tie2 that

disrupts in vivo angiogenesis. *Science*. 1997 Jul 4;277(5322):55-60.

Marshak S, Nikolakopoulou AM, Dirks R, Martens GJ, Cohen-Cory S. Cell-autonomous TrkB signaling in presynaptic retinal ganglion cells mediates axon arbor growth and synapse maturation during the establishment of retinotectal synaptic connectivity. *J Neurosci*. 2007 Mar 7;27(10):2444-56.

Master Z, Jones N, Tran J, Jones J, Kerbel RS, Dumont DJ. Dok-R plays a pivotal role in angiopoietin-1-dependent cell migration through recruitment and activation of Pak. *EMBO J*. 2001 Nov 1;20(21):5919-28.

Murray BW, Padrique ES, Pinko C, McTigue MA. Mechanistic effects of autophosphorylation on receptor tyrosine kinase catalysis: enzymatic characterization of Tie2 and phospho-Tie2. *Biochemistry*. 2001 Aug 28;40(34):10243-53.

Nieuwkoop PD, Faber J. Normal Table of *Xenopus laevis* (Daudin). 2nd ed. North Holland Publishing Company. Amsterdam. 1967

Niu XL, Peters KG, Kontos CD. Deletion of the carboxyl terminus of Tie2 enhances kinase activity, signaling, and function. Evidence for an autoinhibitory mechanism. *J Biol Chem*. 2002 Aug 30;277(35):31768-73.

Osawa M, Swindells MB, Tanikawa J, Tanaka T, Mase T, Furuya T, et al. Solution structure of calmodulin-W-7 complex: the basis of diversity in molecular recognition. *J Mol Biol*. 1998 Feb 13;276(1):165-76.

Sato TN, Tozawa Y, Deutsch U, Wolburg-Buchholz K, Fujiwara Y,

Gendron-Maguire M, et al. Distinct roles of the receptor tyrosine kinases Tie-1 and Tie-2 in blood vessel formation. *Nature*. 1995 Jul 6;376(6535):70-4.

Saharinen P, Eklund L, Miettinen J, Wirkkala R, Anisimov A, Winderlich M, et al. Angiopoietins assemble distinct Tie2 signalling complexes in endothelial cell-cell and cell-matrix contacts. *Nat Cell Biol*. 2008 May;10(5):527-37.

Shewchuk LM, Hassell AM, Ellis B, Holmes WD, Davis R, Horne EL, et al. Structure of the Tie2 RTK domain: self-inhibition by the nucleotide binding loop, activation loop, and C-terminal tail. *Structure*. 2000 Nov 15;8(11):1105-13.

Sturk C, Kim H, Jones N, Dumont DJ. A negative regulatory role for Y1111 on the Tie-2 RTK. *Cell Signal*. 2010 Apr;22(4):676-83.

Suri C, McClain J, Thurston G, McDonald DM, Zhou H, Oldmixon EH, et al. Increased vascularization in mice overexpressing angiopoietin-1. *Science*. 1998 Oct 16;282(5388):468-71.

Thomas M, Augustin HG. The role of the Angiopoietins in vascular morphogenesis. *Angiogenesis*. 2009;12(2):125-37

Winderlich M, Keller L, Cagna G, Broermann A, Kamenyeva O, Kiefer F, et al. VE-PTP controls blood vessel development by balancing Tie-2 activity. *J Cell Biol*. 2009 May 18;185(4):657-71.

Wu FT, Lee CR, Bogdanovic E, Prodeus A, Gariepy J, Kerbel RS.

Vasculotide reduces endothelial permeability and tumor cell extravasation in the absence of binding to or agonistic activation of Tie2. *EMBO Mol Med.* 2015 Jun;7(6):770-87

Ziegler T, Horstkotte J, Schwab C, Pfetsch V, Weinmann K, Dietzel S, et al. Angiopoietin 2 mediates microvascular and hemodynamic alterations in sepsis. *J Clin Invest.* 2013 Jul 1. pii: 66549.

Part II



Epigallocatechin gallate has pleiotropic effects on transmembrane signaling by altering the embedding of transmembrane domains

Received for publication, March 22, 2017, and in revised form, May 1, 2017. Published, Papers in Press, May 9, 2017, DOI 10.1074/jbc.C117.787309

Feng Ye¹, Chansik Yang^{5,6,1}, Jiyeon Kim⁵, Christopher J. MacNevin¹, Klaus M. Hahn¹, Dongeun Park⁴, Mark H. Ginsberg^{2,3}, and Chunggho Kim^{5,3}

From the ¹Department of Medicine, University of California San Diego School of Medicine, La Jolla, California 92093, the ²Department of Life Sciences, Korea University, Seoul 136-701, Republic of Korea, the ³School of Biological Sciences, Seoul National University, Seoul 151-747, Republic of Korea, and the ⁴Department of Pharmacology and Lineberger Cancer Center, University of North Carolina at Chapel Hill, Chapel Hill, North Carolina 27599

Edited by George M. Carman

Epigallocatechin gallate (EGCG) is the principal bioactive ingredient in green tea and has been reported to have many health benefits. EGCG influences multiple signal transduction pathways related to human diseases, including redox, inflammation, cell cycle, and cell adhesion pathways. However, the molecular mechanisms of these varying effects are unclear, limiting further development and utilization of EGCG as a pharmaceutical compound. Here, we examined the effect of EGCG on two representative transmembrane signaling receptors, integrin α IIb β 3 and epidermal growth factor receptor (EGFR). We report that EGCG inhibits talin-induced integrin α IIb β 3 activation, but it activates α IIb β 3 in the absence of talin both in a purified system and in cells. This apparent paradox was explained by the fact that the activation state of α IIb β 3 is tightly regulated by the topology of β 3 transmembrane domain (TMD); increases or decreases in TMD embedding can activate integrins. Talin increases the embedding of integrin β 3 TMD, resulting in integrin activation, whereas we observed here that EGCG decreases the embedding, thus opposing talin-induced integrin activation. In the absence of talin, EGCG decreases the TMD embedding, which can also disrupt the integrin α - β TMD interaction, leading to integrin activation. EGCG exhibited similar paradoxical behavior in EGFR signaling. EGCG alters the topology of EGFR TMD and activates the receptor in the absence of EGF, but inhibits EGF-induced EGFR activation. Thus, this widely ingested polyphenol exhibits pleiotropic effects on transmembrane signaling by modifying the topology of TMDs.

This work was supported by the Basic Science Research Program through the National Research Foundation of Korea (Grant NRF-2016R1A2B4A009755) (to C. K.), by a grant from the Korea Health Technology R&D Project through the Korea Health Industry Development Institute (Grant HI14C0209) (to C. K.), and by National Institutes of Health Grants CA-142833 and P41-EB002025 (to K. M. H.) and HL 078784 and HL 117807 (to M. H. G.). The authors declare that they have no conflicts of interest with the contents of this article. The content is solely the responsibility of the authors and does not necessarily represent the official views of the National Institutes of Health.

This article contains supplemental Fig. 1.

¹Both authors contributed equally to this work.

²To whom correspondence may be addressed. Tel.: 858-822-6432; E-mail: mhginsberg@ucsd.edu.

³To whom correspondence may be addressed. Tel.: 82-2-3290-3402; Fax: 82-2-3290-4144; E-mail: chunggho@korea.ac.kr.

Green tea has been one of the most popular drinks for thousands of years, both as a beverage and as an herbal medicine. Indeed, green tea has many clinically reported health benefits, including the prevention of cardiovascular diseases (1, 2) and cancer (3). Studies on the beneficial effects of green tea using cellular or animal models have recently converged on EGCG,⁴ the most abundant polyphenol considered as a health-promoting phytonutrient in green tea, and have found EGCG to influence multiple signal transduction pathways related to antioxidant, inflammation, cell cycle, and cell adhesion (4). However, the molecular mechanism underlying those effects has remained elusive. Although EGCG has been suggested to have a number of molecular targets (5), only DNA methyltransferase (6) and the 67-kDa laminin receptor (7) have been demonstrated to directly respond to EGCG in an *in vitro* system. On the other hand, recent nuclear magnetic resonance spectroscopy studies clearly showed that EGCG can interact with model lipid membranes (8, 9), which implies that biological membrane can be a molecular target of EGCG. Furthermore, the EGCG-lipid interaction can cause a deformation of the lipid bilayer, e.g. by inducing an expansion of the lipid bilayer (10) and/or altering the thickness of the membrane (11). Because membrane-receptor interactions are important in maintaining the proper TMD topology, structures, and hence function of the transmembrane receptors (12, 13), chemical and physical alteration in biological membrane may cause changes in activities of those proteins (14). However, whether such lipid-EGCG interaction contributes to cell signaling pathways and how it could account for the broad effects of EGCG on many cell signaling pathways are yet to be elucidated.

We hypothesized that EGCG exerts its effect on transmembrane receptor signaling by interacting with a lipid bilayer and thereby changing the TMD topology and signaling of a broad spectrum of transmembrane proteins. We tested this hypothesis using integrin α IIb β 3 and EGFR, two prototypical signaling receptors. Integrin α IIb β 3 is a het-

⁴The abbreviations used are: EGCG, epigallocatechin gallate; EGFR, epidermal growth factor receptor; TMD, transmembrane domain; THD, talin head domain; DMPG, 1,2-dimyristoyl-sn-glycero-3-phosphocholine; DMPG, 1,2-dimyristoyl-sn-glycero-3-phospho-(1'-rac-glycerol); KSI, keto-steroid isomerase; MFI, mean fluorescence intensity.

9858 J. Biol. Chem. (2017) 292(24):9858–9864

© 2017 by The American Society for Biochemistry and Molecular Biology, Inc. Published in the U.S.A.

ASBMB

Downloaded from <http://www.jbc.org/> at Korea University College of Medicine on September 10, 2017

This work published in *J. Biol. Chem.* 2017 Jun
16;292(24):9858–9864,

Study on the Pleiotropic Effects of Transmembrane Signaling by Epigallocatechin Gallate

Chansik Yang

School of biological sciences

The graduate school

Seoul National University

Epigallocatechin gallate (EGCG) is the principal bioactive ingredient in green tea and has been reported to have many health benefits. EGCG influences multiple signal transduction pathways related to human diseases, including redox, inflammation, cell cycle, and cell adhesion pathways. However, the molecular mechanisms of these varying effects are unclear, limiting further development and utilization of EGCG as a pharmaceutical compound. Here, I examined the effect of EGCG on two representative transmembrane signaling receptors, integrin $\alpha\text{IIb}\beta\text{3}$ and epidermal growth factor receptor (EGFR). I report that EGCG inhibits talin-induced integrin $\alpha\text{IIb}\beta\text{3}$ activation, but it activates $\alpha\text{IIb}\beta\text{3}$ in the absence of talin both in a purified system and in cells. This apparent paradox was explained by the fact that the activation state of $\alpha\text{IIb}\beta\text{3}$ is tightly regulated by the topology of β3 transmembrane domain (TMD); increases or decreases in TMD embedding can activate integrins. Talin increases the embedding of integrin β3 TMD, resulting in integrin activation,

whereas I observed here that EGCG decreases the embedding, thus opposing talin-induced integrin activation. In the absence of talin, EGCG decreases the TMD embedding, which can also disrupt the integrin α - β TMD interaction, leading to integrin activation. EGCG exhibited similar paradoxical behavior in EGFR signaling. EGCG alters the topology of EGFR TMD and activates the receptor in the absence of EGF, but inhibits EGF-induced EGFR activation. Thus, this widely ingested polyphenol exhibits pleiotropic effects on transmembrane signaling by modifying the topology of TMDs.⁶⁾

Key Words : EGCG, Integrin α IIb β 3, transmembrane domain, Epidermal growth factor receptor

Student Number : 2013-20302

6) All of contents in here published in *J. Biol. Chem.* 2017 Jun 16;292(24):9858-9864, and I participated as a main author.

INTRODUCTION

Green tea has been one of the most popular drinks for thousands of years, both as a beverage and as an herbal medicine. Indeed, green tea has many clinically reported health benefits, including the prevention of cardiovascular disease (Kuriyama S., 2008; Badu P.V. and Liu D, 2008) and cancer (Shimizu M *et al.*, 2011). Studies on the beneficial effects of green tea using cellular or animal models have recently converged on EGCG (Singh BN *et al.*, 2011), the most abundant polyphenol considered as a health-promoting phytonutrient in green tea, and have found EGCG to influence multiple signal transduction pathways related to antioxidation, inflammation, cell cycle, and cell adhesion (Singh BN *et al.*, 2011). However, the molecular mechanism underlying those effects has remained elusive. Although EGCG has been suggested to have number of molecular targets (Patra SK *et al.*, 2008), only DNA methyltransferase (Lee WJ *et al.*, 2005) and the 67-kDa lamin receptor (Lee WJ *et al.*, 2005) have been demonstrated to directly respond to EGCG in an *in vitro* system. On the other hand, recent nuclear magnetic resonance spectroscopy studies clearly showed that EGCG can interact with model lipid membrane (Uekusa Y *et al.*, 2011; Scheidt HA *et al.*, 2004) which implies that biological membrane can be a molecular target of EGCG. Furthermore, the EGCG-lipid interaction can cause a deformation of the lipid bilayer, e.g. by inducing an expansion of the lipid bilayer (Tamba Y *et al.*, 2007) and/or altering the thickness of the membrane (Sun Y *et al.*, 2009). Because membrane-receptor interactions are important in maintaining the proper TMD topology, structures, and hence function of the transmembrane receptors (Lee AG, 2003; Killian JA *et al.*, 2000), chemical and physical alteration in biological membrane may cause changes in activities of

those proteins (Escriba PV *et al.*, 2008) However, whether such lipid-EGCG interaction contributes to cell signaling pathways and how it could account for the broad effects of EGCG on many cell signaling pathways are yet to be elucidated.

I hypothesized that EGCG exerts its effect on transmembrane receptor signaling by interacting with a lipid bilayer and thereby changing the TMD topology and signaling of a broad spectrum of transmembrane proteins. I tested this hypothesis using integrin $\alpha\text{IIb}\beta\text{3}$ and EGFR, two prototypical signaling receptors. Integrin $\alpha\text{IIb}\beta\text{3}$ is a heterodimeric transmembrane adhesion receptor that has a low affinity for its ligands in the resting state (“inactive”) and a high affinity in the stimulated state (“activate” “or ”activated“). The affinity of integrin $\alpha\text{IIb}\beta\text{3}$ is regulated by TMD interaction of its α and β subunits, which depends on the precise tilt angle of the β3 TMD determined by the lipid-protein interaction (Kim C *et al.*, 2012; Lau TL *et al.*, 2009)). Indeed, the physiological integrin activating protein, talin (Calderwood DA *et al.*, 1999), activates the integrin by altering the tilt angle of integrin β3 TMD (Kim C *et al.*, 2012; Kalli AC *et al.*, 2011). The other model transmembrane receptor, EGFR, normally exists in an inactive monomeric state and is activated upon ligand-induced homodimerization, in which the topology of its TMD may play a role (Endres NF *et al.*, 2013; Arkhipov A *et al.*, 2013). Here, I investigated the effect of EGCG on these two prototypical transmembrane signaling receptors and propose that EGCG can alter the membrane embedding of their TMDs which in turn modulates transmembrane signaling by these receptors.

MATERIAL AND METHODS

Reagents, cell lines, and plasmids

1,2-dimyristoyl-sn-glycero-3-phosphocholine (DMPC) and 1,2-dimyristoyl-sn-glycero-3-phospho-(1'-rac-glycerol) (DMPG) were purchased from Avanti Polar Lipids, Inc. Membrane scaffold protein (MSP1D1) was kindly provided by Dr. Steven Sligar (University of Illinois at Urbana-Champaign). PAC1 and D57 were described previously (Kim C *et al.*, 2012). Anti-FLAG antibody (M2) and Anti-phosphotyrosine antibody (4G10) were purchased from Sigma-Aldrich and Merck Millipore, respectively. CHO/aIIb and CHO/aIIb β 3 cells were generated by infecting CHO cells with lentivirus encoding aIIb and/or β 3 as previously described (Kim C *et al.*, 2012). HEK/EGFR cells were kindly provided by Dr. Seung-Taek Lee (Yonsei University). The β 3 TMD-tail fused with N-terminal 6xHis and ketosteroid isomerase (KSI) in the pET-31 expression vector was described previously (Kim C *et al.*, 2012). Similarly, the EGFR TMD (Pro637 - Gln701) construct containing N-terminal 6xHis and KSI with cysteine mutation at Phe667 was generated by ligation of the PCR-amplified EGFR TMD region into the pET-31 expression vector.

Flow cytometry

CHO or CHO/aIIb cells were transfected with various integrin constructs using Lipofectamine LTX and Plus reagents (Life Technologies) or Lipofectamine 2000 (Life Technologies). CHO/aIIb β 3 cells were transfected with total of 10 μ g plasmids which include 1 μ g tdTomato cDNA as a transfection marker. At 24 h after transfection, cells were detached by trypsinization and treated with EGCG for 10 min. Those cells were stained

with PAC1 followed by allophycocyanin-conjugated anti-mouse IgM antibody. When integrin constructs were transfected, cells were co-stained with D57 to gate cells with similar high α IIb β 3 expression.

EGFR phosphorylation assay

Serum-starved subconfluent HEK/EGFR cells were treated with varying concentration of EGCG for 30 min before EGF treatment (final 50 ng/ml). Cells were lysed by a lysis buffer (20 mM HEPES, pH 7.4, 150 mM NaCl, 1% TritonX-100, 10 mM EDTA, pH 7.4, supplemented with PhosStop (Roche) and protease inhibitor cocktail (Roche)). After clarification by centrifugation at 17,000 g for 30 min, the clarified lysates were incubated at 4°C overnight in the presence of 3 μ g anti-FLAG antibody and the bound proteins were precipitated with protein G sepharose. The bound proteins were analyzed by SDS-PAGE and subsequent western blot with anti-phosphotyrosine antibody and anti-EGFR antibody.

Expression and purification of TMD peptides

6xHis-KSI fused TMD proteins were expressed in E.coli BL21(DE3) and purified using HiTrap Chelating HP column charged with Ni²⁺. The Asp-Pro bond between KSI and TMD peptide in the purified TMD proteins was cleaved in 10% formic acid for 120 mins at 80 °C. The resulting TMD peptide was then dialyzed against a buffer containing 50 mM Tris-HCl, pH 7.4, 500 mM NaCl, and 6 M urea, and then passed through a Ni²⁺-NTA column again to absorb the KSI, leaving the purified TMD peptide in the solution. The TMD peptide was labeled with excess mero60 (1:5 molar ratio). 0.1 % Triton X-100 was added to the labeled TMD peptide and the labeled TMD peptide was then dialyzed extensively against 0.1 % Triton X-100 in Tris-buffered saline (TBS, 20 mM Tris-HCl, pH 7.4, 150 mM NaCl).

Preparation of integrin nanodiscs

DMPC and DMPG lipids were dissolved in chloroform or chloroform-/methanol mixture, mixed into 1:1 ratio, and dried onto a glass tube with steady flow of argon. The lipid mixture was dissolved in 100 mM cholate in TBS. To assemble nanodiscs, 360 μ l of the 1:1 lipid mixture (50 mM), 1 ml of 200 μ M MSP1D1, and the purified TMD peptides (10 μ M) or the purified integrin α IIb β 3 from human platelets (10 μ M) were mixed. The mixture was added with two volumes of Biobeads SM-2 (Bio-Rad) to initiate nanodisc assembly and incubated overnight at room temperature in the dark. The assembled nanodiscs were further purified with a size exclusion column (hi-load 16/60 Superdex 200) with TBS as the column buffer. When necessary, the nanodiscs were concentrated using Ultracel-30k (Millipore).

Fluorescence spectroscopy

200 μ l of the purified nanodiscs were mixed with 50 μ l of various concentrations of EGCG (and THD in the case of β 3 TMD nanodiscs). After 30 min of incubation at room temperature, the emission spectrum (from 605 nm to 655 nm) at the excitation wavelength, 593 nm, was scanned with 1 nm interval using FluoroMax-2 Spectrofluorometer (Instruments S.A., Inc.). The fluorescence from unlabeled TMD peptide, talin, empty nanodiscs, or buffer was negligible. The fluorescence of the samples was re-measured after addition of 2% SDS (final concentration).

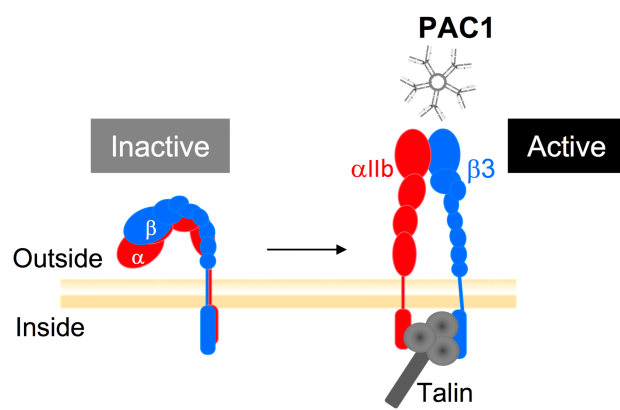
RESULTS

Pleiotropic effect of EGCG on activation of integrin $\alpha\text{IIb}\beta\text{3}$

Although EGCG is reported to have anti-thrombotic effects (Kang WS *et al.*, 1999), the addition of EGCG to platelets, the main cellular mediators of arterial thrombosis, causes complex responses. For example, EGCG inhibited aggregation of thrombin-stimulated platelets, but, paradoxically, caused aggregation of unstimulated platelets at the same dose (Lill G *et al.*, 2003). To better understand the physiological role of this widely consumed polyphenol, I first tested the effect of EGCG on activation of recombinant integrin $\alpha\text{IIb}\beta\text{3}$ in CHO cells where the integrin is normally in a low affinity state; with the addition of increasing concentration of EGCG, there was a progressive increase in activation as measured by binding of PAC1 (Figure 15), a ligand-mimetic, activation-specific integrin $\alpha\text{IIb}\beta\text{3}$ antibody (Shattil SJ *et al.*, 1984) (Figure 16A, white bars). The EGCG-induced increase in PAC1 binding was reduced by washing out EGCG (Figure 17), showing that the effect is reversible and does not require the known oxidation-dependent reactivity toward primary amines (Palhano FL *et al.*, 2013). Physiological activation of this integrin requires binding of talin to the cytoplasmic domain of the β3 subunit (Shattil SJ *et al.*, 2010). To ask whether EGCG induces physiological activation, I utilized a mutant $\alpha\text{IIb}\beta\text{3}$ (Y747A) that does not bind talin (Wegner KL *et al.*, 2007). This mutant showed similar activation by EGCG (Figure 16A, gray bars). Thus, EGCG-induced integrin activation is not dependent on the known intracellular signaling pathway.

Figure 15. Scheme of talin head domain induced integrin $\alpha\text{IIb}\beta_3$ activation.

Conformational states of Integrin $\alpha\text{IIb}\beta_3$ can be changed toward ligand accessible form, from inactive to active when talin head domain, which is constitutively active form of talin, is expressed in cells. PAC1 which is ligand-mimetic antibody can bind to only the active form of Integrin $\alpha\text{IIb}\beta_3$ so can be assessed as integrin activation index.



To directly test the effects of EGCG on talin-induced integrin activation, I introduced talin head domain (THD), the integrin-activating talin fragment (Calderwood DA *et al.*, 1999), into CHO cells expressing integrin α IIb β 3 (CHO/ α IIb β 3), and then examined the effects of EGCG on the talin-induced activation. EGCG blocked THD-induced α IIb β 3 activation in a dose-dependent manner, whereas EGCG alone induced integrin activation (Figure 16B).

Because of the complexity of cellular components that might mediate these paradoxical effects of EGCG, I utilized an *in vitro* reconstitution system in which purified integrin α IIb β 3 was embedded in nanodiscs, islands of 10-nm lipid bilayer encircled by membrane scaffold protein (Denisov IG *et al.*, 2004)⁷). In the reconstituted system, the addition of purified THD can activate the integrin (Ye F *et al.*, 2010). The integrin nanodiscs were first captured to the surface of assay plate coated with anti-integrin β 3 extracellular antibody (AP3), and the degree of integrin activation was measured by PAC1 binding to the immobilized integrin nanodisc (Figure 18A). EGCG activated the integrin nanodiscs in a dose-dependent manner (Figure 18B, green line), as it did in cells. The addition of purified THD increases PAC1 binding in the system as shown previously (Ye F *et al.*, 2010), and the THD-induced increase was inhibited by the addition of an increasing amount of EGCG (Figure 18B, blue line), showing a similar paradoxical effect of EGCG in the purified system as in cells (Figure 16B).

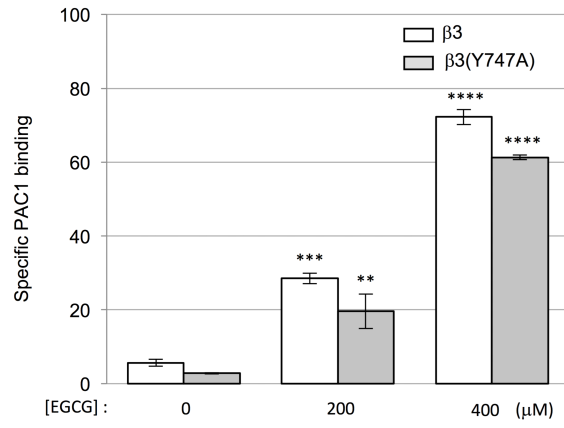
To examine the effect of EGCG on activated integrins in cells, I utilized α IIb β 3(D723R) mutant, which is activated in talin-dependent manner in CHO cells (Wegener KL *et al.*, 2007). The D723R mutation disrupts the electrostatic interaction between α IIb(R995) and β 3(D723), weakening the

7) *in vitro* purified nanodisc assay performed and analyzed by Dr. Feng Ye in UCSD.

Figure 16. EGCG both activates and inhibits activation of integrin α IIb β 3 in cells.

A, CHO cells stably expressing integrin α IIb were transfected with wild-type or talin binding-deficient mutant (Y747A) integrin β 3. EGCG-treated cells with comparable α IIb β 3 expression (high D57 staining) were gated, and the degree of integrin activation of these gated cells was measured by PAC1, an activation-specific integrin α IIb β 3 antibody. Specific PAC1 binding was calculated as $MFI - MFI_0$, where MFI is the mean fluorescence intensity of bound PAC1 and MFI_0 is that in the presence of 10 mM EDTA or 20 μ M eptifibatide, both of which inhibit integrin α IIb β 3-ligand binding. **B**, CHO cells stably expressing α IIb β 3 were transfected with empty vector or THD together with tdTomato cDNA as a transfection marker. Specific PAC1 binding of tdTomato-positive cells treated with different concentrations of EGCG was calculated and shown as described in **A**. error bars represent standard errors (n=3), and analysis of variance multiple comparison using the Bonferroni's test was performed to test for significant differences between EGCG-treated and non-treated samples. **, $p < 0.01$; ***, $p < 0.001$; ****, $p < 0.0001$.

A.



B.

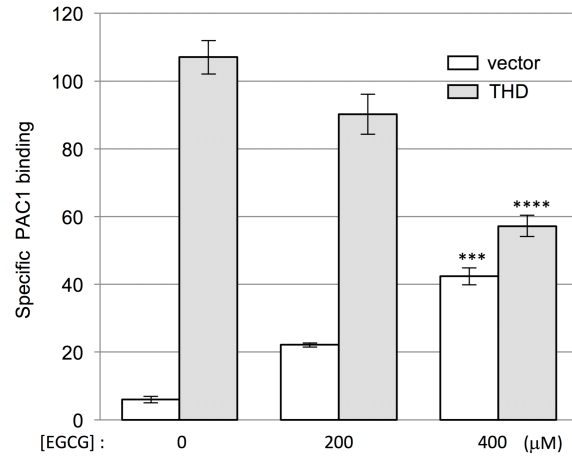


Figure 17. EGCG reversibly induces integrin activation in CHO/ α IIb β 3 cells.

CHO cells stably expressing α IIb β 3 were incubated for 30 min in the absence or presence of 200 μ M EGCG. Those cells were washed twice with Dulbecco Modified Eagle Medium for 10 min per each washing, and then treated with PAC1 in the absence or presence of 200 μ M EGCG again as indicated. PAC1 binding to these cells were analyzed and shown as histogram.

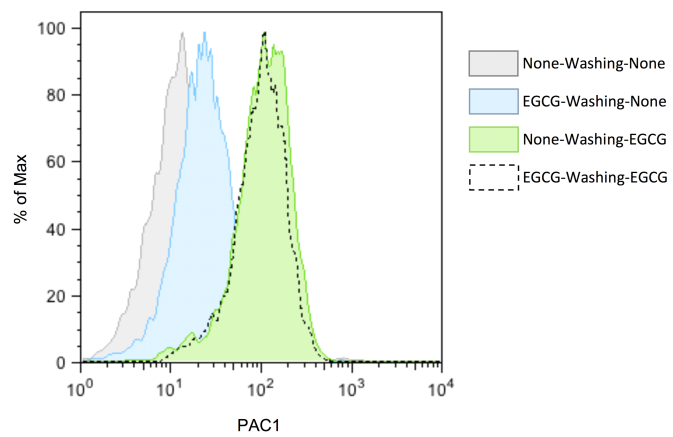
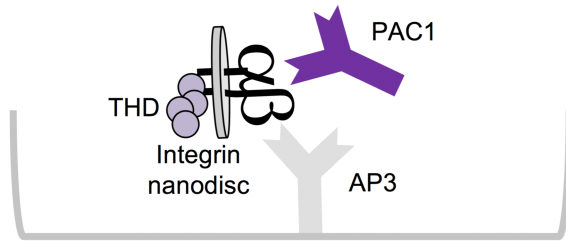


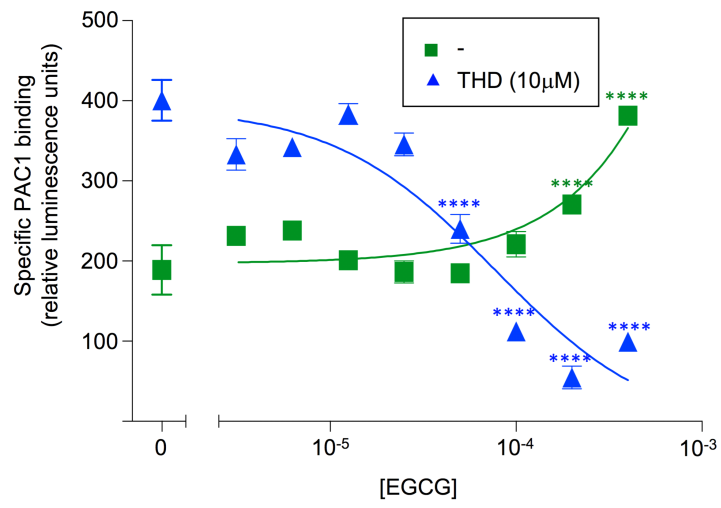
Figure 18. EGCG both activates and inhibits activation of integrin α IIb β 3 in a reconstituted system.

A, The configuration of the integrin nanodisc activation assay. Integrin nanodiscs were captured onto an ELISA plate coated with anti- β 3 antibody (AP3). Specific PAC1 binding was calculated as $L-L_0$, where L is PAC1 binding to the captured integrin nanodisc measured by chemiluminescence and L_0 is that in the presence of eptifibatide. **B**, The effects of EGCG on specific PAC1 binding were measured in the absence (green line) or presence of purified THD (10 μ M) (blue line). error bars represent standard errors (n=3) and statistical analysis performed as in **Figure 16**.

A.



B.



integrin α IIB- β 3 TMD interaction and this favoring the activated state (Hughes PE *et al.*, 1996). The activating effect of the D723R mutant is dependent upon integrin-talin interaction, as its activation is abolished by disrupting integrin binding to endogenous talin, e.g. by the β 3(Y747A) mutation (Wegner KL *et al.*, 2007). When I added EGCG to the cells expressing α IIB β 3(D723R), in sharp contrast to the activating effect observed with the wild-type integrin, I observed that EGCG induced an initial suppression of activation that peaked at 200 μ M EGCG (Figure 19A). At higher concentrations, however, EGCG induced activation, exhibiting a distinct biphasic effect (Figure 19A). Next I tested another activating mutant, α IIB β 3(L712R), in which TMD is predicted to shorten from 29 to 19 amino acids due to the polar residue in the middle of TMD (Patridge AW *et al.*, 2005). The activating effect of the α IIB β 3(L712R) mutant is talin-independent, as its activation is not affected by the loss of the talin-integrin interactions. (Wegner KL, *et al.*, 2007; Nieves B *et al.*, 2010) In contrast to α IIB β 3(D723R), EGCG had no significant effect on the L712R mutant (Figure 19B and C).

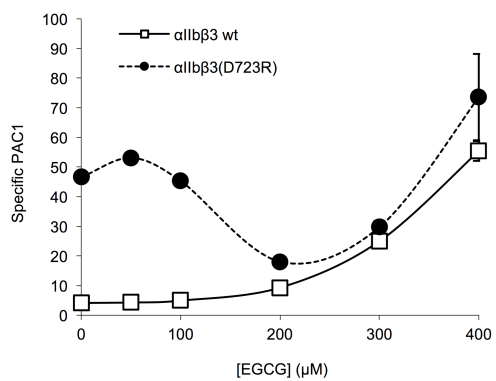
Opposing changes of integrin β 3 TMD topology by EGCG and talin

To find an explanation for these paradoxical effects, I noted the insensitivity of α IIB β 3(L712R) mutant to EGCG. This mutant activates integrin by shortening the β 3 TMD (Patridge AW *et al.*, 2005), whereas talin does it by increasing the lipid embedding of the β 3 TMD (Kim C *et al.*, 2012); both of these changes can alter the β 3 TMD tilt angle, thereby disrupting the α IIB- β 3 TMD interaction and leading to integrin activation (Lau TL *et al.*, 2009). In addition, several studies demonstrated that EGCG

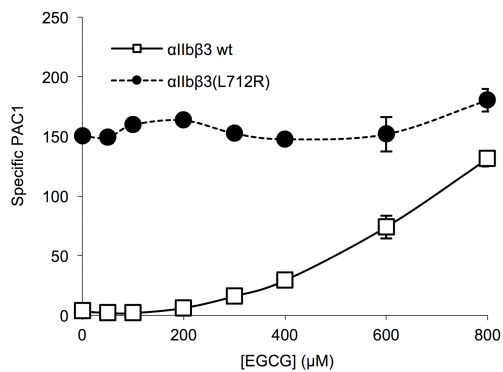
Figure 19. EGCG has distinct effects on talin-dependent and talin-independent α IIb β 3 activation.

A and **B**, CHO cells were transfected with integrin α IIb and activating β 3 mutants, β 3(D723R) (talin-dependent) or β 3(L712R) (talin-independent), and specific PAC1 binding was measured as described in **Figure 16A**. **C**, the percentage of inhibition of integrin activation was calculated as $100 \times (P_0 - P) / P_0$, where P_0 is the specific PAC1 binding in the absence of EGCG and P is that in the presence of EGCG. Note that EGCG initially inhibits and then increases activation of the talin-dependent α IIb β 3(D723R) mutant, whereas it does not inhibit the talin-independent α IIb β 3(L712R) mutant. Error bars represent standard errors (n=3). ****, $p < 0.0001$.

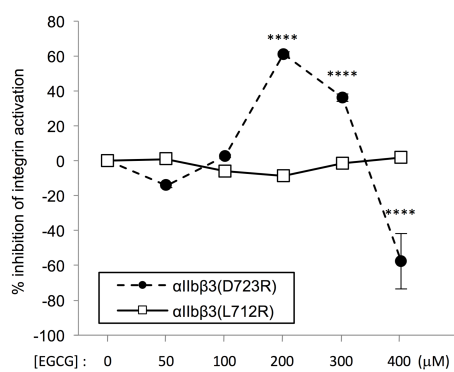
A.



B.



C.



can interact with phospholipids and can even decrease the thickness of a lipid bilayer (Scheidt HA *et al.*, 2004; Tamba Y *et al.*, 2007; Sun Y *et al.*, 2009), which may alter the lipid embedding of TMDs. To test this idea, I investigated whether EGCG can change the embedding of integrin TMD by adapting a $\beta 3$ TMD embedding assay (Kim C *et al.*, 2012). As EGCG had considerable spectral overlap with bimane, the fluorophore used in the previous study, I used another environment sensitive fluorophore, mero60, whose fluorescence increases in a more hydrophobic environment and does not overlap with that of EGCG (MacNevin CJ *et al.*, 2013). I conjugated the dye to either the N-terminal end ($\beta 3$ (L694C)) or the C-terminal end ($\beta 3$ (I721C)) of $\beta 3$ TMD and reconstituted the $\beta 3$ TMD–cytoplasmic tail peptides into phospholipid nanodiscs (Figure 20). EGCG decreased the fluorescence of mero60 at either the N-terminal end or the C-terminal end of $\beta 3$ TMD (Figure 21A and B), indicating that EGCG causes both the N-terminal and the C-terminal ends of $\beta 3$ TMD to become less embedded. The decrease in fluorescence is a specific result from altered membrane embedding of $\beta 3$ TMD, as the EGCG-induced reduction in fluorescence disappeared after the addition of 2% SDS to disassemble the nanodisc (not shown). These data strongly suggest that EGCG reduces the embedding of the $\beta 3$ TMD, although other mechanisms, e.g. EGCG-induced local unraveling of the helix, cannot be ruled out. Because the optimal association of integrin α IIb and $\beta 3$ TMD depends on the precise topology of $\beta 3$ TMD (Lau TL *et al.*, 2009), my data suggest that EGCG alters the $\beta 3$ TMD topology, thereby destabilizing the α - β TMD association and inducing integrin activation.

Figure 20. Diagram of environment sensitive fluorescence spectroscopy.

The environment-sensitive dye, mero60, was conjugated to $\beta 3$ TMD-tail peptide through the cysteine mutation at Leu⁶⁹⁴ residue to probe the embedding change of $\beta 3$ TMD at the outer membrane leaflet or at Ile⁷²¹ residue at the inner membrane leaflet. The mero60-labeled $\beta 3$ TMD-tail peptides were then incorporated into phospholipid nanodiscs.

Nanodisc

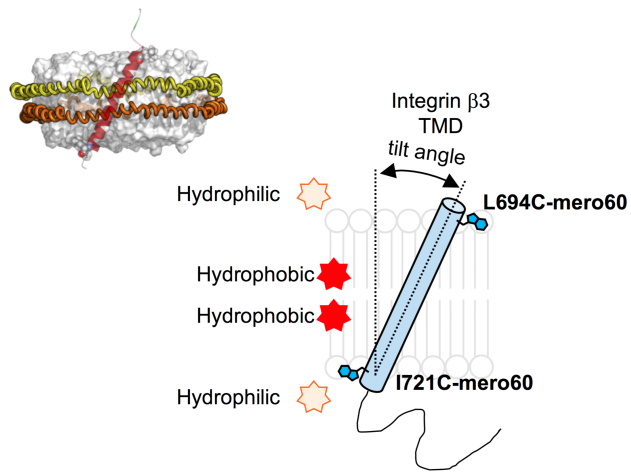
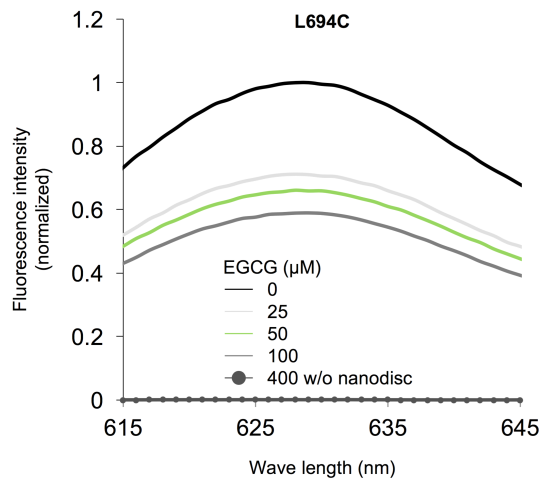


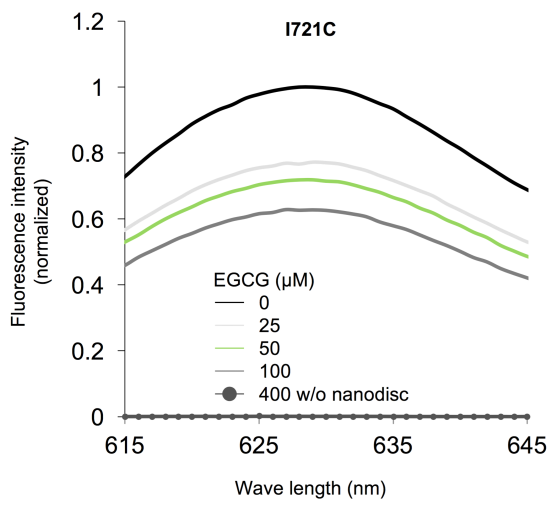
Figure 21. EGCG decreases embedding angle of β 3 TMD.

A, EGCG decreases the fluorescence intensity of L694C-mero60 nanodisc. EGCG is not fluorescent at the wavelength range measured in the analysis. Fluorescence intensities were normalized to the maximum fluorescence intensity in the L694C-mero nanodiscs without EGCG. **B**, the fluorescence of I721C-mero60 nanodiscs was analyzed as in **A**.

A.



B.



Consistent with previous report (Kim C *et al.*, 2012) that THD increases the embedding of the $\beta 3$ TMD domain, THD increased the fluorescence intensities of mero60 conjugated to $\beta 3$ (L694C) or $\beta 3$ (I721C) (Figure 22A and B, black dotted lines). The increased fluorescence reflects an altered topology of the $\beta 3$ TMD (Kim C *et al.*, 2012), which can also disrupt the association of integrin α and β TMDs. Intriguingly, EGCG reversed the THD-induced increase in the fluorescence of mero60 in both $\beta 3$ (L694C) and $\beta 3$ (I721C) (Figure 22A and B, green dotted lines), indicating that EGCG alters the topology of the $\beta 3$ TMD in a manner that opposes the effect of THD (Figure 23). I propose that EGCG-induced change of the $\beta 3$ TMD topology opposes that induced by talin. Thus, it can offset the talin-induced changes in TMD topology and integrin activation. The embedding assay using integrin $\beta 3$ TMD appears more sensitive to EGCG than the integrin activation assay. In the embedding assay, concentration of EGCG from 25 to 100 μ M caused large fluorescence changes both in the absence of talin (Figure 21A and B) and in the presence of talin (Figure 22A and B), whereas higher concentrations of EGCG were required to affect the integrin activation assay (Figure 18B). This may be due to the additional stabilizing effect of the presence of the extracellular domains, which are absent in the $\beta 3$ TMD embedding assays, on integrin $\alpha\beta$ association and activation.

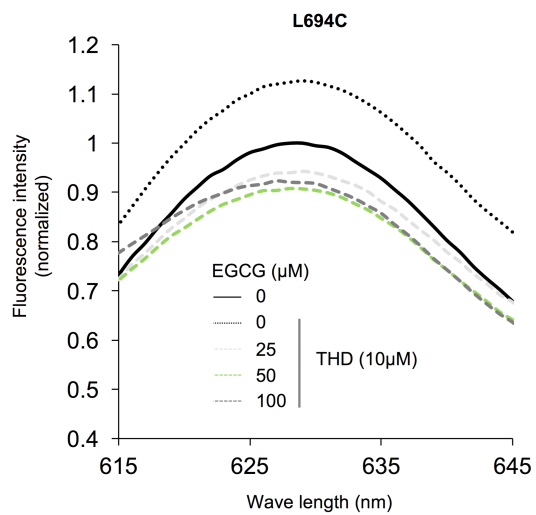
Effects of EGCG on transmembrane signaling through a receptor tyrosine kinase

If the EGCG-induced topological change of integrin $\beta 3$ TMD is due to an EGCG-lipid interaction, we reasoned that EGCG should also have effects on other transmembrane proteins with signaling functions. To test this hypothesis, I focused on the receptor tyrosine kinase because the

Figure 22. EGCG induces β 3 TMD topological changes in the opposite direction to talin.

A, L694C-mero60 nanodiscs were incubated with 10 μ M THD with or without varying concentration of EGCG. EGCG reverse the increase of mero60 fluorescence intensity induced by THD. **B**, the effect of EGCG on I721C-mero60 nanodiscs was analyzed as in **A**.

A.



B.

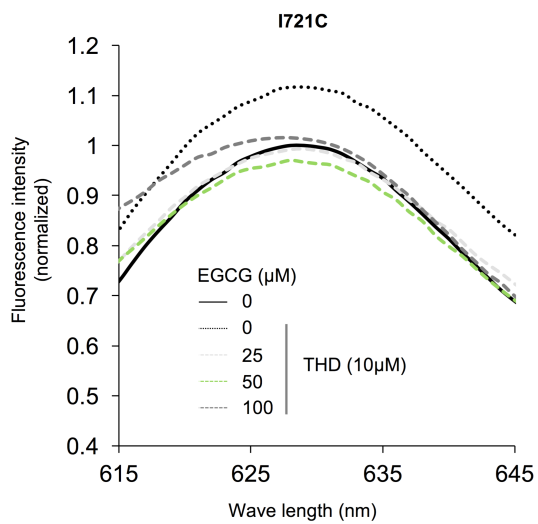
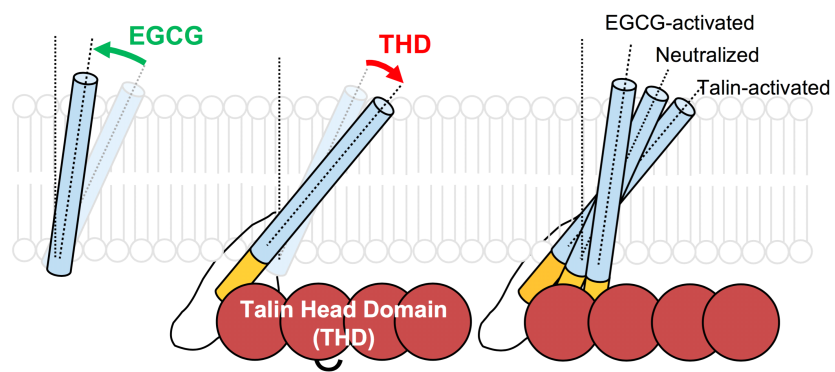


Figure 23. Proposed model of EGCG's action.

Because the association of integrin α IIb and β 3 TMD depends on the precise tilt angle of β 3 TMD, either increased or decreased embedding of the β 3 TMD can disrupt the α - β TMD association and activate the integrin. Talin binding to integrin β 3 tail increases the TMD tilt angle, thereby activating integrin. EGCG interacts with the phospholipid bilayer and reduces the integrin TMD tilting angle. When both effects are present, EGCG first neutralize the effect of talin, but continued reduction in the tilt angle by EGCG activates the integrin.



dimerization of their TMDs in the lipid bilayer may play a role in activation of those receptors (Endres NF *et al.*, 2013; Arkhipov A *et al.*, 2013). Indeed, EGCG was reported to inhibit activation of receptor tyrosine kinases such as EGFR (Liang YC *et al.*, 1997; Adachi S *et al.*, 2007), possibly due to effects on lipid order (Adachi S *et al.*, 2007). Pretreatment of HEK293 cells stably expressing EGFR with EGCG inhibited EGF-induced EGFR phosphorylation. (Figure 24) In contrast, EGCG treatment in the absence of EGF induced EGFR phosphorylation in a concentration-dependent manner. (Figure 25) Furthermore, EGCG decreased the fluorescence intensity of mero60 attached to the C-terminal region of the nanodisc-embedded EFGR TMD. (Figure 26) These data suggest that a topological change of EGFR TMD induced by EGF (Moriki T *et al.*, 2001) can be reversed by the action of EGCG, and that EGCG-induced topological change in the absence of EGF may favor dimerization of EGFR TMDs, leading to activation.

Figure 24. EGCG decreases EGF induced phosphorylation of EGFR.

HEK293 cells expressing FLAG-tagged human EGFR (HEK/EGFR) were serum-starved overnight and pretreated with different concentrations of EGCG. 30min after EGCG treatment, cells were stimulated with 50 ng/ml EGF for an additional 30 min. EGFR was immunoprecipitated (IP) and analyzed by western blotting (WB) with anti-phosphotyrosine antibody (4G10) and anti-EGFR antibody. The degree of phosphotyrosine signal per precipitated EGFR band intensities was normalized to unstimulated control (0%) and EGF-treated control (100%), and shown as a bar graph for each sample. Error bars represent standard errors (n=3). Representative western blots are shown above.

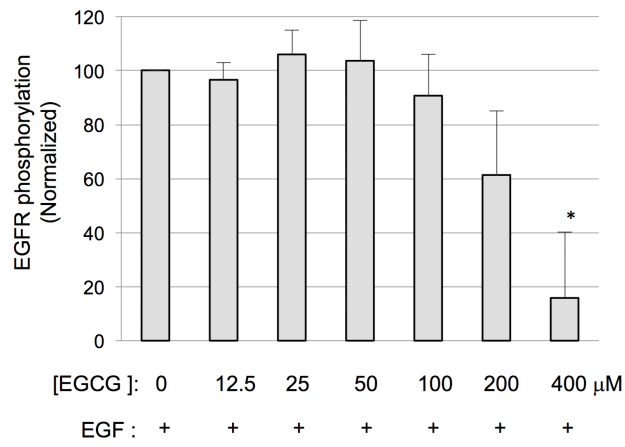
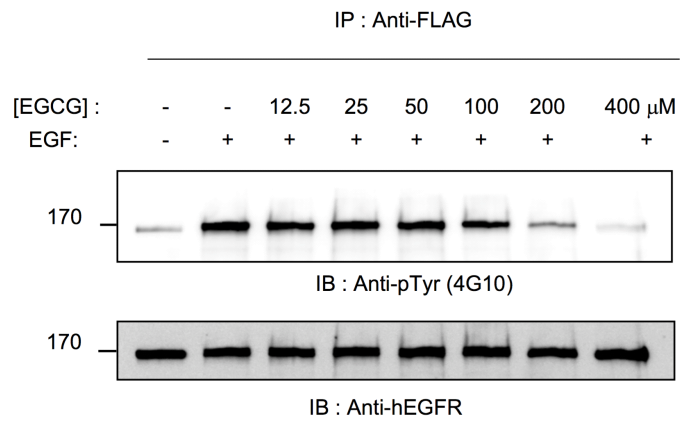


Figure 25. EGCG alone increases phosphorylation of EGFR

EGCG treated as in Figure 10. EGCG induced EGFR phosphorylation in a dose-dependent manner. Error bars represent standard errors (n=3). Statistical analysis performed as in **Figure 16A**. *, $p < 0.05$; ****, $p < 0.0001$.

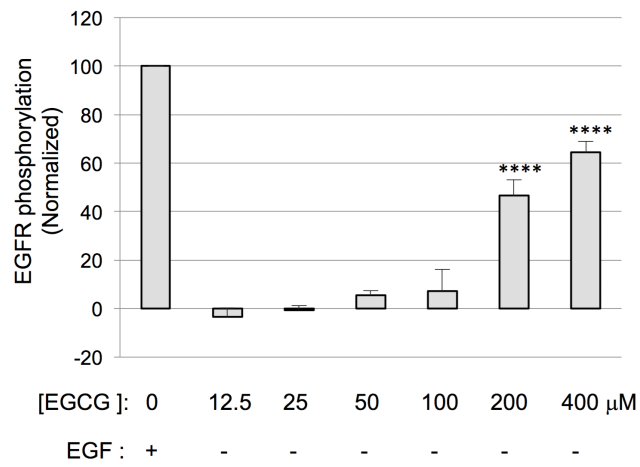
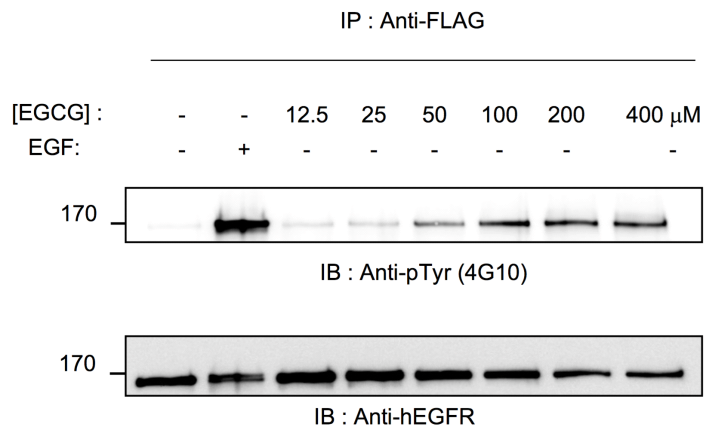
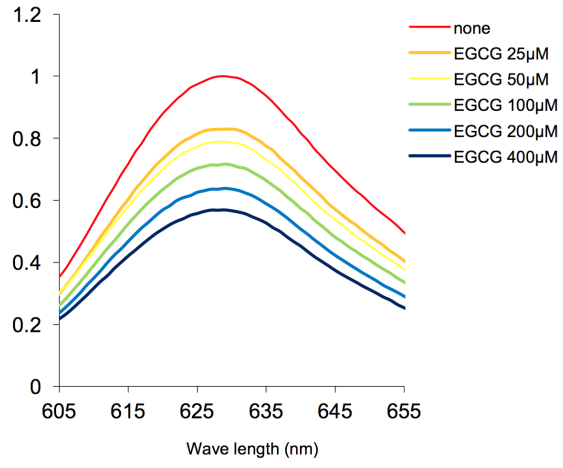


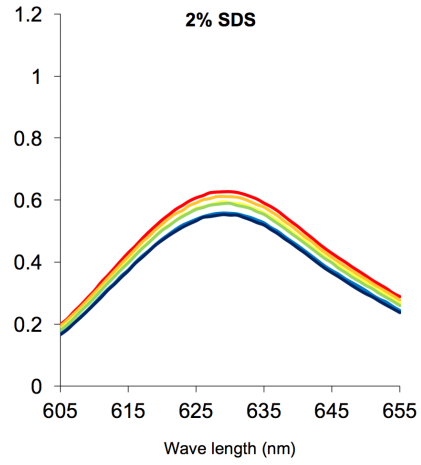
Figure 26. Effects of EGCG on lipid embedding of EGFR TMD.

Left, purified EGFR TMD peptide (EGFR(F667C)) labeled with mero60 was reconstituted into nanodiscs, and the effect of EGCG on the embedding of EGFR TMD was analyzed as in **Figure 21A**. **Right**, EGCG had little effect on mero60 fluorescence when EGFR TMD nanodiscs were solubilized with 2% SDS.

EGFR(F667C)



2% SDS



CONCLUSION

My results show that EGCG can change the TMD topologies of receptors and activate those receptors. Conversely, when physiological activation involves shifts in TMD topology, then EGCG can oppose those shifts and inhibit transmembrane signaling. I propose that such a dual effect can account for the conflicting reported effects of EGCG. Recent studies showed that EGCG can bind to lipid bilayers and reside near the phosphate head groups of phospholipids, and that the interaction is further stabilized by cation- π interaction between one of the ring structures in EGCG and the quaternary amine of the phospholipid head group (Uekusa Y *et al.*, 2011). Because the interaction between TMDs and phospholipids can influence the topology of TMDs in a lipid bilayer by mechanisms such as snorkeling of the basic lysine side chain into the phosphate head groups of the phospholipids (Kim C *et al.*, 2012), EGCG may alter the interaction of the TMD with the phosphate head group, thus leading to changes in TMD topology. Alternatively, the rigidity of lipids induced by insertion of EGCG into hydrophobic lipid bilayer, as suggested by molecular simulation study (Sirk TW *et al.*, 2009), or the rigidity of lipid-inserted EGCG itself, due to its less flexible aromatic rings, might alter the tilt angle of TMDs, causing less embedding. Future studies will be required to address these hypothesis; however, my observation that EGCG has a dual effect on transmembrane signaling by modulating lipid embedding of TMDs provides an attractive mechanism to explain some of EGCG's pleiotropic effects on transmembrane signaling.

REFERENCES

Adachi S, Nagao T, Ingolfsson HI, Maxfield FR, Andersen OS, Kopelovich L, Weinstein IB. The inhibitory effect of (-)-epigallocatechin gallate on activation of the epidermal growth factor receptor is associated with altered lipid order in HT29 colon cancer cells. *Cancer Res.* 2007 Jul 1;67(13):6493-501.

Arkipov A, Shan Y, Das R, Endres NF, Eastwood MP, Wemmer DE, Kuriyan J, Shaw DE. Architecture and membrane interactions of the EGF receptor. *Cell.* 2013 Jan 31;152(3):557-69

Babu PV, Liu D. Green tea catechins and cardiovascular health: an update. *Curr Med Chem.* 2008;15(18):1840-50.

Calderwood DA, Zent R, Grant R, Rees DJ, Hynes RO, Ginsberg MH. The Talin head domain binds to integrin beta subunit cytoplasmic tails and regulates integrin activation. *J Biol Chem.* 1999 Oct 1;274(40):28071-4.

Denisov IG, Grinkova YV, Lazarides AA, Sligar SG. Directed self-assembly of monodisperse phospholipid bilayer Nanodiscs with controlled size. *J Am Chem Soc.* 2004 Mar 24;126(11):3477-87.

Endres NF, Das R, Smith AW, Arkipov A, Kovacs E, Huang Y, Pelton JG, Shan Y, Shaw DE, Wemmer DE, Groves JT, Kuriyan J. Conformational coupling across the plasma membrane in activation of the EGF receptor. *Cell.* 2013 Jan 31;152(3):543-56.

Escribá PV, González-Ros JM, Goñi FM, Kinnunen PK, Vigh L, Sánchez-Magraner L, Fernández AM, Busquets X, Horváth I, Barceló-Coblijn G. Membranes: a meeting point for lipids, proteins and therapies. *J Cell Mol Med.* 2008 Jun;12(3):829-75.

Hughes PE, Diaz-Gonzalez F, Leong L, Wu C, McDonald JA, Shattil SJ, Ginsberg MH. Breaking the integrin hinge. A defined structural constraint regulates integrin signaling. *J Biol Chem.* 1996 Mar 22;271(12):6571-4.

Iwamoto DV, Calderwood DA. Regulation of integrin-mediated adhesions. *Curr Opin Cell Biol.* 2015 Oct;36:41-7.

Kalli AC, Campbell ID, Sansom MS. Multiscale simulations suggest a mechanism for integrin inside-out activation. *Proc Natl Acad Sci U S A.* 2011 Jul 19;108(29):11890-5.

Kang WS, Lim IH, Yuk DY, Chung KH, Park JB, Yoo HS, Yun YP. Antithrombotic activities of green tea catechins and (-)-epigallocatechin gallate. *Thromb Res.* 1999 Nov 1;96(3):229-37.

Killian JA, von Heijne G. How proteins adapt to a membrane-water interface. *Trends Biochem Sci.* 2000 Sep;25(9):429-34.

Kim C, Schmidt T, Cho EG, Ye F, Ulmer TS, Ginsberg MH. Basic amino-acid side chains regulate transmembrane integrin signalling. *Nature.* 2011 Dec 18;481(7380):209-13

Kim C, Ye F, Hu X, Ginsberg MH. Talin activates integrins by altering the topology of the beta transmembrane domain. *J Cell Biol.* 2012 May

28;197(5):605-11.

Kuriyama S. The relation between green tea consumption and cardiovascular disease as evidenced by epidemiological studies. *J Nutr.* 2008 Aug;138(8):1548S-1553S.

Lau TL, Kim C, Ginsberg MH, Ulmer TS. The structure of the integrin alphaIIb beta3 transmembrane complex explains integrin transmembrane signalling. *EMBO J.* 2009 May 6;28(9):1351-61.

Lee AG. Lipid-protein interactions in biological membranes: a structural perspective. *Biochim Biophys Acta.* 2003 May 2;1612(1):1-40.

Lee WJ, Shim JY, Zhu BT. Mechanisms for the inhibition of DNA methyltransferases by tea catechins and bioflavonoids. *Mol Pharmacol.* 2005 Oct;68(4):1018-30

Liang YC, Lin-shiau SY, Chen CF, Lin JK. Suppression of extracellular signals and cell proliferation through EGF receptor binding by (-)-epigallocatechin gallate in human A431 epidermoid carcinoma cells. *J Cell Biochem.* 1997 Oct 1;67(1):55-65.

Lill G, Voit S, Schrör K, Weber AA. Complex effects of different green tea catechins on human platelets. *FEBS Lett.* 2003 Jul 10;546(2-3):265-70.

MacNevin CJ, Gremyachinskiy D, Hsu CW, Li L, Rougie M, Davis TT, Hahn KM. Environment-sensing merocyanine dyes for live cell imaging applications. *Bioconjug Chem.* 2013 Feb 20;24(2):215-23.

Moriki T, Maruyama H, Maruyama IN. Activation of preformed EGF receptor dimers by ligand-induced rotation of the transmembrane domain. *J Mol Biol.* 2001 Aug 31;311(5):1011-26.

Nieves B, Jones CW, Ward R, Ohta Y, Reverte CG, LaFlamme SE. The NPIY motif in the integrin beta1 tail dictates the requirement for talin-1 in outside-in signaling. *J Cell Sci.* 2010 Apr 15;123(Pt 8):1216-26.

Palhano FL, Lee J, Grimster NP, Kelly JW. Toward the molecular mechanism(s) by which EGCG treatment remodels mature amyloid fibrils. *J Am Chem Soc.* 2013 May 22;135(20):7503-10.

Patra SK, Rizzi F, Silva A, Rugina DO, Bettuzzi S. Molecular targets of (-)-epigallocatechin-3-gallate (EGCG): specificity and interaction with membrane lipid rafts. *J Physiol Pharmacol.* 2008 Dec;59 Suppl 9:217-35.

Partridge AW, Liu S, Kim S, Bowie JU, Ginsberg MH. Transmembrane domain helix packing stabilizes integrin alphaIIb beta3 in the low affinity state. *J Biol Chem.* 2005 Feb 25;280(8):7294-300.

Scheidt HA, Pampel A, Nissler L, Gebhardt R, Huster D. Investigation of the membrane localization and distribution of flavonoids by high-resolution magic angle spinning NMR spectroscopy. *Biochim Biophys Acta.* 2004 May 27;1663(1-2):97-107.

Shattil SJ, Hoxie JA, Cunningham M, Brass LF. Changes in the platelet membrane glycoprotein IIb/IIIa complex during platelet activation. *J Biol Chem.* 1985 Sep 15;260(20):11107-14.

Shattil SJ, Kim C, Ginsberg MH. The final steps of integrin activation: the end game. *Nat Rev Mol Cell Biol.* 2010 Apr;11(4):288-300.

Shimizu M, Adachi S, Masuda M, Kozawa O, Moriwaki H. Cancer chemoprevention with green tea catechins by targeting receptor tyrosine kinases. *Mol Nutr Food Res.* 2011 Jun;55(6):832-43.

Singh BN, Shankar S, Srivastava RK. Green tea catechin, epigallocatechin-3-gallate (EGCG): mechanisms, perspectives and clinical applications. *Biochem Pharmacol.* 2011 Dec 15;82(12):1807-21.

Sirk TW, Brown EF, Friedman M, Sum AK. Molecular binding of catechins to biomembranes: relationship to biological activity. *J Agric Food Chem.* 2009 Aug 12;57(15):6720-8

Sun Y, Hung WC, Chen FY, Lee CC, Huang HW. Interaction of tea catechin (-)-epigallocatechin gallate with lipid bilayers. *Biophys J.* 2009 Feb;96(3):1026-35.

Tachibana H, Koga K, Fujimura Y, Yamada K. A receptor for green tea polyphenol EGCG. *Nat Struct Mol Biol.* 2004 Apr;11(4):380-1

Tamba Y, Ohba S, Kubota M, Yoshioka H, Yoshioka H, Yamazaki M. Single GUV method reveals interaction of tea catechin (-)-epigallocatechin gallate with lipid membranes. *Biophys J.* 2007 May 1;92(9):3178-94.

Uekusa Y, Kamihira-Ishijima M, Sugimoto O, Ishii T, Kumazawa S, Nakamura K, Tanji K, Naito A, Nakayama T. Interaction of epicatechin gallate with phospholipid membranes as revealed by solid-state NMR



spectroscopy. *Biochim Biophys Acta*. 2011 Jun;1808(6):1654-60.

Wegener KL, Partridge AW, Han J, Pickford AR, Liddington RC, Ginsberg MH, Campbell ID. Structural basis of integrin activation by talin. *Cell*. 2007 Jan 12;128(1):171-82.

Ye F, Hu G, Taylor D, Ratnikov B, Bobkov AA, McLean MA, Sligar SG, Taylor KA, Ginsberg MH. Recreation of the terminal events in physiological integrin activation. *J Cell Biol*. 2010 Jan 11;188(1):157-73.

Part III

Identification of indothiazinone as a natural antiplatelet agent

Chansik Yang^{1,2,†}  | Sugyeong Kwon^{3,†} | Se-Jong Kim¹ | Minseon Jeong³ |
Ji-Young Park⁴ | Dongeun Park² | Soon Jun Hong⁵ | Jong-Wha Jung³ |
Chungho Kim¹ 

¹Department of Life Sciences, Korea University, Seoul, Korea

²School of Biological Sciences, Seoul National University, Seoul, Korea

³College of Pharmacy, Research Institute of Pharmaceutical Sciences, Kyungpook National University, Daegu, Korea

⁴Department of Clinical Pharmacology and Toxicology, Korea University Anam Hospital, Seoul, Korea

⁵Department of Cardiology, Cardiovascular Center, Korea University Anam Hospital, Seoul, Korea

Correspondence

Chungho Kim, Department of Life Sciences, Korea University, Seoul, Korea.
Email: chungho@korea.ac.kr
and

Jong-Wha Jung, College of Pharmacy, Research Institute of Pharmaceutical Sciences, Kyungpook National University, Daegu, Korea.

Email: jungj@knu.ac.kr

Funding information

Korean Health Technology R&D Project, Grant/Award Number: HI14C0209

Cardiovascular disease, which is caused by unregulated platelet aggregation, is one of the main causes of deaths worldwide. Many studies have focused on natural products with antiplatelet effects as a safe alternative therapy to prevent the disease. In this context, an in-house chemical library was screened to find natural products capable of inhibiting the interaction between platelet integrin α IIb β 3 and fibrinogen, which is an essential step in platelet aggregation. On the basis of the screening results, indothiazinone, an alkaloid found in microbial cultures, was identified as a potential antiplatelet agent. Specifically, indothiazinone treatment significantly inhibited the binding of fibrinogen to Chinese hamster ovary cells expressing integrin α IIb β 3. It also restricted thrombin- and adenosine diphosphate-dependent spreading of human platelets on a fibrinogen matrix. More importantly, surface plasmon resonance and molecular dynamics studies suggested that indothiazinone suppressed talin-induced activation of integrin α IIb β 3 presumably by inhibiting talin-integrin interaction. In conclusion, these results suggest that indothiazinone can be used as a lead compound for the development of antiplatelet drugs with a novel mode of action.

KEYWORDS

antiplatelet drug, indothiazinone, integrin α IIb β 3, platelet, talin

1 | INTRODUCTION

Platelets circulating in blood are essential for hemostasis. Upon injury to the blood vessels, platelets rapidly adhere to injured sites and form fibrinogen-mediated platelet aggregates, or thrombus, thus preventing further bleeding.^[1] Unregulated thrombus formation, however, can block blood flow leading to cardiovascular diseases, such as myocardial infarction.^[1] Thus, antiplatelet drugs that can reduce platelet aggregation are beneficial for patients with a high risk of thrombosis.

[†]These authors contribute equally to the work.

Antiplatelet effects of natural products are of considerable interest for the prevention as well as treatment of cardiovascular diseases.^[2] Dietary food-derived bioactive compounds have gained much attention as the consumption of healthy dietary food increases, and growing amount of data have shown the antiplatelet activities exerted by these compounds.^[3] For instance, unsaturated fatty acids,^[4] sulfides,^[5] carotenoids,^[6] and polyphenols including flavonols^[7] are well-known cardioprotective agents from dietary sources, and have proven to be effective in decreasing platelet activation by various mechanisms. Compared to the exhaustive studies on dietary constituents showing antiplatelet activities, natural antiplatelet compounds from other sources have been

This work published in *Chem. Biol. Drug Design* 2017 Nov;90(5): 873–882,

Study on the Mechanism of Integrin $\alpha\text{IIb}\beta\text{3}$ Activation by Natural products

Chansik Yang
School of biological sciences
The graduate school
Seoul National University

Cardiovascular disease, which is caused by unregulated platelet aggregation, is one of the main causes of deaths worldwide. Many studies have focused on natural products with antiplatelet effects as a safe alternative therapy to prevent the disease. In this context, an in-house chemical library was screened to find natural products capable of inhibiting the interaction between platelet integrin $\alpha\text{IIb}\beta\text{3}$ and fibrinogen, which is an essential step in platelet aggregation. On the basis of the screening results, indothiazinone, an alkaloid found in microbial culture, was identified as a potential antiplatelet agent. Specifically, indothiazinone treatment significantly inhibited the binding of fibrinogen to Chinese hamster ovary cells expressing integrin $\alpha\text{IIb}\beta\text{3}$. It also restricted thrombin- and adenosine diphosphate-dependent spreading of human platelets on a fibrinogen matrix. More importantly, surface plasmon resonance and molecular dynamics studies suggested that indothiazinone suppressed talin-induced activation of integrin $\alpha\text{IIb}\beta\text{3}$ presumably by inhibiting talin-integrin interaction. In conclusion, these results suggest that indothiazinone can be used as a lead compound for the development

of antiplatelet drugs with a novel mode of action.⁸⁾

Key Words : antiplatelet drug, indothiazinone, integrin $\alpha\text{IIb}\beta\text{3}$, platelet, talin

Student Number : 2013-20302

8) All of contents in here published in *Chem. Biol. Drug Design* 2017 Nov;90(5): 873-882, and I participated as a main author.

Introduction

Platelets circulating in blood are essential for hemostasis. Upon injury to the blood vessels, platelets rapidly adhere to injured sites and form fibrinogen-mediated platelet aggregates, or thrombus, thus preventing further bleeding (Jackson SP, 2011). Unregulated thrombus formation, however, can block blood flow leading to cardiovascular disease, such as myocardial infarction (Jackson SP, 2011). Thus, antiplatelet drugs that can reduce platelet aggregation are beneficial for patients with a high risk of thrombosis.

Antiplatelet effects of natural products are of considerable interest for the prevention as well as treatment of cardiovascular diseases (Vilahur G *et al.*, 2013). Dietary food-derived bioactive compounds have gained much attention as the consumption of healthy dietary food increases, and growing amount of data have shown the antiplatelet activities exerted by these compounds (Alissa EM *et al.*, 2012). For instance, unsaturated fatty acids (Dimitrow PP *et al.*, 2009), sulfides (Kram L *et al.*, 2013), carotenoids (Hsiao G *et al.*, 2005), and polyphenols including flavonols (Santhakumar AB *et al.*, 2014) are well-known cardioprotective agents from dietary sources, and have proven to be efficient in decreasing platelet activation by various mechanisms. Compared to the exhaustive studies on dietary constituents showing antiplatelet activities, natural antiplatelet compounds from other sources have been rarely explored. Considering that cardiovascular disease are major causes of death globally, identification of antiplatelet compounds with structural novelties from natural sources is of great importance.

I was interested in the identification of integrin $\alpha\text{IIb}\beta\text{3}$ -dependent antiplatelet compounds from various natural sources, particularly those that meet the criteria of “lead-likeness” for the development of pharmaceutical

agents. Integrin $\alpha\text{IIb}\beta\text{3}$, also called glycoprotein IIb/IIIa, is well known for its pivotal role in platelet aggregation (Nieswandt B *et al.*, 2009; Hynes RO, 2002). Unlike other integrins found on other cells, integrin $\alpha\text{IIb}\beta\text{3}$ is selectively expressed on platelets (Hynes RO, 2002). During platelet aggregation, conformational changes in the extracellular domain of the integrin, also termed as integrin activation, facilitate fibrinogen binding. Because fibrinogen has multiple integrin binding sites (Lishko VK *et al.*, 2004), the activated integrins in the surface of platelets can adhere to the same fibrinogen molecule that form bridges between adjacent platelets, leading to platelet aggregation. Thus, integrin $\alpha\text{IIb}\beta\text{3}$ is considered a promising target in the discovery and development of antiplatelet agents (Bledzka K *et al.*, 2013). A majority of integrin $\alpha\text{IIb}\beta\text{3}$ -dependent antiplatelet agents are competitive inhibitors that directly interfere with the binding of fibrinogen to integrin $\alpha\text{IIb}\beta\text{3}$. Antibodies, disintegrins, and Arg-Gly-Asp sequence analogs with the mode of action have been developed as potent antiplatelet agents (Bledzka K *et al.*, 2013) and three of them, abciximab, eptifibatid, and tirofiban, are clinically available (Estevez B *et al.*, 2015). Despite the clinical efficacy of these antiplatelet agents, severe thrombocytopenia, paradoxical induction of thrombosis, as well as bleeding have been reported as adverse side effects (Bledzka K *et al.*, 2013). Several studies have also revealed that binding of such ligand-mimetic compounds results in conformational changes in the extracellular domains of integrin $\alpha\text{IIb}\beta\text{3}$, which may even induce integrin-dependent downstream signaling (Reynolds AR *et al.*, 2009; Du XP *et al.*, 1991). Thus, the identification of novel compounds possessing integrin $\alpha\text{IIb}\beta\text{3}$ -dependent antiplatelet activity with a different mode of action is still in need for the development of new classes of antiplatelet agents.

In this study, antiplatelet activity of indothiazinone, also known as 1H-indol-3-yl(1,3-thiazol-2-yl)methanone, is described. Unlike other natural

antiplatelet agents from dietary sources, indothiazinone is an alkaloid isolated from microbial cultures (Jasen R *et al.*, 2014; Kwon S *et al.*, 2015). Because indothiazinone possess a novel scaffold rarely found in nature, this study suggest that it can be a useful lead compound in the development of antiplatelet drugs with novel mode of action.

MATERIALS AND METHODS

Synthesis of indothiazinone and its derivatives

Synthesis of in house library containing indothiazinone and its derivatives performed and provided by Prof. Jong-Wha Jung in Kyungpook National University.

Cell culture and cell adhesion assay

Chinese hamster ovary cell lines expressing integrin $\alpha\text{IIb}\beta\text{3}$, A5 provided by Dr. Mark Ginsberg (University of California, San Diego) or H2 generated by lentivirus infection as described previously (Kim J *et al.*, 2016) were maintained in Dulbecco's modified Eagle's medium (DMEM) supplemented with 10% fetal bovine serum, 100 U/mL penicillin, 100 $\mu\text{g}/\text{mL}$ streptomycin, 2 mM L-glutamine, and non-essential amino acids. For cell adhesion assay, 96-well plates were first coated with 5-10 $\mu\text{g}/\text{mL}$ fibrinogen in phosphate-buffered saline (PBS) overnight at 4 °C, and then blocked to prevent non-specific cell adhesion by further incubation with 2% bovine serum albumin in PBS for 2 h at room temperature. Subconfluent cells were detached by trypsinization and the cell suspension was washed twice with DMEM. Aliquots of these cells were added to the wells of the fibrinogen-coated 96-well plates and incubated for 0.5-1 h at 37 °C in a CO₂ incubator in the presence of indothiazinone, KCH-1569, or other indothiazinone derivatives. After washing three times with DMEM, the remaining cells were quantified using the Cell Counting Kit-8 (Dojindo Molecular Technologies, Rockville, MD, USA) according to the manufacturer's instructions.

Platelet isolation and spreading assay

Blood was collected from a healthy donor in accordance with the protocol approved by the institutional review board of the Korea University Anam Hospital (IRB Number: ED14130). For platelet isolation, blood samples from a healthy donor were collected into BD Vacutainer tubes containing 3.2% sodium citrate buffer (BD, Franklin Lakes, NJ, USA). A 3-mL sample of the blood/citrate mixture was then added to 875 μ L of modified Tyrode's solution (140 mM NaCl, 2.7 mM KCl, 0.4 mM NaH₂PO₄, 10 mM NaHCO₃, 5 mM dextrose, and 10 mM HEPES, pH 7.4), 175 μ L of ACD buffer (85 mM sodium citrate, 65 mM citric acid, and 104 mM D-glucose, pH 4.4), and 1 U/ μ L apyrase. The mixture was centrifuged at 200 g at room temperature, and the supernatant (platelet-rich plasma, PRP) was treated with 1 U/ μ L apyrase and 0.375 mM prostaglandin E1, before incubation for 10 min in the dark. The PRP was then centrifuged at 700 g for 5 min at room temperature, and the pellet was resuspended in Walsh buffer (137 mM NaCl, 2.7 mM KCl, 1 mM MgCl₂, 3.3 mM NaH₂PO₄, and 20 mM HEPES, pH 7.4). The platelet suspension was incubated on the 10 μ g/mL fibrinogen-coated cover glass for 1 h in the presence of agonist (ADP or thrombin), indothiazinone, KCH-1569, and/or vehicle. Unbound platelets were washed with Walsh buffer, and bound platelets were fixed with 3.5% formaldehyde and stained with rhodamine-phalloidin for visualization.

Platelet imaging and quantitation

Fluorescence and differential interference contrast images of the stained platelets were taken using an inverted fluorescence microscope (TI-E; Nikon, Tokyo, Japan) equipped with a charge-coupled device camera and a 100 \times oil lens. Three random fields were captured per coverslip for each experimental condition. The ratio of total adherent platelet area divided by total number of platelets was calculated using the ImageJ software.

Integrin activation assay

A5 cells were transfected with green fluorescent protein (GFP)-fused talin head domain or GFP alone. After 24h, the cells were detached and washed with DMEM. Then, cells were first incubated with indothiazinone or KCH-1569 for 10 min at room temperature, followed by further incubation with the anti-integrin $\alpha\text{IIb}\beta\text{3}$ activation-specific antibody, PAC1, for 30 min. After washing, allophycocyanin-conjugated anti-mouse IgM antibody was added to the reaction mixture. Stained cells were analyzed using a FACS Calibur cytometer (BD Biosciences). Cells were gated and grouped according to their GFP fluorescence, and the mean fluorescence from PAC1 binding to these cells was analyzed using MatLab software as previously described. (Kim J *et al.*, 2016)

Surface plasmon resonance binding assay

6xHis-tagged talin F2 and F3 subdomains (6xHis-talin F2/F3) of talin head domains was purified using HisPurTM Ni-NTA resin (Thermo Scientific). Surface plasmon resonance response curves were obtained using a range of indothiazinone concentration. A ProteOn XPR36 system (Bio-Rad, Hercules, CA, USA) equipped with a sensor chip was used for real-time binding studies. A solution of PBS and 0.005% Tween 20 was used as the running buffer and for sample preparation. The 6xHis-talin F2/F3 was immobilized onto the channels of an HTE chip (Bio-Rad), leaving one channel as reference. A 210- μL sample of talin (2.5 mg/mL, His-tagged) was injected into the flow cells (30 $\mu\text{L}/\text{min}$) to allow saturation of the HTE chip. Binding kinetics analysis was performed by injecting 100- μl aliquots of serially diluted indothiazinone (50 to 800 μM) containing 4% DMSO in TBS-T buffer into the channels of the HTE chip for 1 min at 100 $\mu\text{L}/\text{min}$. The recorded resonance units (RU) were plotted against indothiazinone concentration. To obtain the dissociation curves, PBS-T

buffer (100 $\mu\text{L}/\text{min}$) was flushed over the chip for 200s to dissociate the bound analytes. The ProteOn XPR36 control software, ProteOn Manager v.3.1.0.6, was used to record changes in the RUs, as well as to plot and analyze the binding curves. The RUs were normalized by subtracting the RU of the empty channel. The kinetic and equilibrium constants were obtained by global fitting of the Langmuir 1:1 bimolecular kinetic model.

RESULTS

Identification of indothiazinone as a natural antiplatelet agents

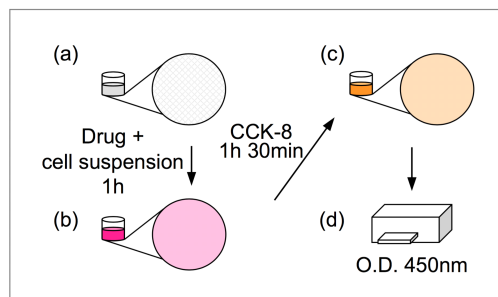
To screen natural products showing antiplatelet activity, I set up an easy and robust cellular assay that can mimic the platelet–fibrinogen interaction, the essential step in platelet aggregation (Phillips DR *et al.*, 1988). As platelets depend on integrin $\alpha\text{IIb}\beta\text{3}$ for fibrinogen binding (Aslan JE *et al.*, 2012) and cells expressing the integrin can specifically adhere to fibrinogen-coated surfaces, I used the Chinese hamster ovary (CHO) cell line stably expressing human integrin $\alpha\text{IIb}\beta\text{3}$ (CHO/ $\alpha\text{IIb}\beta\text{3}$) (Kim J *et al.*, 2016) and fibrinogen-coated 96-well plates as the screening platform. Adhesion of the cells to the plate was quantified by assessing the cellular dehydrogenase activity (Figure 27A and B). In this assay, I screened in-house chemical library (provided from Professor Jong-Wha Jung in Kyungpook National University) and found that indothiazinone (Figure 27C) inhibited the adhesion of CHO/ $\alpha\text{IIb}\beta\text{3}$ to fibrinogen.

To confirm the antiplatelet activity of indothiazinone, I investigated its effect on agonist-induced platelet spreading on fibrinogen-coated surface, one of the assays widely used to monitor platelet activity (Aslan JE *et al.*, 2012). Unstimulated platelets isolated from healthy donors bound to immobilized fibrinogen and formed filopodia-like protrusions within an hour (Top left panels of Figure 28A and B), while platelets stimulated by 10 μM adenosine diphosphate (ADP) (bottom left panels of Figure 28 A and B) or 1.6 U/ml thrombin (not shown) spread fully on the surface. Interestingly, treatment with 200 μM indothiazinone dramatically inhibited

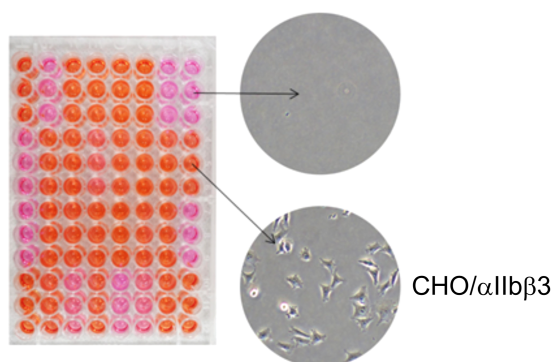
Figure 27. Antiplatelet activity of indothiazinone.

A, Schematic diagram of 96-well plate-based cell adhesion assay. Wells were coated with fibrinogen (a), and CHO/ α IIb β 3 cells in the presence of individual chemicals were incubated on the well surface for 1 hr (b). After washing, bound cells were incubated with CCK-8 reagents (c). Optical density of the media was measured at 450nm to quantify the degree of cell adhesion (d). **B**, Representative images of cell adhesion assay after O.D. measured. As described in A, CCK-8 reagents turn to orange by adherent cells(right, bottom) and non of cells adherent in BSA coated well(right upper). **C**, Chemical structure of indothiazinone.

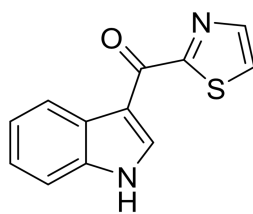
A.



B.



C.

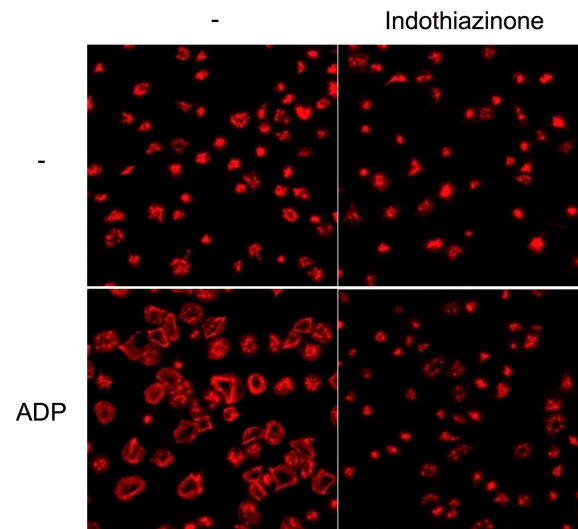


Indothiazinone (1)

Figure 28. Representative images of platelet spreading on fibrinogen matrix.

A, Isolated human platelets were incubated on a fibrinogen-coated cover glass for 1 hr in the presence of indothiazinone and/or adenosine diphosphate (ADP) (10 μ M). Platelets were then stained for actin with rhodamine-phalloidin. **B**, Differential interference contrast images of platelets in **A**. Scale bar, 10 μ m

A.



B.

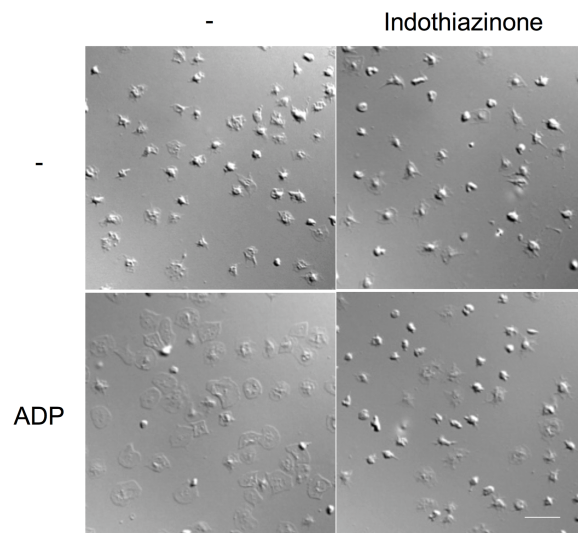
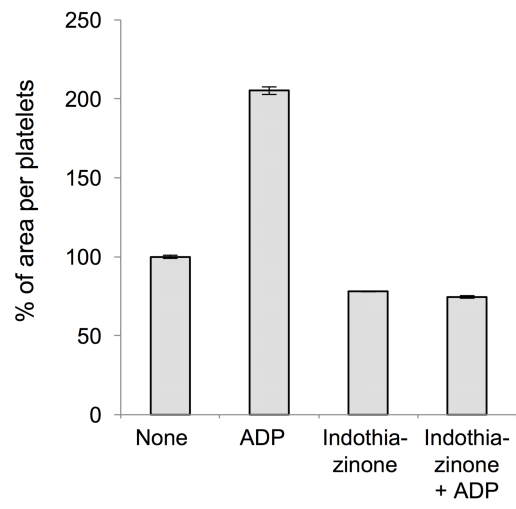


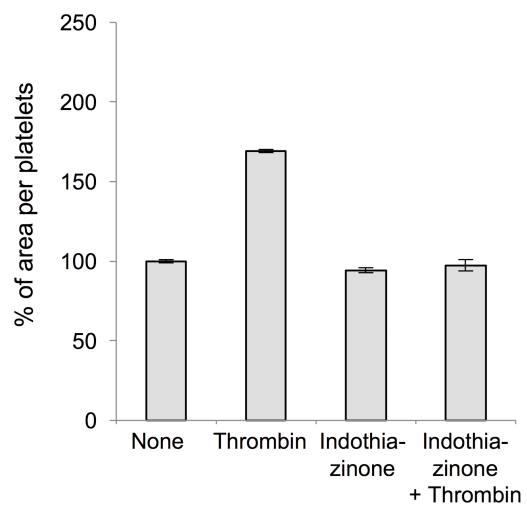
Figure 29. Quantification of Indothiazinone effects on platelet spreading.

A ADP- and **B** thropmbin- induced platelet spreading in the presence of indothiazinone is quantified by measuring the surface area of spread platelets. Average areas of the treated platelets were normalized to those of untreated platelets. Error bars represent the standard error (n=3)

A.



B.



the ADP-induced platelet spreading (bottom right panels of Figure 28A and B). Measurement of the spread area of platelets for quantifying the results revealed that 10 μ M ADP and 1.6 U/ml thrombin treatments increased the spread area up to 20.22% and 169.24%, respectively, relative to that of unstimulated platelets (Figure 29A and B). In contrast, treatment with 200 μ M indothiazinone reduced the platelet area to 74.58% and 97.49%, less than that of the unstimulated controls (Figure 29A and B). Thus, these results showed that indothiazinone exhibited antiplatelet activity, presumably by inhibiting integrin α IIb β 3-dependent fibrinogen binding.

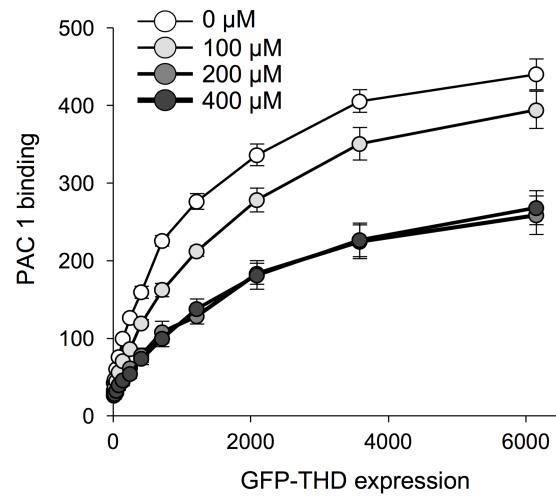
Effect of indothiazinone on talin-induced PAC1 binding

Integrin-dependent cell adhesion and spreading are largely dependent on the affinity of integrin (Chigaev A *et al.*, 2007; Pinon P *et al.*, 2014; Green JA *et al.*, 2009). Talin, a cytoplasmic protein, is known to bind to the cytoplasmic tail of integrin and increase its affinity in response to various agonists acting on platelets (Tadokoro S *et al.*, 2003; Kasirer-Friede A *et al.*, 2014). Thus, I hypothesized that indothiazinone's antiplatelet activity may be ascribed to its ability to inhibit the function of talin. Overexpression of the talin head domain, a constitutively active form of talin (Calderwood DA *et al.*, 2002), in the CHO/ α IIb β 3 cell line induced integrin activation, which was detected using increase in binding to PAC1 (Figure 30A, empty circles), a ligand-mimetic integrin α IIb β 3-specific antibody (Shattil SJ *et al.*, 1985). Importantly, treatment with indothiazinone reduced the talin head domain-mediated integrin activation in a dose-dependent manner (Figure 30A).

Figure 30. Effect of indothiazinone on talin-induced integrin activation.

A, CHO/ α IIb β 3 cells transfected with green fluorescent protein (GFP)-fused talin head domain (GFP-THD) or **B**, GFP only were stained with PAC1 in the presence of the indicated concentration of indothiazinone. The mean fluorescence intensities produced by binding of PAC1 to cells expressing different concentrations of GFP-talin head domain or GFP were plotted as line graphs. Error bars represent standard errors of two independent experiments with duplicated sample.

A.



B.

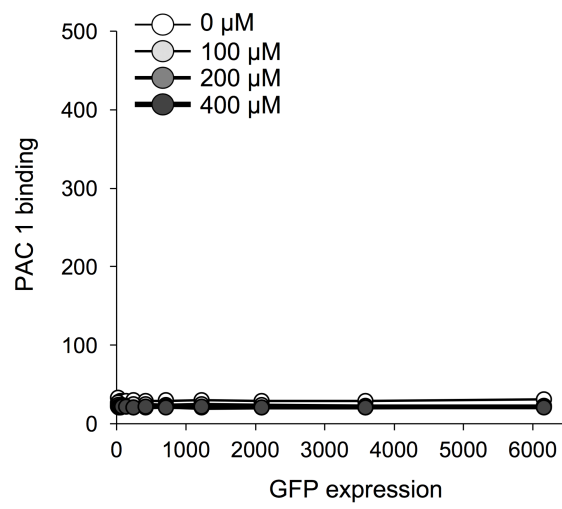
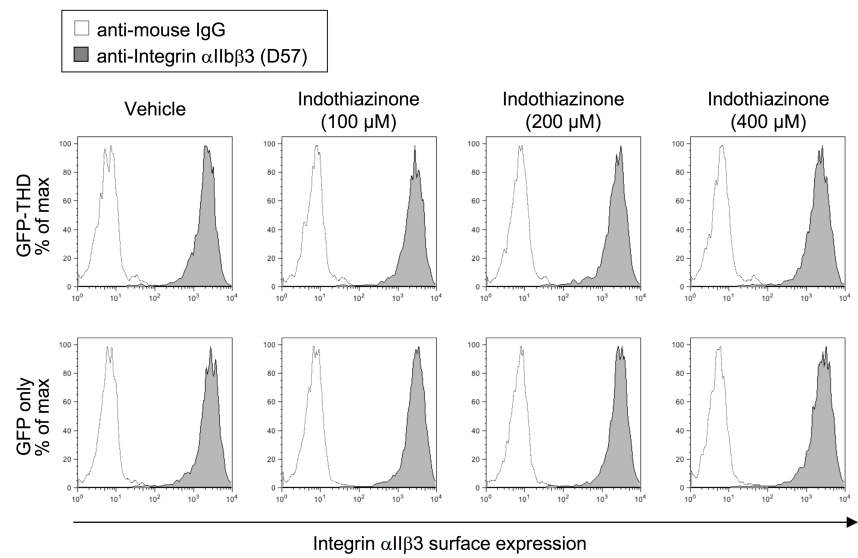


Figure 31. Effect of indothiazinone on cell surface expression of integrin α IIb β 3.

Effects of indothiazinone on integrin α IIb β 3 surface expression levels in GFP-THD-(top panels) and GFP-transfected cells (low panels) were analyzed using D57, integrin α IIb β 3 complex specific antibody, or its isotype control. Representative histograms were shown.



Indothiazinone at 200 μ M reduced PAC1 binding by about 50%; however, it showed a saturation effect at concentrations higher than 200 μ M, possible due to decrease in water solubility. Interestingly, when integrin surface expression was measured using D57, an integrin α IIb β 3 complex-specific antibody, it was found that indothiazinone treatment did not induce noticeable changes in the surface expression of the integrin (Figure 31). These results showed that the inhibitory effect of indothiazinone is probably because of its suppressive action on talin-mediated integrin activation.

Possible mechanism of indothiazinone action

The binding of talin to the cytoplasmic tail of integrin β activates integrin by disrupting the α - β transmembrane domain interaction (Kim C *et al.*, 2012). Structural and molecular dynamics simulation studies have revealed that disruption of the transmembrane domain interaction as well as integrin activation requires talin-integrin interaction at two different regions of integrin β subunit, that is, the membrane proximal (MP) and membrane distal (MD) regions (Kim C *et al.*, 2011). Talin binds strongly to the MD region, where an NPxY (Asn-Pro-X-Tyr) motif in the integrin β cytoplasmic tail plays a dominant role in talin-integrin interaction (Kim C *et al.*, 2011). However, interaction between talin and integrin in the MP region is relatively weak; (Wegner KL *et al.*, 2007) nevertheless, the interaction is essential for integrin activation. (Wegner KL *et al.*, 2007)

The fact that indothiazinone was able to inhibit talin-induced integrin activation raised a possibility that it may bind to talin, rather than to the unstructured integrin tail (Ulmer TS *et al.*, 2001), and interfere with integrin-talin interaction. To test this hypothesis, I purified the F2/F3

subdomains (talin F2/F3) of talin head domain and the direct binding of indothiazinone to talin was first tested using surface plasmon resonance.⁹⁾ The real-time binding of indothiazinone to the purified talin F2/F3 immobilized on sensor chip proceeded in a dose-dependent manner, with a KD value of 2.03×10^{-4} M (Figure 32A) This observation supported the direct binding of indothiazinone to the talin head domain, which possibly contributed to its antiplatelet activity. My molecular docking simulation using known crystal structure of talin F2/F3 (Anthis NJ *et al.*, 2010) also predicted possible interactions between them with considerably high score (Figure 32B). Interestingly, two indothiazinone binding sites were predicted in the talin-integrin binding interface around the MP (Figure 32B, red dotted circle) and MD interacting regions (Figure 32B, blue dotted circle). In the MP interacting region, indothiazinone occupies the position where talin forms a hydrophobic bond with two phenylalanine residues of the cytoplasmic tail of integrin β (Figure 32B, right). In the MD interacting region on the other hand, binding of indothiazinone to talin inhibits the interaction between talin and tyrosine residue of the NPxY region of the integrin β 3 cytoplasmic tail (Figure 32B). Thus, one of the possible interactions between indothiazinone and talin at either region might form the molecular basis of suppression of talin-mediated integrin activation. To determine which of these regions are responsible for indothiazinone binding, I generated talin F2/F3 proteins with mutations in the MP interacting region (L325A/K318A) and in the MD interacting region (D372A/Y373A/I396A) (Figure 33A and B) as well as talin F2 protein as a negative controls and tested their binding to indothiazinone as in Figure 32A. Interestingly, introduction of the mutations at the MD interacting region reduced the binding by about 50%, while the mutation at the MP

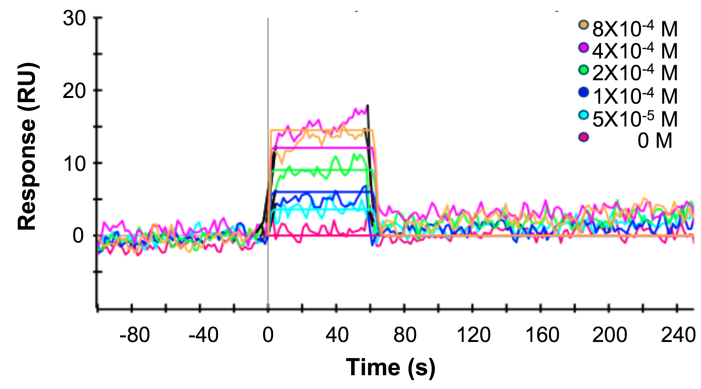
9) Surface plasmon resonance assay performed and analyzed by professor Jong-Wha Jung in Kyungpook National University

interacting region has no noticeable effect (Figure 34). The binding was specific because the negative control, talin F2 protein, showed almost no binding with indothiazinone (Figure 34). These results suggest that indothiazinone can occupy the MD interacting region in talin, this inhibiting talin-integrin binding and integrin activation.

Figure 32. Interaction between indothiazinone and talin.

A, surface plasmon resonance analysis of the binding of indothiazinone to purified 6xHis-tagged talin F2/F3. RU, resonance units. **B**, Complex structure of integrin $\beta 1$ cytoplasmic tail and talin F2/F3 domains (Protein Data Bank accession no. 3G9W) is depicted in left. Shown are two phenylalanines, F763 and F766, involved in the talin-membrane proximal (MP) region interaction, and tyrosine, Y783, involved in the talin-membrane distal (MD) region interaction, with corresponding integrin $\beta 3$ residues in parentheses. Possible indothiazinone binding site at the MP (red dotted circle) or MD interacting regions in talin (blue dotted circle) were predicted by molecular docking simulation. Integrin β cytoplasmic tail, talin F2/F3 domain, and indothiazinone are colored as blue, gray, and red, respectively. At the MP interacting region, indothiazinone occupies the binding interface where two phenylalanines, F753 and F756 of integrin $\beta 3$, are located. At the MD region, indothiazinone occupies the binding interface where the tyrosine in NPxY motif, Y747 of integrin $\beta 3$, is located.

A.



B.

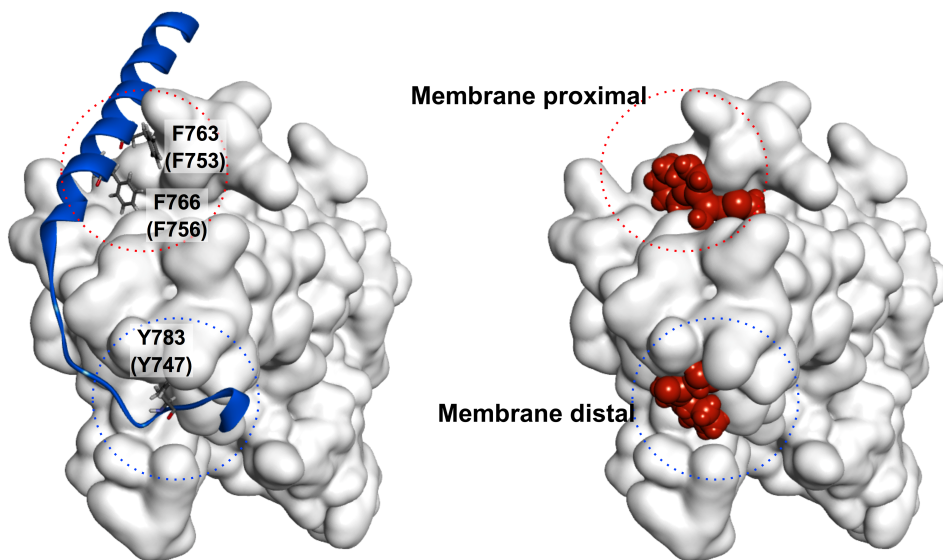
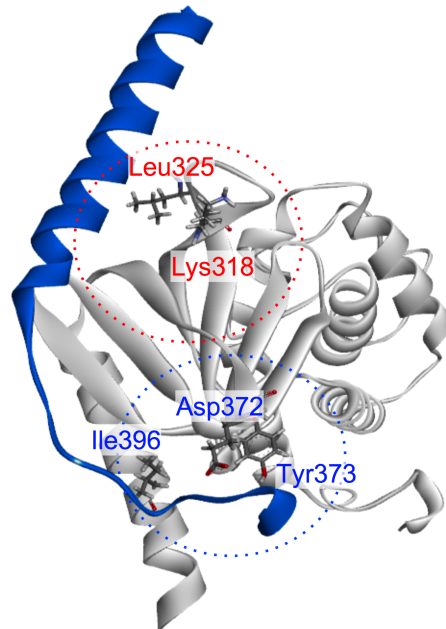


Figure 33. Purification of mutant talin head domain.

A, The amino acid residues at the MP interacting region (red dotted circle, Lys318 and Leu325) or at the MD interacting region (blue dotted circle, Asp372, Tyr373 and Ile396) of talin F2/F3 domain were mutated into alanines, to generate talin F2/F3(L325A/K318A) and talin F2/F3(D372A/Y373A/I396A). **B**, Coomassie blue staining of purified His-tagged talin F2/F3 wild type and mutants.

A.



B.

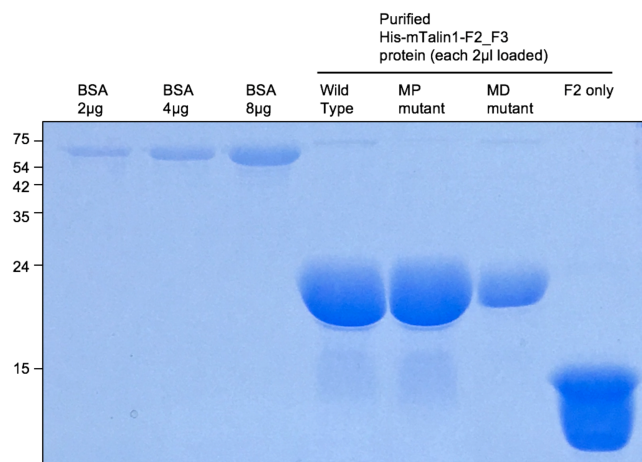
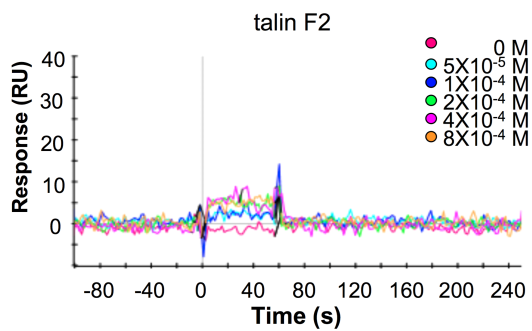
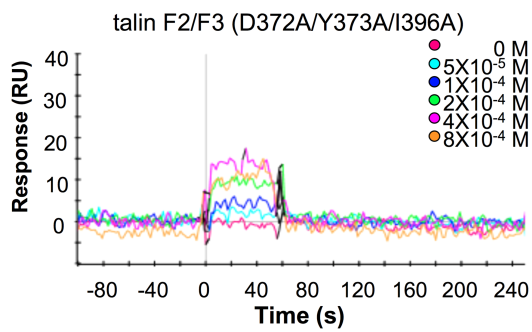
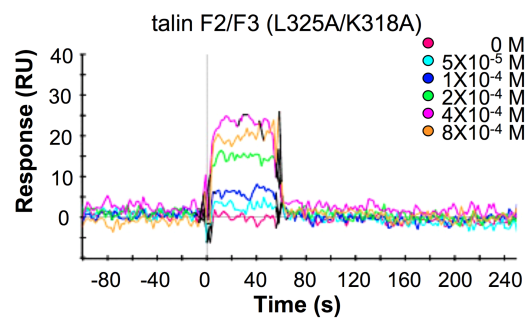
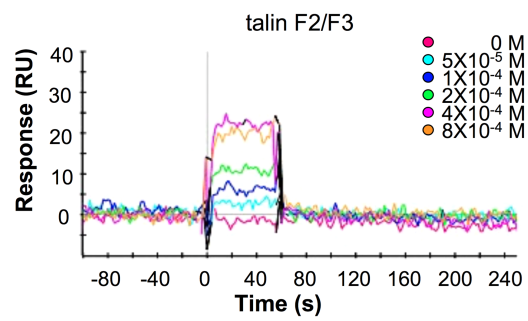


Figure 34. Effects of mutation in talin on talin-indothiazinone interaction.

The degrees of binding between indothiazinone and wild type talin F2/F3 domain, L325A/K318A mutant, D372A/Y373A/I396A mutant, or talin f2 domain were analyzed by surface plasmon resonance as in Figure 32A. RU, resonance units.



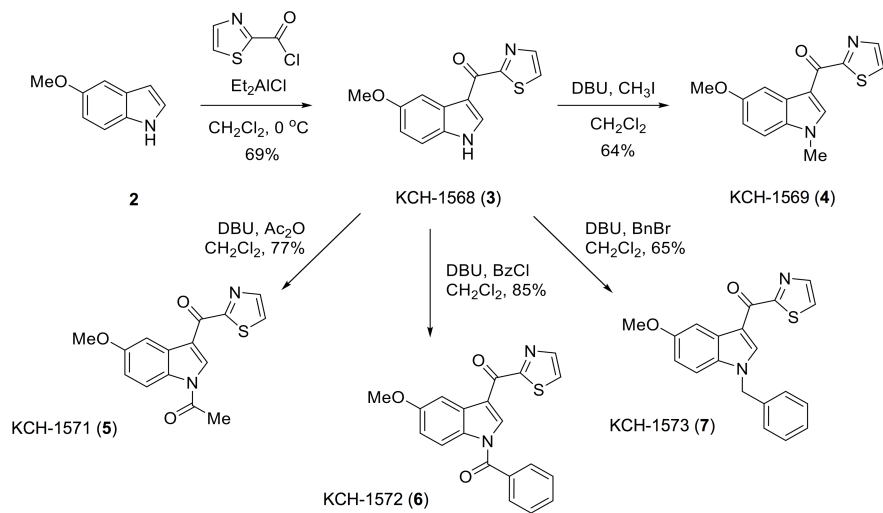
Synthesis of KCH-1569, a derivative of indothiazinone, and its antiplatelet effects

The results described above suggest that indothiazinone might be a useful lead compound for the development of antiplatelet drugs capable of inhibiting integrin $\alpha\text{IIb}\beta\text{3}$ activation. As a proof of concept, I tested CHO/ $\alpha\text{IIb}\beta\text{3}$ -fibrinogen binding as illustrated in Figure 27A using several compounds which modified of indothiazinone. In this experiment, one of the compounds containing additional methoxyl and methyl groups in the benzimidazole ring of indothiazinone (KCH-1569) effectively inhibited CHO/ $\alpha\text{IIb}\beta\text{3}$ adhesion to the fibrinogen-coated surface (Figure 35) At a concentration of 200 μM especially, the inhibitory effect of KCH-1569 was significantly enhanced compared to that of indothiazinone (Figure 36A). Moreover, in the PAC1 binding assay, 100 μM KCH-1569 significantly inhibited talin head domain-induced integrin activation (Figure 36B, blue line), whereas the same concentration of indothiazinone only partially (not statistically significant) inhibited the talin head domain-induced PAC1 binding (Figure 36B, red line). Finally, KCH-1569 was proven not to exhibit noticeable influence on integrin $\alpha\text{IIb}\beta\text{3}$ surface expression (Figure 37), confirming that the inhibitory effects of the compound are due to its ability to decrease the affinity but not the surface expression of the integrin.

Figure 35. Effect of indothiazinone and its derivatives.

A, Structures of synthesized of 5-methoxy-indothiazinone derivatives **B**, CHO/ α IIb β 3 cells were incubated on fibrinogen coated surface in the presence of 400 μ M chemicals as indicated. Bound cells were analyzed as described in **Figure 27A**. Error bars represent standard error of the means of two independent experiments with triplicated samples.

A.



B.

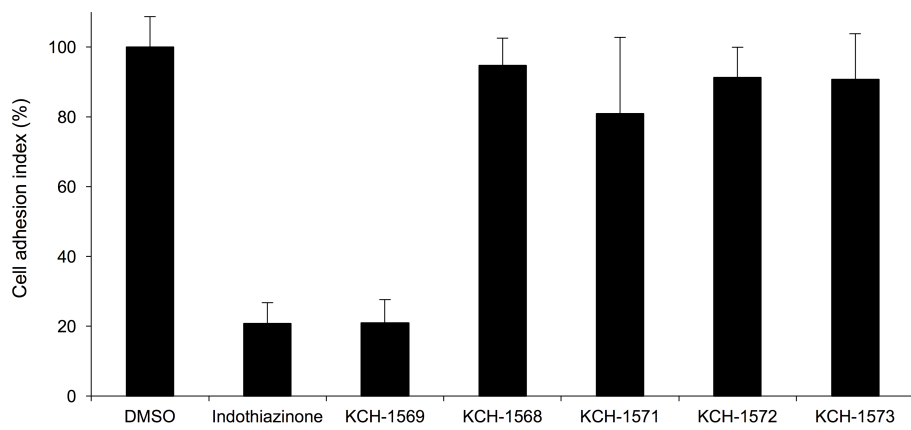
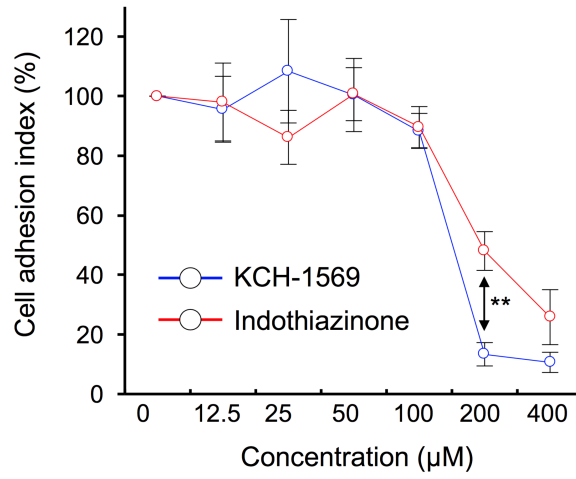


Figure 36. Enhanced antiplatelet effect of KCH-1569.

A, Adhesion of CHO/ α IIb β 3 cells to fibrinogen-coated wells in the presence of different concentrations of indothiazinone (red) or KCH-1569 (blue). Error bars represent standard deviation of two independent experiments with triplicated samples. ** $p < 0.01$ (two-way analysis of variance with multiple comparison using Fisher's least significant difference test). **B**, PAC1 binding of cells treated with either 100 μ M indothiazinone (red) or 100 μ M KCH-1569 (blue). The degree of PAC1 binding was normalized to the maximum binding to vehicle-treated sample. * $p < 0.05$, ** $p < 0.01$, *** $p < 0.001$ (two-way analysis of variance with multiple comparison using Fisher's least significant difference test.) Error bars represent standard error of the means of three independent experiments with duplicated samples.

A.



B.

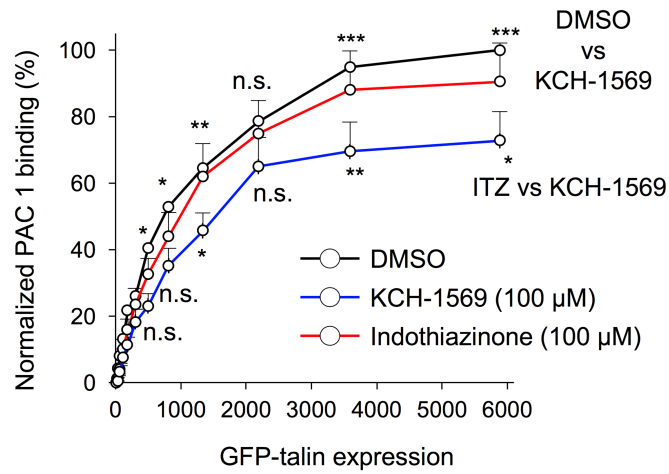
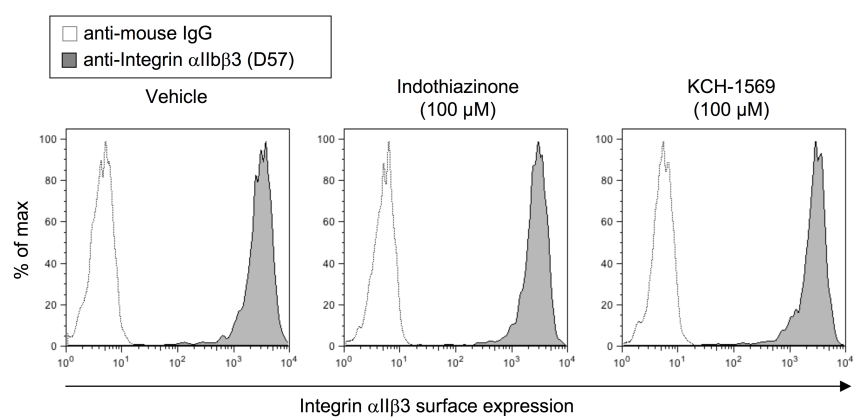


Figure 37. Effects of indothiazinone (middle) or KCH1569 (right) on integrin α IIb β 3 surface expression levels in GFP-THD-transfected cells.

Surface expression level of integrin α IIb β 3 analyzed as in **Figure 31**

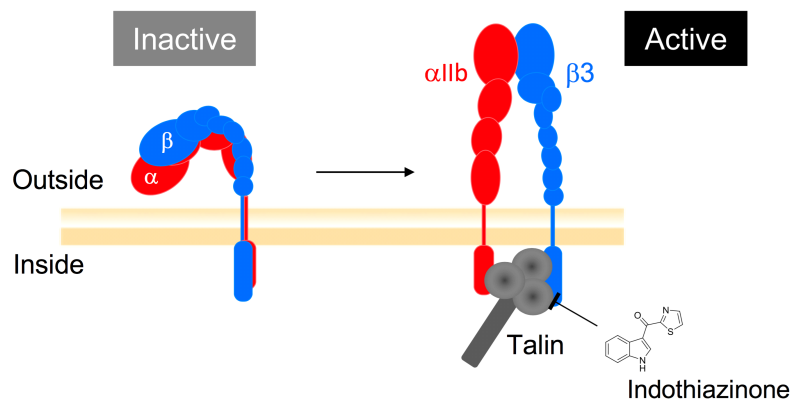


CONCLUSION

Taken together, I identified the natural product, indothiazinone, exhibited antiplatelet activity, by showing suppressive effects of the compound on integrin $\alpha\text{IIb}\beta\text{3}$ -dependent cell adhesion, platelet spreading, and talin-induced integrin activation. I also tested a derivative of indothiazinone showing enhanced antiplatelet activity, and demonstrated that indothiazinone can be used a novel lead compound for development of new antiplatelet drugs (Figure 38). Considering that direct inhibition of integrin–ligand interaction has severe adverse effects (Bledzka K *et al.*, 2013) as described above, suppression of integrin activation by inhibiting talin–integrin interaction has been considered as an alternative therapy for reducing the risk of thrombosis. (Petrich BG *et al.*, 2007) For example, studies using mice expressing integrin β3 (L746A) (Petrich BG *et al.*, 2007) or talin (L325R) (Stefanini L *et al.*, 2014) mutant, both of which can inhibit integrin–talin interaction, elegantly showed that disruption of the interaction can reduce integrin activation while preventing pathological bleeding, the main adverse effect of strong antiplatelet therapy. (Bledzka K *et al.*, 2013) Thus, I believe that indothiazinone capable of inhibiting talin–integrin interaction can provide the chemical basis for development of novel antiplatelet drugs with superior mode of action.

Figure 38. Graphical abstract

Indothiazinone, a natural product from myxobacteria, was shown to inhibit agonist-induced platelet spreading by suppressing talin-mediated integrin α IIb β 3 activation. This study also shows that indothiazinone can be used as a lead compound in the development of antiplatelet drugs with a novel mode of action.



REFERENCES

- Alissa EM, Ferns GA. Functional foods and nutraceuticals in the primary prevention of cardiovascular diseases. *J Nutr Metab*. 2012;2012:569486.
- Anthis NJ, Wegener KL, Critchley DR, Campbell ID. Structural diversity in integrin/talin interactions. *Structure*. 2010 Dec 8;18(12):1654–66.
- Aslan JE, Itakura A, Gertz JM, McCarty OJ. Platelet shape change and spreading. *Methods Mol Biol* 2012, 788, 91.
- Bledzka K, Smyth SS, Plow EF. Integrin $\alpha\text{IIb}\beta\text{3}$: from discovery to efficacious therapeutic target. *Circ Res*. 2013 Apr 12;112(8):1189–200.
- Calderwood DA, Yan B, de Pereda JM, Alvarez BG, Fujioka Y, Liddington RC, Ginsberg MH. The phosphotyrosine binding-like domain of talin activates integrins. *J Biol Chem* 2002, 277, 21749.
- Chigaev A, Waller A, Zwartz GJ, Buranda T, Sklar LA. Regulation of cell adhesion by affinity and conformational unbending of $\alpha\text{4}\beta\text{1}$ integrin. *J Immunol* 2007, 178, 6828.
- Dimitrow PP, Jawien M. Pleiotropic, cardioprotective effects of omega-3 polyunsaturated fatty acids. *Mini Rev Med Chem*. 2009 Aug;9(9):1030–9.
- Du XP, Plow EF, Frelinger AL 3rd, O'Toole TE, Loftus JC, Ginsberg MH. Ligands "activate" integrin $\alpha\text{IIb}\beta\text{3}$ (platelet GPIIb-IIIa). *Cell*. 1991 May 3;65(3):409–16.

Estevez B, Shen B, Du X. Targeting integrin and integrin signaling in treating thrombosis. *Arterioscler Thromb Vasc Biol.* 2015 Jan;35(1):24-9.

Green JA, Berrier AL, Pankov R, Yamada KM. beta1 integrin cytoplasmic domain residues selectively modulate fibronectin matrix assembly and cell spreading through talin and Akt-1. *J Biol Chem.* 2009 Mar 20;284(12):8148-59.

Hsiao G, Wang Y, Tzu NH, Fong TH, Shen MY, Lin KH, Chou DS, Sheu JR. Inhibitory effects of lycopene on in vitro platelet activation and in vivo prevention of thrombus formation. *J Lab Clin Med.* 2005 Oct;146(4):216-26.

Humphries JD, Byron A, Humphries MJ. Integrin ligands at a glance. *J Cell Sci.* 2006 Oct 1;119(Pt 19):3901-3.

Hynes RO. Integrins: bidirectional, allosteric signaling machines. *Cell* 2002, 110, 673.

Jackson SP. Arterial thrombosis--insidious, unpredictable and deadly. *Nat Med.* 2011 Nov 7;17(11):1423-36.

Jansen R, Mohr KI, Bernecker S, Stadler M, Muller R, Indothiazinone, an indolyl thiazolyl ketone from a novel myxobacterium belonging to the Sorangiineae. *J Nat Prod.* 2014 Apr 25;77(4):1054-60.

Kasirer-Friede A, Kang J, Kahner B, Ye F, Ginsberg MH, Shattil SJ. ADAP interactions with talin and kindlin promote platelet integrin $\alpha\text{IIb}\beta\text{3}$ activation and stable fibrinogen binding. *Blood.* 2014 May 15;123(20):3156-65.

Kim C, Ye F, Ginsberg MH. Regulation of integrin activation. *Annu Rev Cell Dev Biol.* 2011;27:321-45.

Kim C, Schmidt T, Cho EG, Ye F, Ulmer TS, Ginsberg MH. Basic amino-acid side chains regulate transmembrane integrin signalling. *Nature.* 2011 Dec 18;481(7380):209-13.

Kim C, Ye F, Hu X, Ginsberg MH. Talin activates integrins by altering the topology of the β transmembrane domain. *J Cell Biol.* 2012 May 28;197(5):605-11.

Kim J, Yang C, Kim EJ, Jang J, Kim SJ, Kang SM, *et al.* Vimentin filaments regulate integrin-ligand interactions by binding to the cytoplasmic tail of integrin β 3. *J Cell Sci.* 2016 May 15;129(10):2030-42.

Kram L, Grambow E, Mueller-Graf F, Sorg H, Vollmar B. The anti-thrombotic effect of hydrogen sulfide is partly mediated by an upregulation of nitric oxide synthases. *Thromb Res.* 2013 Aug;132(2):e112-7.

Kwon S, Han YT, Jung J-W. Studies on the Synthesis of Indothiazinone and Its Derivatives via Direct 3-Acylation of Indole. *Synthetic Communications* 2015, May (45):1662-1668.

Lishko VK, Podolnikova NP, Yakubenko VP, Yakovlev S, Medved L, Yadav SP, Ugarova TP. Multiple binding sites in fibrinogen for integrin α 5 β 1 (Mac-1). *J Biol Chem.* 2004 Oct 22;279(43):44897-906.

Nieswandt B, Varga-Szabo D, Elvers M. Integrins in platelet activation. *J Thromb Haemost.* 2009 Jul;7 Suppl 1:206-9.

Petrich BG, Fogelstrand P, Partridge AW, Yousefi N, Ablooglu AJ, Shattil SJ, et al. The antithrombotic potential of selective blockade of talin-dependent integrin alpha IIb beta 3 (platelet GPIIb-IIIa) activation. *J Clin Invest.* 2007 Aug;117(8):2250-9.

Phillips DR, Charo IF, Parise LV, Fitzgerald LA. The platelet membrane glycoprotein IIb-IIIa complex. *Blood.* 1988 Apr;71(4):831-43.

Pinon P, Parssinen J, Vazquez P, Bachmann M, Rahikainen R, Jacquier MC, et al. Talin-bound NPLY motif recruits integrin-signaling adapters to regulate cell spreading and mechanosensing. *J Cell Biol.* 2014 Apr 28;205(2):265-81.

Reynolds AR, Hart IR, Watson AR, Welti JC, Silva RG, Robinson SD, et al. Stimulation of tumor growth and angiogenesis by low concentrations of RGD-mimetic integrin inhibitors. *Nat Med.* 2009 Apr;15(4):392-400.

Santhakumar AB, Bulmer AC, Singh I. A review of the mechanisms and effectiveness of dietary polyphenols in reducing oxidative stress and thrombotic risk. *J Hum Nutr Diet.* 2014 Feb;27(1):1-21.

Shattil SJ, Hoxie JA, Cunningham M, Brass LF. Changes in the platelet membrane glycoprotein IIb-IIIa complex during platelet activation. *J Biol Chem.* 1985 Sep 15;260(20):11107-14.

Stefanini L, Ye F, Snider AK, Sarabakhsh K, Piatt R, Paul DS, et al. A

talin mutant that impairs talin-integrin binding in platelets decelerates α IIb β 3 activation without pathological bleeding. *Blood*. 2014 Apr 24;123(17):2722-31.

Tadokoro S, Shattil SJ, Eto K, Tai V, Liddington RC, de Pereda JM, et al. Talin binding to integrin beta tails: a final common step in integrin activation. *Science*. 2003 Oct 3;302(5642):103-6.

Ulmer TS, Yaspan B, Ginsberg MH, Campbell ID. NMR analysis of structure and dynamics of the cytosolic tails of integrin alpha IIb beta 3 in aqueous solution. *Biochemistry*. 2001 Jun 26;40(25):7498-508.

Vilahur G, Badimon L. Antiplatelet properties of natural products. *Vascul Pharmacol*. 2013 Sep-Oct;59(3-4):67-75.

Wegener KL, Partridge AW, Han J, Pickford AR, Liddington RC, Ginsberg MH, Campbell ID. Structural basis of integrin activation by talin. *Cell*. 2007 Jan 12;128(1):171-82.

국문초록

혈관내피세포에서 주로 발현되는 Tie2는 막단백질 키나아제로, 발달 단계에서의 혈관 형성 또는 암의 성장에 필수 과정인 혈관 신생에 중요한 역할을 하는 것이 잘 알려져 있다. 본 연구에서는 Tie2의 활성이 칼슘/칼모둘린에 의해 음성적으로 조절되는 기작을 생화학적, 세포생물학적 기법 및 *in vivo* 실험으로 다음의 내용을 통해 검증하였다. 첫째, 혈관내피세포(HUVEC)에 calcium ionophore 처리에 의한 세포내 칼슘농도를 증가시켰을 때, Tie2 리간드인 Ang1에 의해 증가된 Tie2 활성이 감소하는 현상을 확인하였다. 둘째, Tie2 세포외도메인이 제거된 돌연변이 모델 시스템을 이용한 기작 연구결과, Tie2 활성 저해 현상은 칼슘이온 특이적임을 확인하였다. 셋째, 칼슘 수용체인 칼모둘린과 Tie2가 상호작용을 하는 것을 확인하였으며, Tie2의 1113번째 티로신 잔기가 칼모둘린-Tie2 상호작용에 필수적임을 확인하였다. 넷째, calcium ionophore 처리에 의한 Tie2의 활성 저해 현상은 칼모둘린과-Tie2간의 상호작용이 존재할 때만 관찰되는 것을 확인하였으며 다섯째, 칼모둘린이 결합하지 못하는 Tie2 돌연변이를 아프리카 발톱 개구리 혈관 형성 모델에 적용한 결과 혈관이 비정상적으로 형성되는 것을 관찰하였다. Tie2의 양성조절 기작을 통해 혈관 신생과정을 저해하기 위한 기존의 연구와 달리, 본 연구를 통해 혈관이 정상적인 구조를 형성함에 Tie2의 음성조절 기작이 기여함을 밝혔다.

세포부착 막 단백질인 인테그린은 α 와 β 서브유닛이 조직에 따라 다양한 조합을 이루며 발현한다. 그 중 인테그린 α IIb β 3는 혈소판 특이적으로 발현되며, 세포내 작용제인 탈린 단백질이 β 3 세포내 도메인에 결합하여 β 3의 인지질 이중층에서의 위상차 변화를 야기하고, α 와 β 의 막 통관부위의 상호결합을 저해함으로써 구조적 변화를 유도한다. 이로 인해 리간드인 피브리노젠과의 결합부위가 노출되어 혈소판 응집을 형성하기 때문에 지혈 작용에 중요함이 잘 알려져 있다. 인테그린의 리간드 결합부위에 경쟁적으로 결합하는 기존의 항혈소판제의 경우 인테그린의 정상적인 기능을 위한 활성조차 저해하기 때문에 출혈의 부작용이 있다. 따라서 본 연구는 리간드 결합부위가 아닌 세포내 인

테그린 작용제 탈린을 타깃하는 새로운 작용기작의 항혈소판제 개발을 위한 연구 내용으로 심혈관 질환 개선에 도움을 주는 것으로 잘 알려진 녹차의 주 성분인 EGCG를 이용한 연구와, 미소박테리아에서 발견되는 천연물 유도체인 Indothiazinone을 이용한 연구 결과이다.

EGCG를 인테그린 $\alpha\text{IIb}\beta_3$ 를 지속적으로 활성화 시키도록 탈린을 발현시킨 세포주에 처리하였을 때, 인테그린 $\alpha\text{IIb}\beta_3$ 활성이 저해되는 현상을 관찰하였다. 하지만, 탈린을 발현시키지 않은 세포주에 EGCG를 처리하였을 때에도 인테그린 $\alpha\text{IIb}\beta_3$ 활성이 증가되는 현상을 관찰하였다. 본 현상의 기작을 규명하기 위해 정제된 인공세포막인 나노디스크 시스템을 이용하였다. 인테그린 $\alpha\text{IIb}\beta_3$ 의 활성은 β_3 막 통관부위가 인지질 이중층에서의 위상차 변화에 의해 조절되므로, 나노디스크로 불리는 인공세포막에 인테그린 β_3 막통관부위를 삽입하여 위상 변화를 확인하였다. 이를 위해 인테그린 β_3 막통관부위 양 끝에 소수성/친수성 환경에 따라 발광 증감의 성질을 지닌 mero60 형광물질을 결합하여 발광 정도를 측정하였다. 인테그린 β_3 가 삽입된 나노디스크에 탈린을 넣어주었을 때, 형광물질의 발광이 증가함을 확인하였으며 이는 나노디스크에 삽입된 인테그린 β_3 막 통관부위의 기울기가 증가하여 형광물질이 소수성인 인지질 이중층 안쪽으로 향한 것을 의미한다. 이 조건에서 EGCG를 처리하였을 때 이러한 증가된 인테그린 β_3 막 통관부위의 기울기가 감소되는 현상을 관찰했으며, 탈린이 없는 조건에서도 인테그린 β_3 막 통관부위 기울기를 감소시키는 현상을 확인하였다. 이와 같은 EGCG의 pleiotropic 한 효과는 EGFR 발현 세포주에서도 확인 하였으며, EGFR의 막통관부위를 정제하여 나노디스크에 삽입 후 위상 변화를 관찰한 결과 인테그린과 마찬가지로 EGFR 막통관부위 위상변화를 감소시키는 것을 확인하였다.

Pleiotropic 효과가 없는 항혈소판제 개발을 위하여 EGCG 화학구조 기반의 천연물 유도체 라이브러리를 이용한 스크리닝을 수행하였다. 인테그린 $\alpha\text{IIb}\beta_3$ 발현 세포주에 천연물 유도체 라이브러리 전처리를 한 후 피브리노겐이 코팅된 96-well plate에 세포 부착을 저해하는 유효물질을 선별하였다. 그 중 미소박테리아에서 발견되는 천연물 유도체인 Indothiazinone을 발견하였다. Indothiazinone은 ADP 또는 thrombin 처리에 의한 인간 혈소판의 피브리노겐

매트릭스 위에서 퍼짐을 저해하였으며, 탈린을 발현시킨 인테그린 $\alpha\text{IIb}\beta\text{3}$ 발현 세포주의 활성을 저해함을 확인하였다. EGCG와 달리 Indothiazinone 단독 처리에 의한 인테그린 $\alpha\text{IIb}\beta\text{3}$ 의 활성이 증가하지 않음을 확인하였고, 탈린에 의해 증가된 인테그린 $\alpha\text{IIb}\beta\text{3}$ 활성이 세포 표면에서 인테그린의 발현을 감소시키지 않음을 확인했다. 분자 동역학 모델링 기법을 이용하여 인테그린 β 와 탈린이 결합하는 부위에 Indothiazinone이 결합할 수 있는 가능성을 확인하였으며, 이를 바탕으로 탈린 야생형 및 돌연변이 단백질을 정제하여 SPR 실험을 수행했다. 그 결과 Indothiazinone이 탈린 야생형에 농도 의존적으로 직접 결합하는 것을 확인하였으며, 돌연변이 탈린에는 결합정도가 감소한 것을 관찰했다. 이는 Indothiazinone이 인테그린 β 와 탈린간의 상호작용을 저해함으로써 인테그린 $\alpha\text{IIb}\beta\text{3}$ 의 활성을 저해할 가능성이 있음을 시사한다. 결과적으로 본 연구는 EGCG의 pleiotropic 한 효과가 막 단백질 인테그린과 EGFR의 막 통관부위 기울기를 조절함으로써 막단백질의 활성이 조절될 수 있음을 규명했으며, 탈린을 타겟으로 하는 새로운 작용기전의 항혈소판제로써 Indothiazinone이 선도 물질로 개발될 가능성을 검증한 연구 결과이다.